NATIONAL AERONAUTICS AND SPACE ADMINISTRATION



Technical Report 32-1274

# Design and Construction of the 15-ft-Beam Solar Simulator SS15B

R. P. Eddy

JET PROPULSION LABORATORY
CALIFORNIA INSTITUTE OF TECHNOLOGY
PASADENA, CALIFORNIA

October 1, 1968

NATIONAL AERONAUTICS AND SPACE ADMINISTRATION

*Technical Report 32-1274*

# *Design and Construction of the 15-ft-Beam Solar Simulator SS15B*

*R. P. Eddy*

JET PROPULSION LABORATORY
CALIFORNIA INSTITUTE OF TECHNOLOGY
PASADENA, CALIFORNIA

October 1, 1968

***TECHNICAL REPORT 32-1274***



Prepared Under Contract No. NAS 7-100
National Aeronautics and Space Administration

## Preface

The work described in this report was performed by the Environmental Sciences Division of the Jet Propulsion Laboratory.

# Contents

## Contents (contd)



## Tables



## Figures

## Contents (contd)

### Figures (contd)

## Contents (contd)

### Figures (contd)

## Abstract

The modification of the JPL 25-ft space simulator to incorporate a larger, higher quality solar simulator produced an initial 15-ft-diam beam of better than ±5% uniformity measured throughout the test volume. Although similar in general arrangement to the SS6A system developed for the 10-ft simulator, it employs several improvements. The uniformity and collimation are improved by defocusing and rotating the collimator and by using the aberration effect of the condensing lenses in the mixer lens assembly. The efficiency has been improved by incorporating a lens in the vacuum interface window. The use of water-cooled, 20-kW xenon arc lamps allows the system to be operated with a fewer number of lamps and related support equipment. Every effort was made toward combining potential and flexibility into the design by utilizing the latest advances in solar simulation technology. The conservative design of the SS15B simulator makes available sufficient reserve power which can be used for enlarging the beam to the ultimate 20-ft diam, providing up to planet Mercury irradiance, reducing the collimation angle, or improving the spectrum by selective filtering.

# Design and Construction of the 15-ft-Beam Solar Simulator SS15B

## I. Introduction

The 15-ft-beam solar simulator (SS15B)[1] (Fig. 1) is a high-quality, off-axis, single-beam system utilizing a single-piece collimator, an integrating lens system, and a 37-lamp cluster of 20-kW xenon arc lamps. Although similar to the 6-ft beam system (SS6A) developed for the JPL 10-ft space simulator (Refs. 1, 2), it incorporates several improvements and certain changes required because of size scaling. Many of the changes involved in building this new simulator produced state-of-the-art components and techniques previously untried.

The design of the SS15B simulator started on June 1, 1964, and acceptance testing was completed on August 28, 1967. The performance specifications were either equaled or exceeded in all instances, as shown in Table 1.

Some of the built-in flexibility and future potential for the SS15B system include the 276-in.-diam collimator, the 42-in.-diam free aperture at the vacuum-solar penetration, and the provision for future addition of 24 lamp positions. The simulator is initially sized to produce a 15-ft-diam beam, but the 23-ft collimator will accommodate a beam of up to 20 ft in diameter. Additional power obtained by enlarging the system aperture, or increasing the lamp cluster size from thirty-seven to sixty-one 30 kW lamps can be used in varying combinations to increase irradiance levels, alter the collimation angle, or modify the spectrum by selective filtration.

[1]The first version, the SS15A solar simulator, used a window in the side of the space simulator, instead of a lens.

**Table 1. SS15B specification and performance**

| Parameter | Specification | Performance |
|---|---|---|
| Test volume | 15 ft diam × 25 ft high | 15 ft diam × 25 ft high |
| Irradiance | 50 to 135 W/ft$^2$ | 50 to 135 W/ft$^2$ with 100% reserve |
| Uniformity of irradiance | ±5% | ±4% |
| Collimation | ±2 deg | ±1 deg |
| Spectral match with sun | Good | That of xenon lamps as modified by optics |

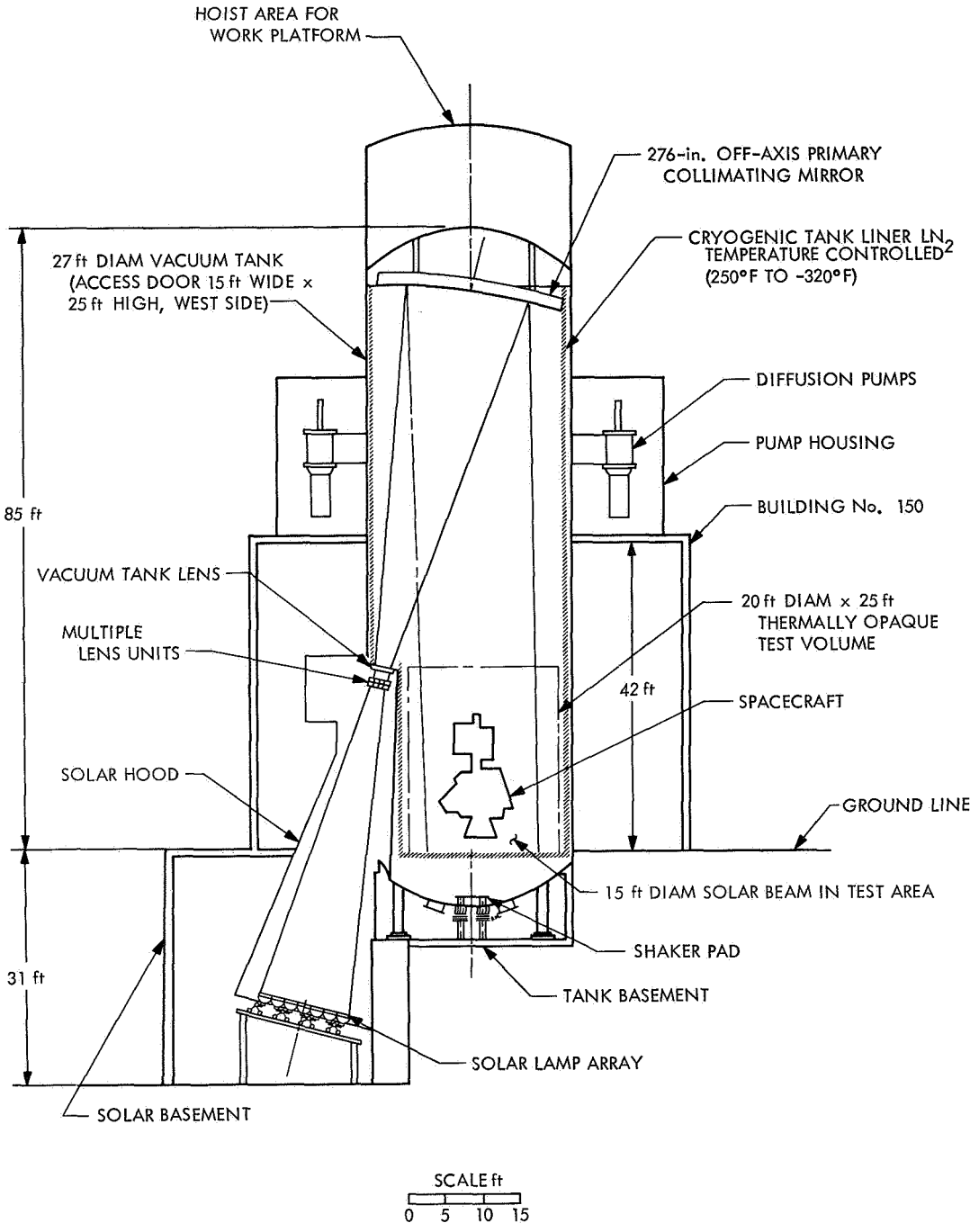


**Fig. 1. JPL 25-ft space simulator**

## II. Collimating Mirror

The SS15B collimator is a 23-ft-diam, highly polished, aluminized, nickel-plated mirror with a 100-ft radius of curvature and 50-ft focal length. It is temperature-controlled with a closed-loop nitrogen gas system and has an operating temperature range of −100 to +200°F (Ref. 3).

The uniformity and collimation of the light from the mirror to the test volume is optimized in the SS15B system by using a very small off-axis angle (14 deg) and by

placing the collimator 18 in. off focus and rotated 0.206 deg (Ref. 4). Figure 2 shows how the decollimation due to spherical aberration of the mirror is overcome somewhat by defocusing the virtual source (mixer-lens array), then equalizing the resulting beam collimation so that no ray exceeds ±1.078 deg from the vertical. Note that the position and rotation of the collimating mirror is determined by the maximum 20-ft-diam beam.

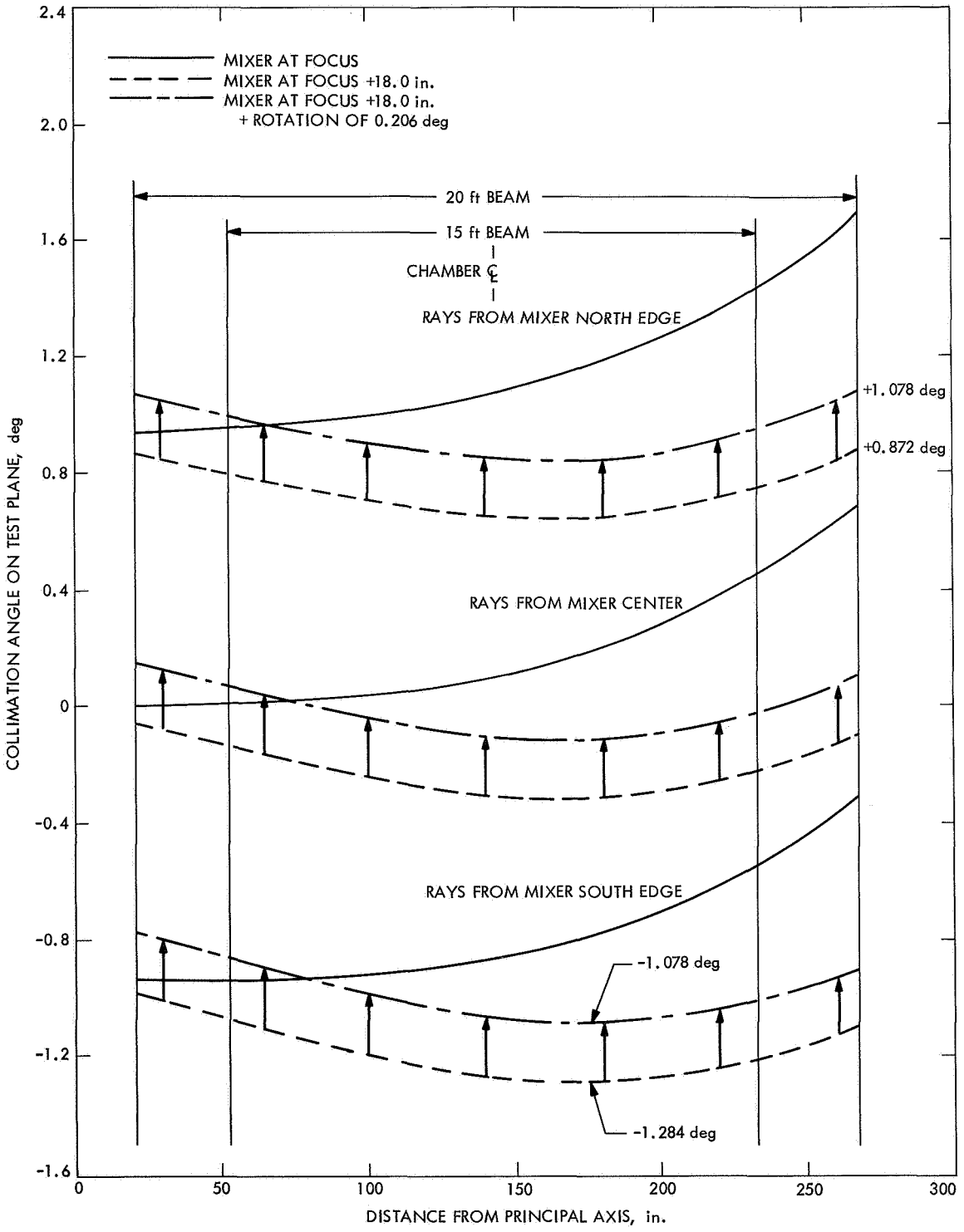


**Fig. 2. Collimation angle vs mirror location**

Figure 3 shows the effect of moving the virtual source with respect to the mirror on the uniformity of irradiance in the test volume. Here again, the uniformity has been optimized for the maximum potential 20-ft-diam beam. Figure 4 shows the collimating mirror being hoisted into position in the top of the space simulator.

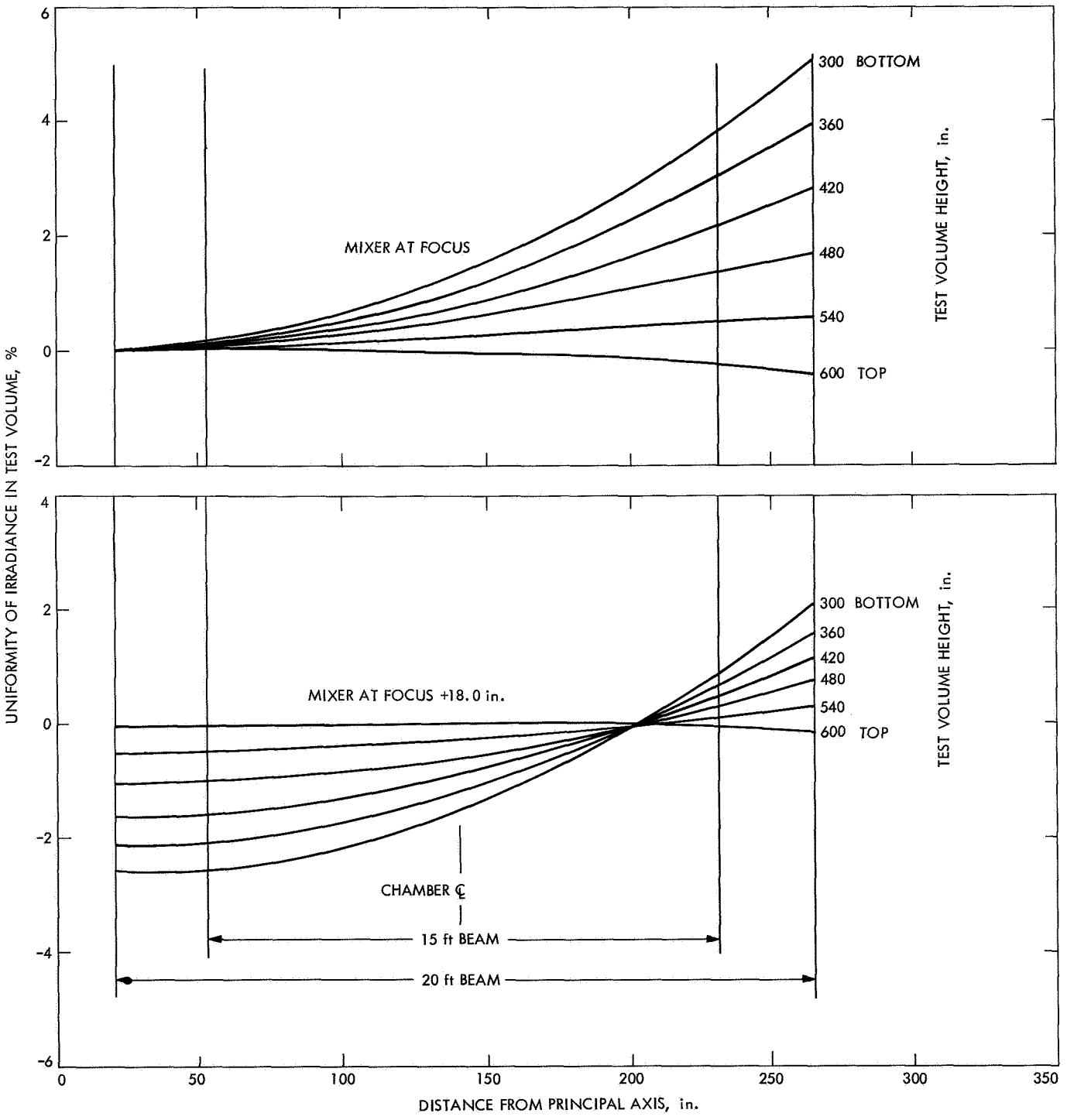


**Fig. 3. Uniformity of irradiance vs mirror location**

**Fig. 4. 23-ft mirror in hoisting position**

The uniformity of the irradiance in the test volume is highly dependent on the quality of the collimating mirror. Once the spherical aberration has been minimized and the uniformity of the irradiance at the collimator plane has been optimized by the mixer lens array, then every effort must be made to have uniform, high reflectivity and minimum slope deviation — or minimum gap size, in the case of segmented mirrors. The effects of slope deviation and gap size are a function of collimation angle of the system and become more pronounced as the collimation angle becomes smaller. The SS15B system was designed for a 1-deg collimation half-angle, which fact made the one-piece design more practical.

## III. Transmission Optics

### A. Description

The transmission optics, housed in an extension of the solar hood, consist of an integrating lens system and a vacuum interface window lens. The integrating lens system, because of its weight and size, is mounted on a carriage that is electrically operated and retractable from the light beam to the maintenance position (Fig. 5). The mixer carriage is fully adjustable for focus and positioning on the optical axis and is capable of expansion to handle a 30-in.-diam integrating lens assembly. The entire assembly is water-cooled (Fig. 6) and is partially shielded by a water-cooled aperture that blocks off all the energy from the lamps not directed at the entrance optics.

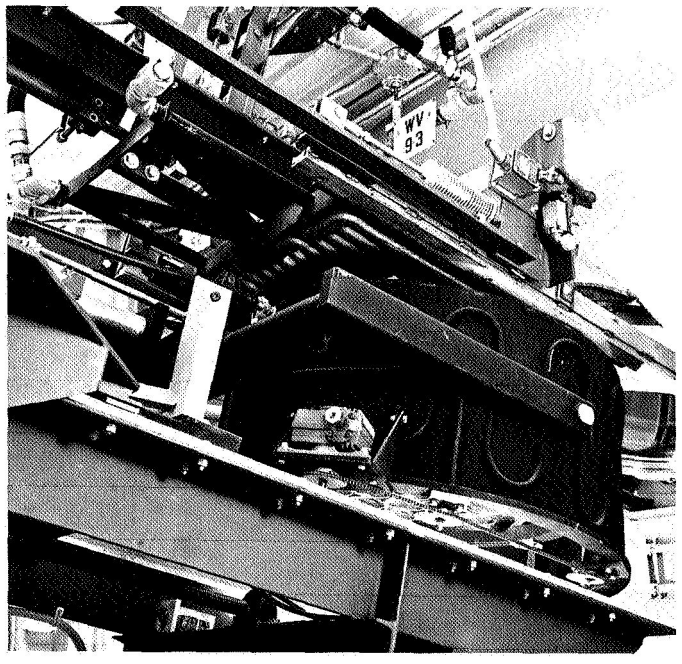


**Fig. 5. Lens carriage, safety door, and window lens**

There is a safety or tare door that operates between the integrating lens system and the window lens to seal tightly against the window lens opening. This door is water-cooled and designed to absorb the heat load of the entire solar simulator. It can be used to provide safe access to the lens room when the chamber is under vacuum or to operate the solar simulator without light in the test volume for simulating eclipses or taking radiometer tare measurements. The safety door is air operated either from the console or from the lens room and is safety-interlocked with mechanical, as well as electrical, stops.

There is a maintenance platform that can roll in or out of the optical path to form a solid floor beneath the lens system. When the safety door and lens carriage are retracted, the maintenance platform can be rolled in to give full standing access for two men at the window lens. The maintenance platform is interlocked with the solar hood blower to prevent low-pressure implosion of the filter housing in event the platform were to block off the air flow. Since it is not cooled, it is also interlocked with the lamp-operating system such that the platform must be completely stowed before any lamps can be operated.

### B. Design of Transmission Optics

The transmission optics of the SS15B system present an interesting problem from a thermal, as well as an optical, design point of view. Since all of the energy in the test volume must pass through a single aperture, a thermal bottleneck, with resulting high-flux densities, develops at the mixer lens system. Tests conducted with a prototype collector and 20-kW lamps at rated power (Ref. 5) demonstrated peak flux levels of 13.5 W/in.$^2$ and an energy distribution roughly cosine shaped, as shown in Fig. 7, for a single lamp. The power that passed through the SS15B aperture for these flux levels was approximately 3900 W/lamp. An estimate of the maximum expected flux levels and power through the mixer can be obtained by multiplying these numbers by the maximum system-design parameters:

$$\Phi_{max} = 13.5 \frac{\text{W}}{\text{in.}^2\text{-lamp}} \times 61 \text{ lamps} \times \frac{30}{20} = 1{,}235 \frac{\text{W}}{\text{in.}^2}$$

$$\text{or } 6.05 \times 10^5 \frac{\text{Btu}}{\text{h-ft}^2}$$

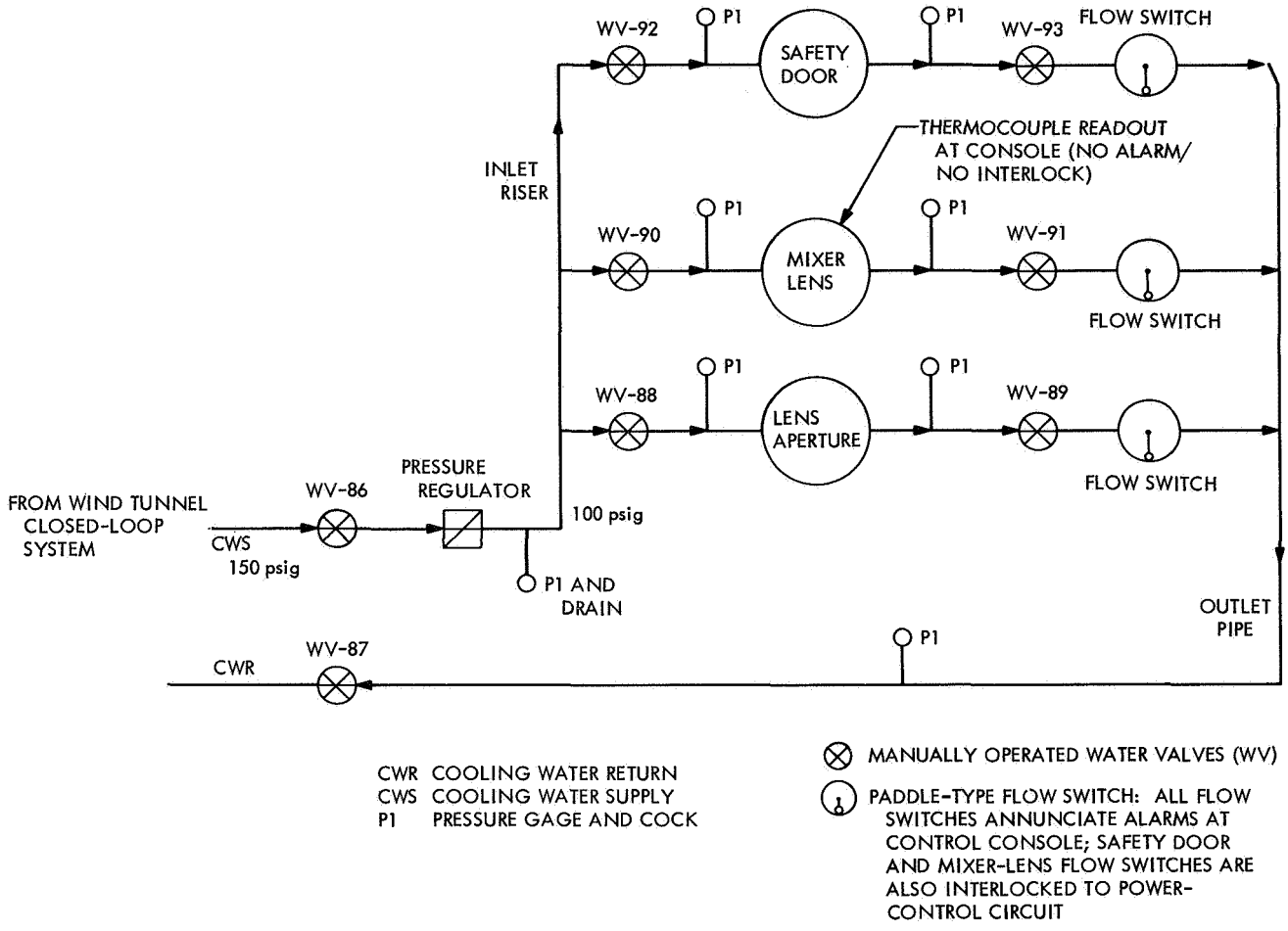


**Fig. 6. Lens room water schematic**

$$P_{max} = 3900 \frac{W}{\text{lamp}} \times 61 \text{ lamps} \times \frac{30}{20} = 357{,}000 \text{ W}$$

$$\text{or } 1.22 \times 10^6 \frac{\text{Btu}}{\text{h}}$$

Lamp-power output has been demonstrated to vary linearly with input power for the range examined.

Several studies and lens-mounting designs were accomplished for the type A solar simulator at JPL. The testing, which was conducted at flux levels approximately 20% of the expected levels in the SS15B system, demonstrated that uncooled metal lens-supports subjected to direct radiation were unsuitable. A 19-element lens system, supported at the edge and maintained in position by sapphire balls at the intersection of the lenses, was developed which has proven satisfactory for use in the smaller A-type system, but was not considered for use in the B system for the following reasons:

(1) The high level and nonuniformity of the flux distribution at the mixer aperture makes it extremely difficult to calculate the combined thermal-structural stress levels of a 19-element lens matrix.

(2) The tolerances, fitting, and support of such a lens system would make the resulting cost high.

(3) There would be considerable risk involved in a failure of such a lens system located above the lamp array.

The lens-support system chosen for the SS15B system is a water-cooled, chrome-plated, copper block, suitably machined to accept the lenses with an 0.07-in. copper web between lenses. The losses associated with this type of support system are only 3.5% over that of a system with lenses in direct contact (Fig. 8). The shape of the simulator beam is determined by the shape of the condenser lens aperture. A circular lens aperture was chosen for the SS15B system because of the limiting aperture of

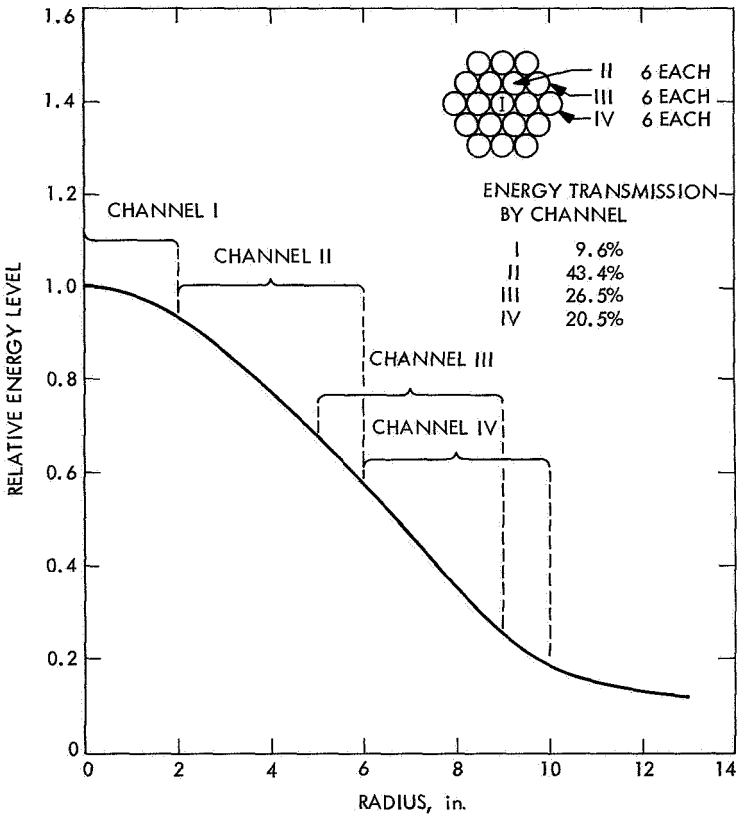


**Fig. 7. Energy distribution and transmission through the mixer aperture**

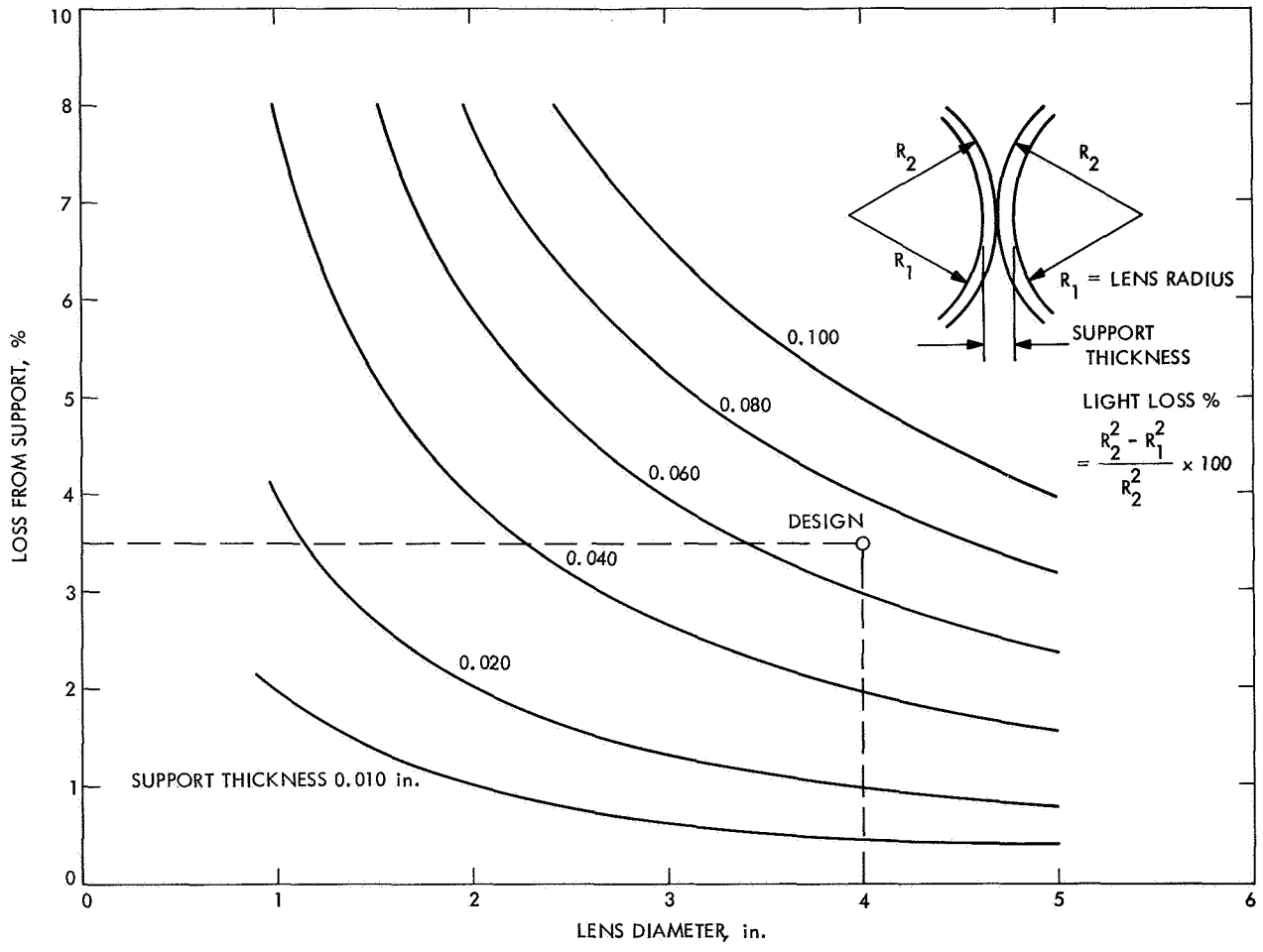


**Fig. 8. Mixer-support light loss**

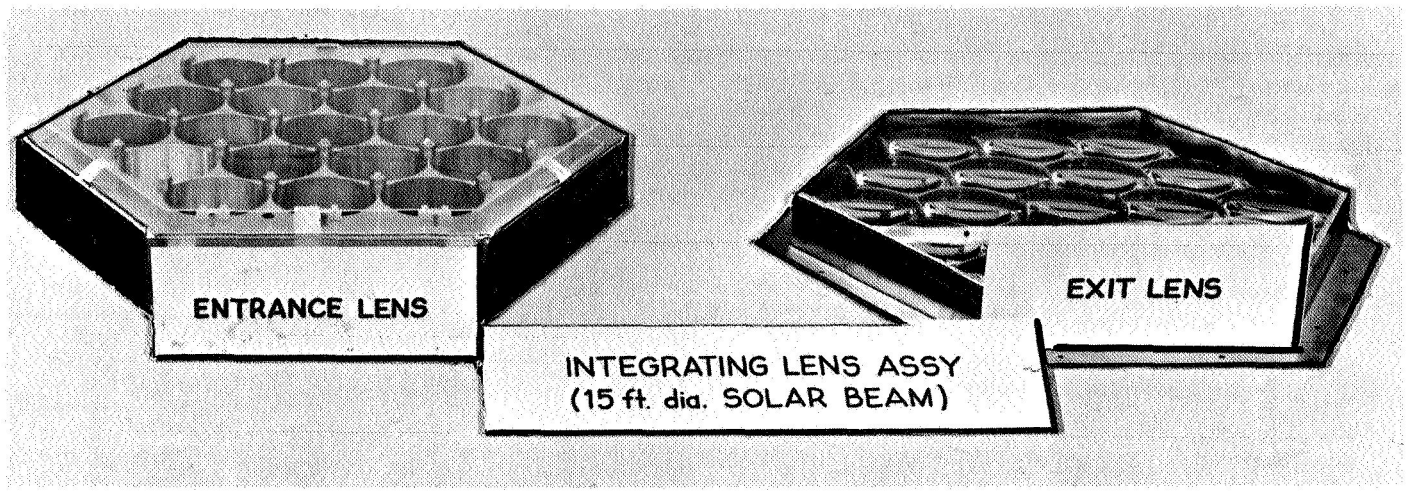


**Fig. 9. SS15B holder**

the 23-ft collimating mirror in projecting the maximum 20-ft-diam beam.

Figure 9 shows the water-cooled condensing lens holder and the air-cooled projection lens holder. The projection lens holder is fixed rigidly to the top of the lens carriage. The condensing lens holder is mounted in the lens carriage below the projection lenses on an elevator-type mount, which allows minor focal length adjustments between the two 19-element lens arrays for various mixer configurations. All the lenses are manufactured from Corning 7940, optical-grade fused silica in the shapes shown in Fig. 10.

The original lens support for the SS15B system was designed to accommodate the energy required for an operational earth constant (133 W/ft$^2$) at the test volume. The center portion of the copper lens holder is conductively cooled to a water passage along the outer periphery. The lens holder is necessarily limited to temperatures below 600°F because, above those temperatures, the chrome plating would oxidize and the holder would get progressively hotter. Figure 11 shows the maximum lens support temperatures achieved during system tuning and calibration testing.

A more sophisticated lens support design has recently been completed which will accommodate the full thermal load of the potential sixty-one 30-kW lamps (Fig. 12). This water-cooled, stainless-steel tubing braze-ment will directly cool all portions of the lens support and provide the following advantages:

(1) The existing lenses can be utilized.

(2) The energy transmission losses due to web thickness are eliminated.

(3) The design is adaptable to a wide range of beam sizes and test volume irradiance levels.

The window lens is also manufactured of Corning 7940 fused silica. It is mounted directly onto the vacuum seal, silicone rubber O-ring and Teflon cushion pad to provide uniform edge support. To prevent excess strains or chipping, the window is fully cushioned with silicone rubber pads and a mounting ring (Fig. 13). The focal length of the window lens is 724.0 $\pm$ 12 in. — plano-convex with the plane side towards the vacuum.

Figure 14 shows an optical schematic of the SS15B solar simulator with object and image sizes and interlens distances. Figure 15 is the optical alignment drawing for the 25-ft space simulator modification and shows the relationship of the various optical elements to the vacuum chamber. For a general description and history of this type of system see also Ref. 2.

### C. Mixer Lens Aberration and Uniformity

The primary function of the mixer lens system is to improve the uniformity of irradiance in the test volume.

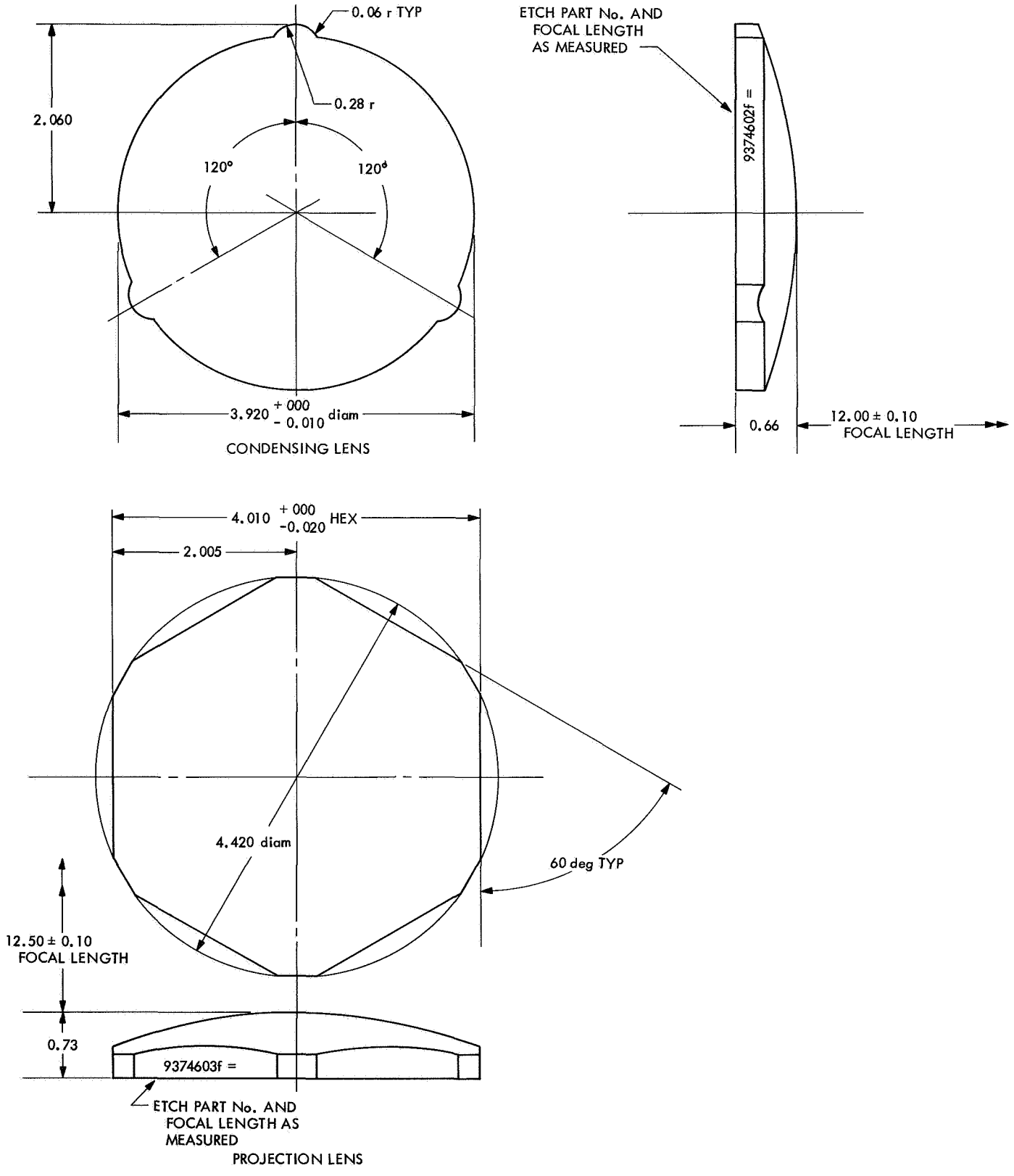


**Fig. 10. Condensing and projection lens shapes**

This is accomplished by dividing the energy at the mixer aperture into a number of symmetrical beam channels, which are then integrated into a single beam at the test volume. Theoretically, a greater number of lens channels will produce a more uniform beam, but there are practical limitations on the number of lens elements to be used. Figure 16 shows the theoretical uniformity that is possible by dividing and integrating the energy available at the SS15B mixer aperture with 19 symmetrical lens channels. The 3.5% uniformity is obtained with more than 50% of the total energy passing through the center seven lens channels. The positive distribution of channels I, II, and III are not balanced by the negative distribution of channel IV; other methods must be found to further improve the test volume uniformity.

If the energy distribution at the mixer aperture were flat, the theoretical uniformity obtained from a properly designed mixer lens system might be good, but this requires a stable light source and a rather sophisticated collector design, which is not as efficient as an elliptical figure for passing energy through the system aperture. Other methods, such as selective zonal transmission of lens elements or reflectivity of the collimator, could be considered if overall efficiency of the system could be ignored.

A technique of improving the test volume uniformity, which was accidentally discovered during the assembly and tuning of the SS6A system at JPL, involves use of the aberration properties of the condensing lens elements in the mixer lens assembly. By inverting the condensing lenses with respect to the projection lenses, it is possible to cause a shift in the uniformity at the condensing lens exit pupil, which is at the focus of the projection lens. Figure 17 shows how the test volume uniformity in the SS15B system is altered by incremental and symmetrical changes in the condensing lens orientation of various lens channels. It should be noted here that symmetrical orientation produces symmetrical changes in test volume uniformity. Also, this change in test volume uniformity is accomplished without efficiency losses because the energy transferred through the mixer lens channels is merely redistributed. Note that the waviness in the Fig. 17 curves is due to the variations in collimator reflectivity (see Section VII).

Confirmation of this empirical system turning data and a better understanding of the mechanism of change involved was accomplished by using existing JPL computer ray-trace programs (Refs. 5, 6). The density of many ray trace points at the exit pupil of the condensing lens

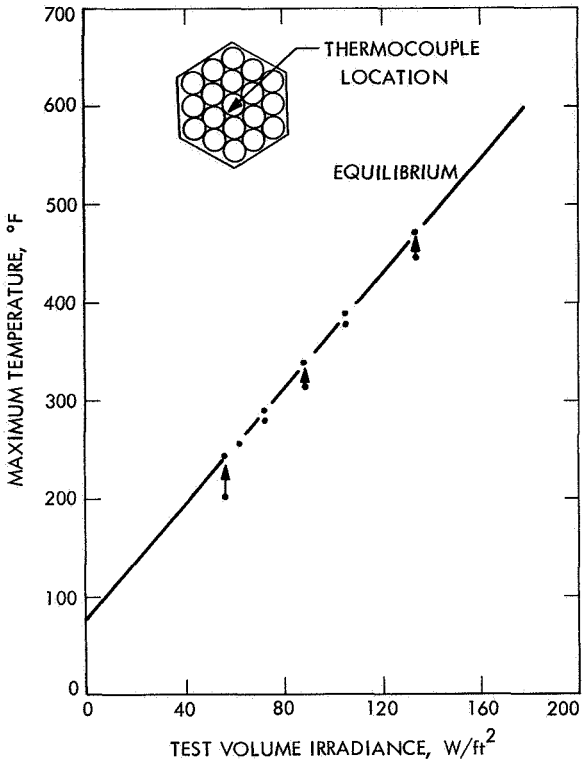


**Fig. 11. Lens holder temperature vs test volume irradiance**

through a uniform field at the entrance pupil was used to calculate the uniformity at the exit pupil field. The field uniformity at the condensing lens exit pupil is projected to the collimator and to the test volume and directly affects the test volume uniformity. Figure 18 shows the magnitude of change at the condensing lens exit pupil due to the inversion of the plano-convex (spherical) lens element used in the SS15B system.

Although it has not yet been tried in the SS15B system, there are two possibilities that seem evident from this study:

(1) The condensing lens elements can be designed to correct nonuniformities caused by the energy distribution at the mixer aperture and the number of lens elements used.

(2) The test volume nonuniformities due to the spherical aberration of the collimator (see Fig. 3) can be improved by asymmetric utilization of the condensing lens aberration in the mixer lens assembly. Figure 19 shows how diametrically opposed lens channels can be used to accomplish this effect for off-axis systems.

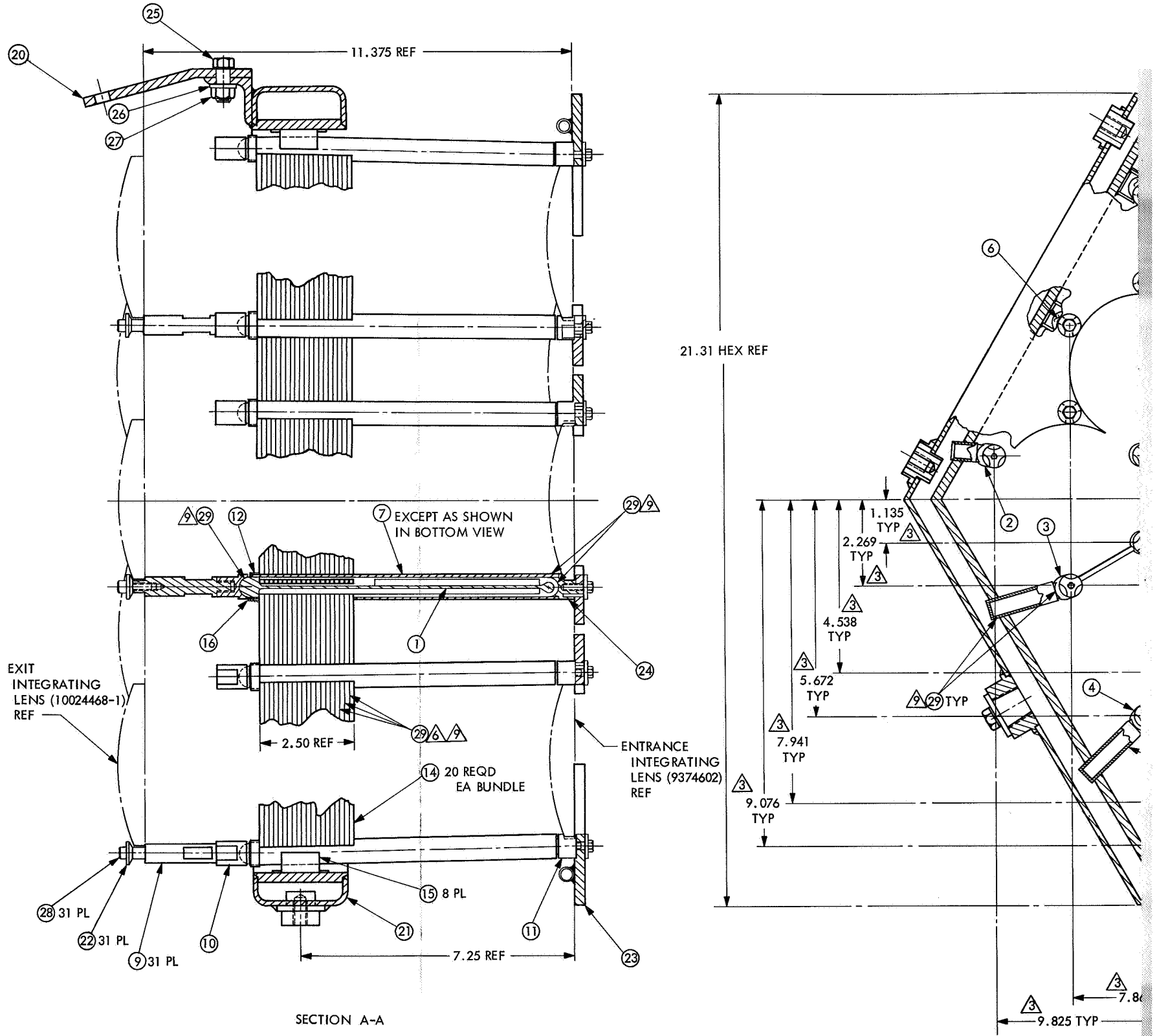
11.375 REF
EXCEPT AS SHOWN IN BOTTOM VIEW
EXIT INTEGRATING LENS (10024468-1) REF
ENTRANCE INTEGRATING LENS (9374602) REF
20 REQD EA BUNDLE
2.50 REF
7.25 REF
31 PL
8 PL
21.31 HEX REF
1.135 TYP
2.269 TYP
4.538 TYP
5.672 TYP
7.941 TYP
9.076 TYP
TYP
9.825 TYP

SECTION A-A

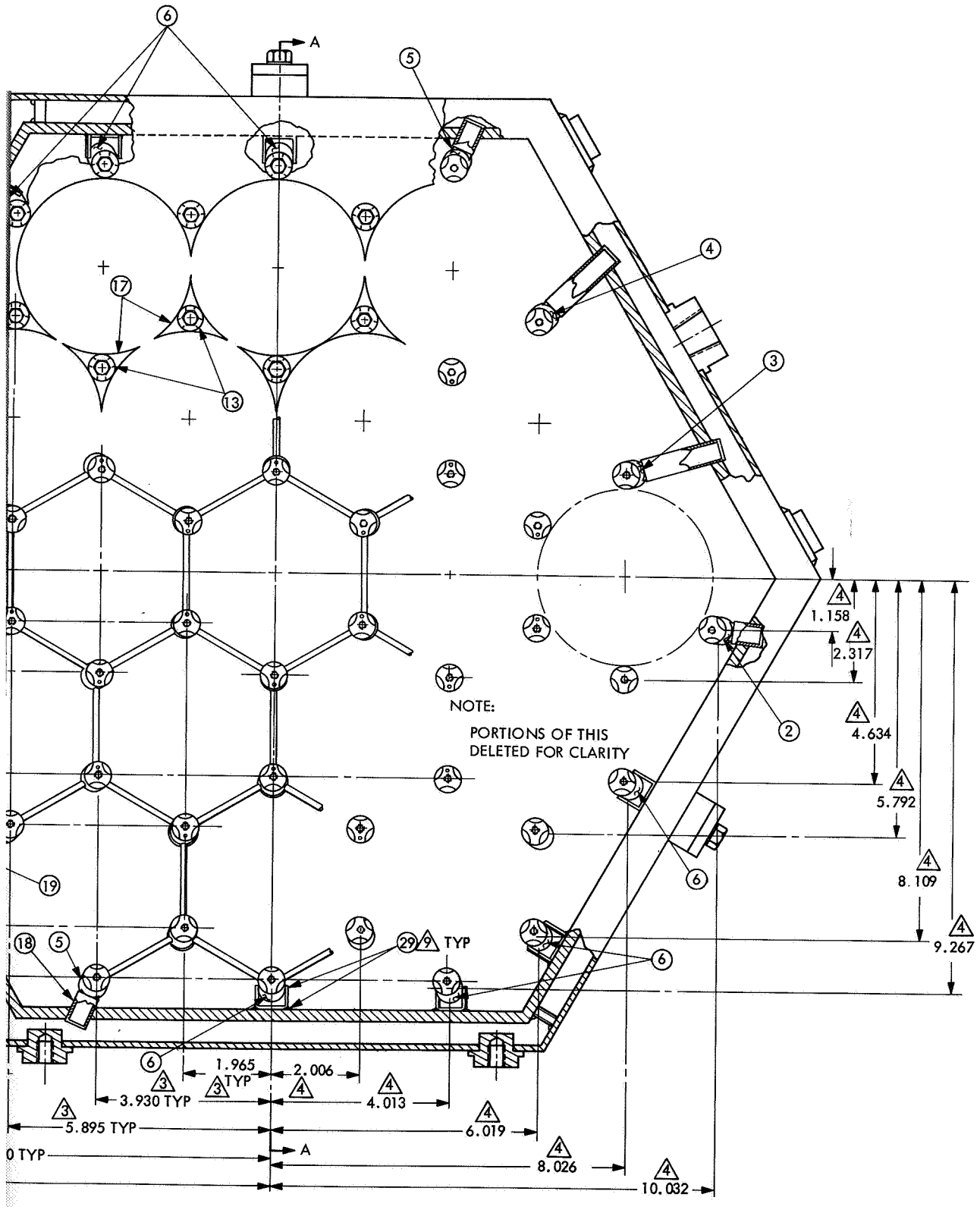


NOTE: (UNLESS OTHERWISE SPECIFIED)

1 REMOVE ALL BURRS AND SHARP EDGES 0.003 MIN - 0.010 MAX

2 MACHINED FILLET RADIUS 0.010 MAX

△3 COORDINATE DIM GIVEN ARE TO THE CENTER LINE OF THE POST ENDS ON NEAR SIDE OF ASSY (TYP 4 QUADRANTS)

△4 COORDINATE DIM GIVEN ARE TO THE CENTERLINE OF THE POST ENDS ON FAR SIDE OF ASSY (TYP 4 QUADRANTS)

5 BOTTOM LENSES HAVE A NOMINAL 0.010 CLEARANCE BETWEEN EACH LENS WHEN INSTALLED IN SUPPORT ASSY

△6 BRAZE EACH TUBE BUNDLE WITH A MINIMUM OF 50% BOND BETWEEN TUBES

△7 PASSIVATE ITEMS (2) THRU (7), (10), (12), (14), (15) (16), (18), AND (19) PER JPL SPEC GMO-50295-PRS AFTER MACHINING AND PRIOR TO BRAZING, POLISHING, AND PLATING

△8 TOLERANCES AT BRAZED JOINTS TO BE SPECIFIED BY THE BRAZING MANUFACTURER

△9 BRAZE ALLOY TO BE SPECIFIED BY BRAZING VENDOR. NO BRAZING ALLOYS TO BE USED WITH A MELTING TEMP BELOW 400°F

△10 STRESS RELIEVE TUBES (2) THRU (7) PRIOR TO MACHINING SLOTS

△11 DIMENSIONS AND TOLERANCES OF SLOTS IN ITEMS (2) THRU (7) TO BE SPECIFIED BY BRAZING VENDOR

△12 ELECTROPOLISH ITEM (9)

△13 POLISH AND CHROME PLATE ASSY PER FEDERAL SPEC QQ-C-320, CL 2 AFTER BRAZING EXCEPT SURFACES INDICATED NP DO NOT PLATE ITEMS (1), (9), (20), (22), (25), (26), (27), AND (28)

14 FINAL ASSY TO BE CERTIFIED PRESSURE CHECKED AT 200 psig WATER. NO LEAKS PERMITTED

15 IDENTIFY PER JPL SPEC FS 500451

**Fig. 12. Mixer lens support assembly, Mark II**

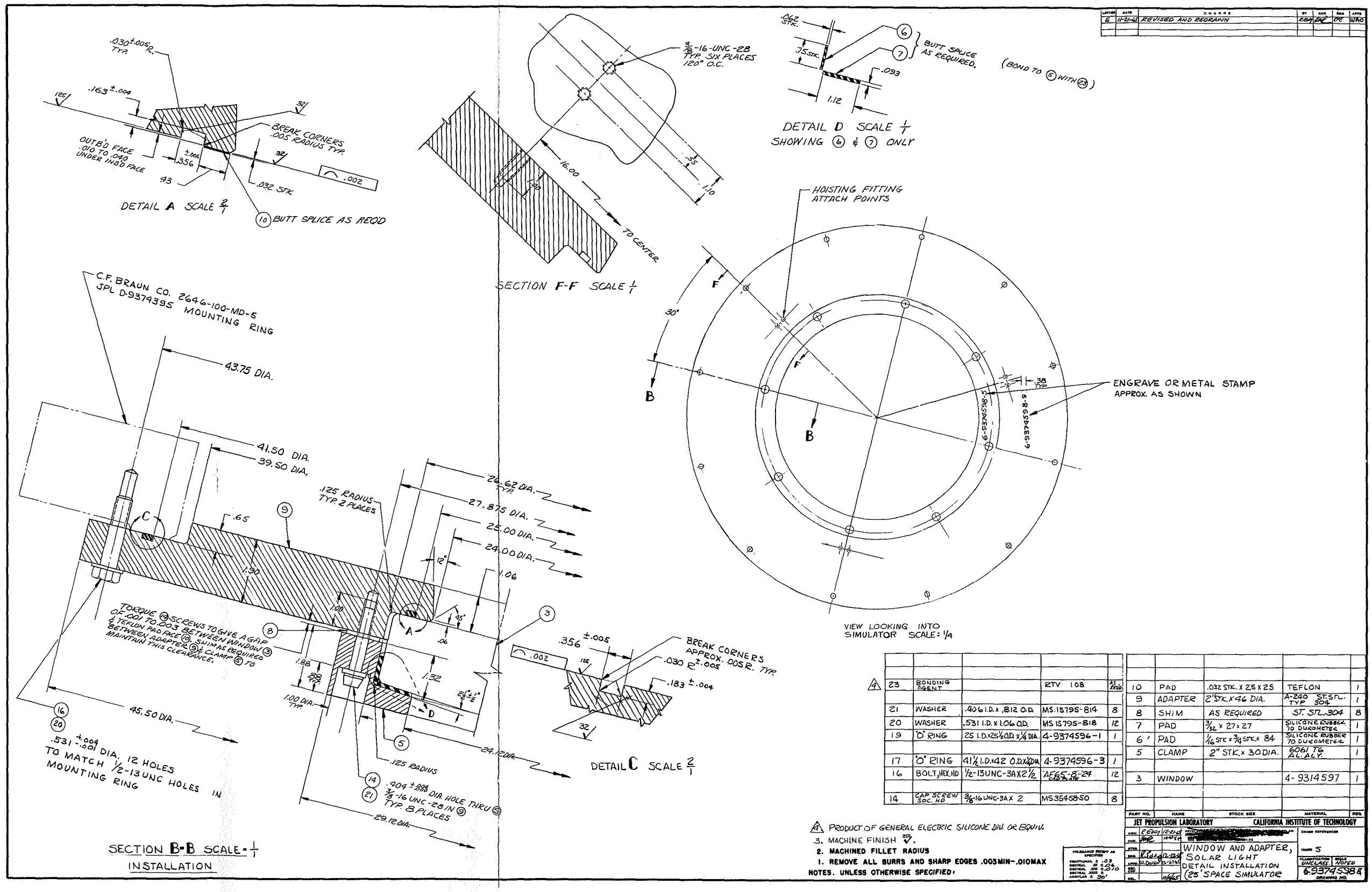


| LETTER | DATE | CHANGES | BY | CHK | Engr | APPR |
|---|---|---|---|---|---|---|
| E | 11-21-66 | REVISED AND REDRAWN | [redacted] | [redacted] | PE | WKO |

| | | | | | |
|---|---|---|---|---|---|
| 4 | 23 | BONDING AGENT | | RTV 108 | AS REQD |
| | 21 | WASHER | .406 I.D. x .812 O.D. | MS 15795-814 | 8 |
| | 20 | WASHER | .531 I.D. x 1.06 O.D. | MS 15795-818 | 12 |
| | 19 | "O" RING | 25 I.D. x 25¼ O.D. x ¼ DIA. | 4-9374596-1 | 1 |
| | 17 | "O" RING | 41½ I.D. x 42 O.D. x ½ DIA. | 4-9374596-3 | 1 |
| | 16 | BOLT, HEX. HD | ½-13UNC-3A X 2½ | AF65-8-24 | 12 |
| | 14 | CAP SCREW SOC. HD | ⅜-16 UNC-3A X 2 | MS 35458-50 | 8 |

| | | | | |
|---|---|---|---|---|
| 10 | PAD | .032 STK. X 25 X 25 | TEFLON | 1 |
| 9 | ADAPTER | 2" STK. X 46 DIA. | A-240 ST. STL. TYP 304 | 1 |
| 8 | SHIM | AS REQUIRED | ST. STL. 304 | 8 |
| 7 | PAD | 3/32 x 27 x 27 | SILICONE RUBBER 70 DUROMETER | 1 |
| 6 | PAD | 1/16 STK. x 3/4 STK. x 84 | SILICONE RUBBER 70 DUROMETER | 1 |
| 5 | CLAMP | 2" STK. x 30 DIA. | 6061 T6 AL. ALY. | 1 |
| 3 | WINDOW | | 4-9314597 | 1 |

PART NO. | NAME | STOCK SIZE | MATERIAL | REQ.

NOTES. UNLESS OTHERWISE SPECIFIED:
1. REMOVE ALL BURRS AND SHARP EDGES .003 MIN-.010 MAX
2. MACHINED FILLET RADIUS
3. MACHINE FINISH 63 √.
4 PRODUCT OF GENERAL ELECTRIC SILICONE DIV. OR EQUIV.

TOLERANCE EXCEPT AS SPECIFIED
FRACTIONAL ± .03
DECIMAL .XX ± .25
DECIMAL .XXX ± .070
DECIMAL .XXXX ± .30'
ANGULAR ± 30'

JET PROPULSION LABORATORY — CALIFORNIA INSTITUTE OF TECHNOLOGY

| | | | |
|---|---|---|---|
| DRAWN | E Eng | 12-21-66 | |
| CHK | [redacted] | 12-21-66 | |
| ENGR | [redacted] | | |
| SUPV | [redacted] | | |
| APPR | [redacted] | 12-21-66 | |
| MGR | [redacted] | | |
| REL | | 1/19/65 | |

ENGR DISTRIBUTION
ISSUE S

WINDOW AND ADAPTER, SOLAR LIGHT DETAIL INSTALLATION (25' SPACE SIMULATOR

CLASSIFICATION (UNCLASS.) MARK NOTED
DRAWING NO. 6-9374598-4

**Fig. 13. Window lens and adapter**

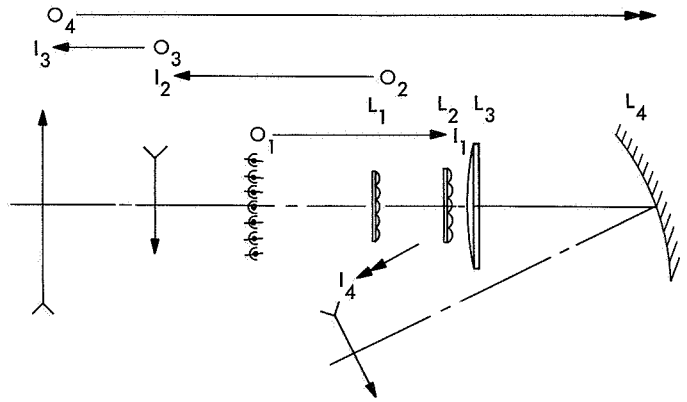


O = OBJECT
I = IMAGE
$O_1$ = LAMP ARRAY (37 ea)
$L_1$ = CONDENSING LENS (19 ea)
$L_2$ = PROJECTION LENS (19 ea)
$L_3$ = WINDOW LENS
$L_4$ = COLLIMATOR SURFACE
$O_2$ = EXIT PUPIL OF $L_1$
$I_4$ = TEST VOLUME RE-IMAGE PLANE

**Fig. 14. SS15B optical schematic**

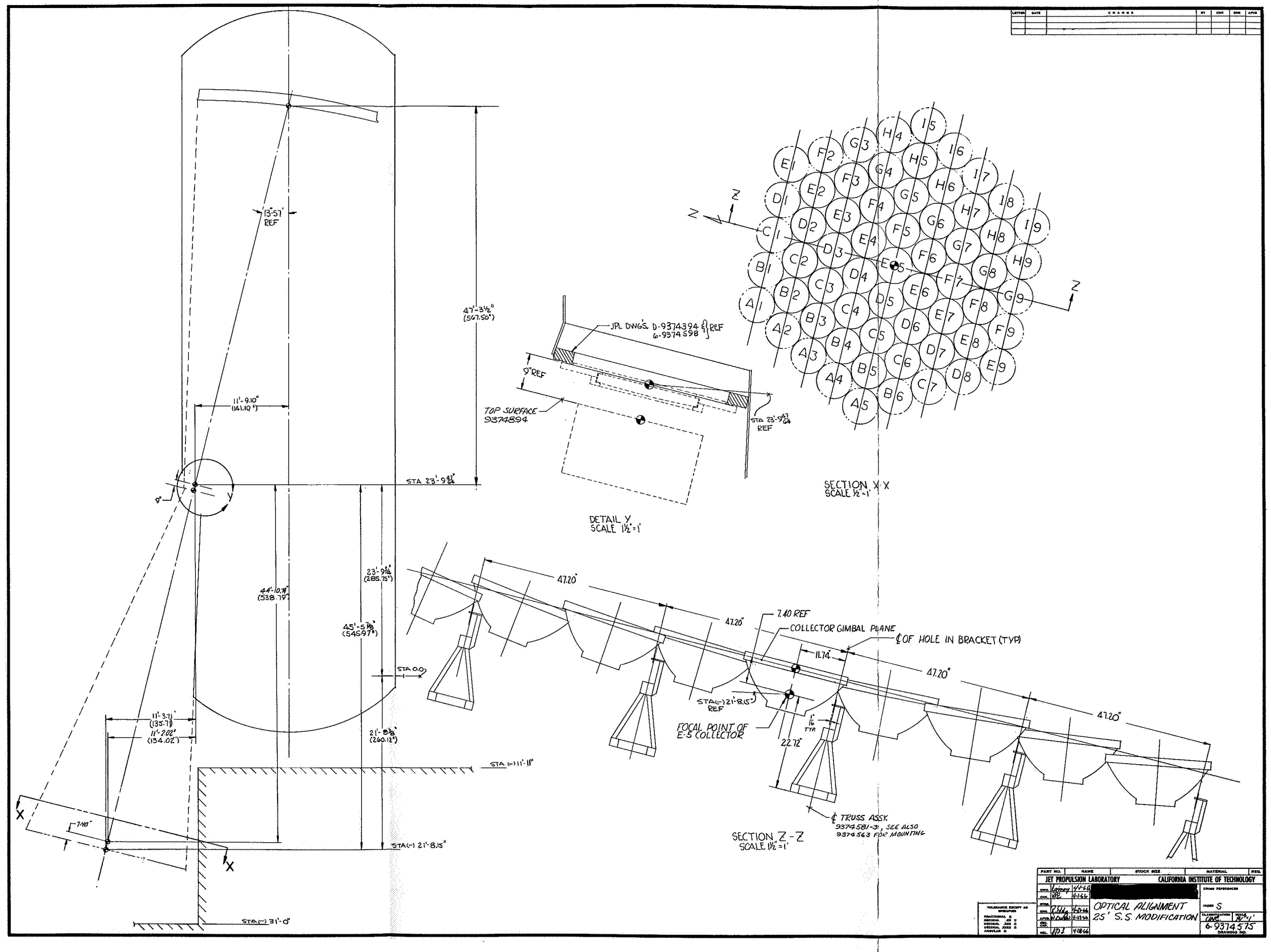


**Fig. 15. Optical alignment—24-ft space simulator modification**

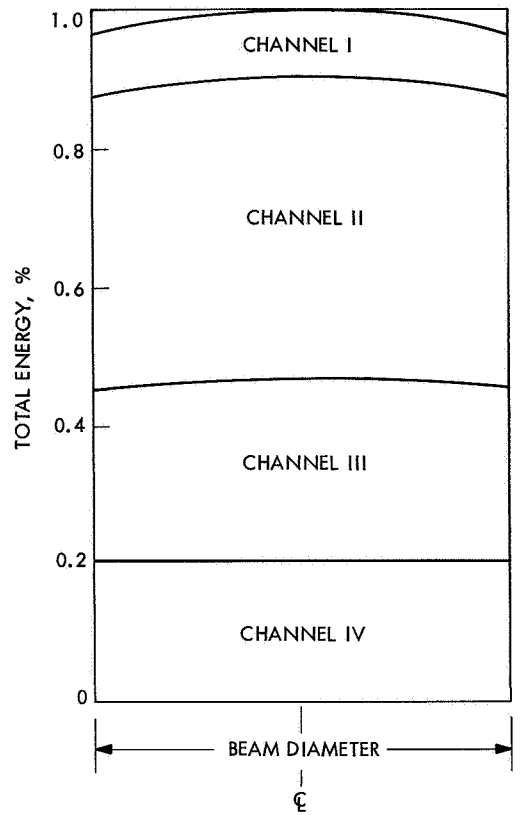


**Fig. 16. Uniformity contribution by lens channel**

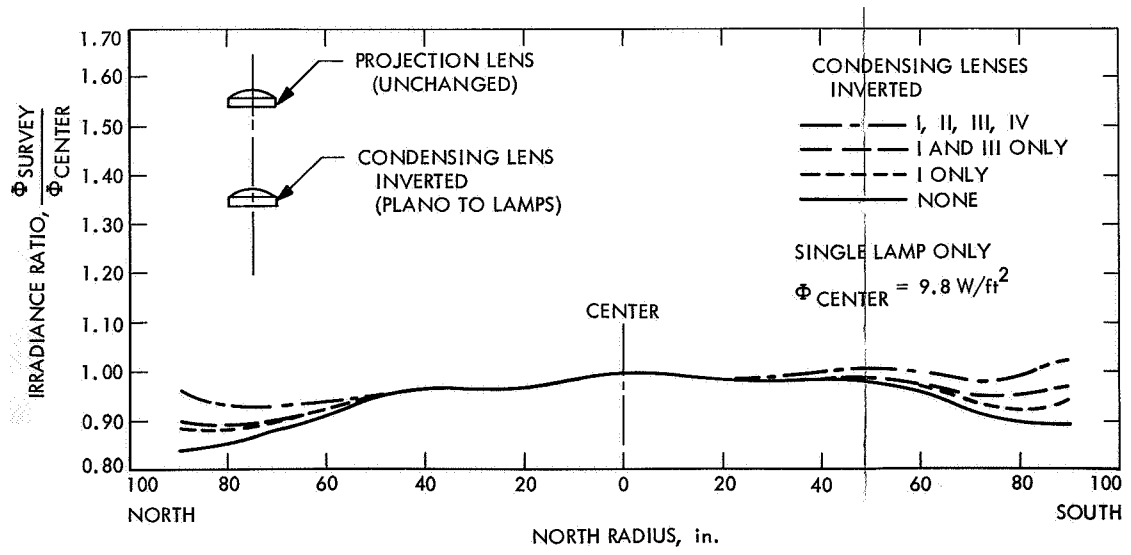


**Fig. 17. Test volume uniformity vs lens inversion**

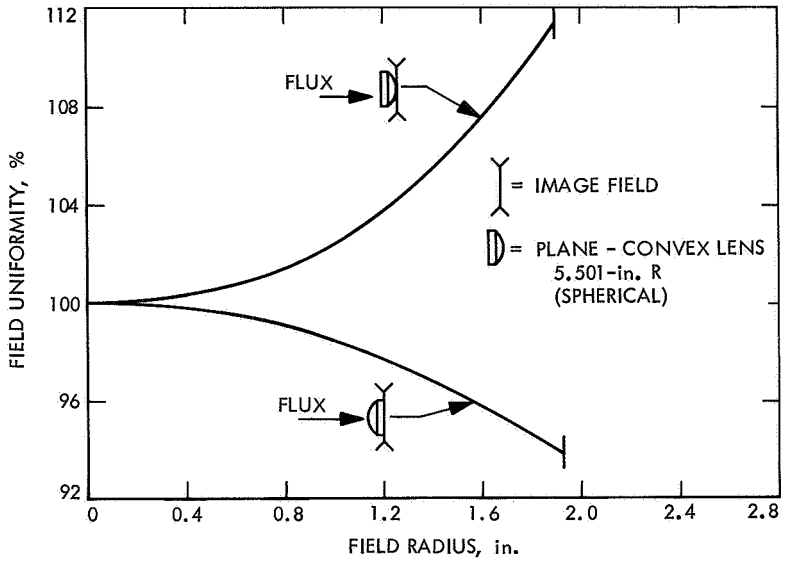


**Fig. 18. Field uniformity vs field radius**

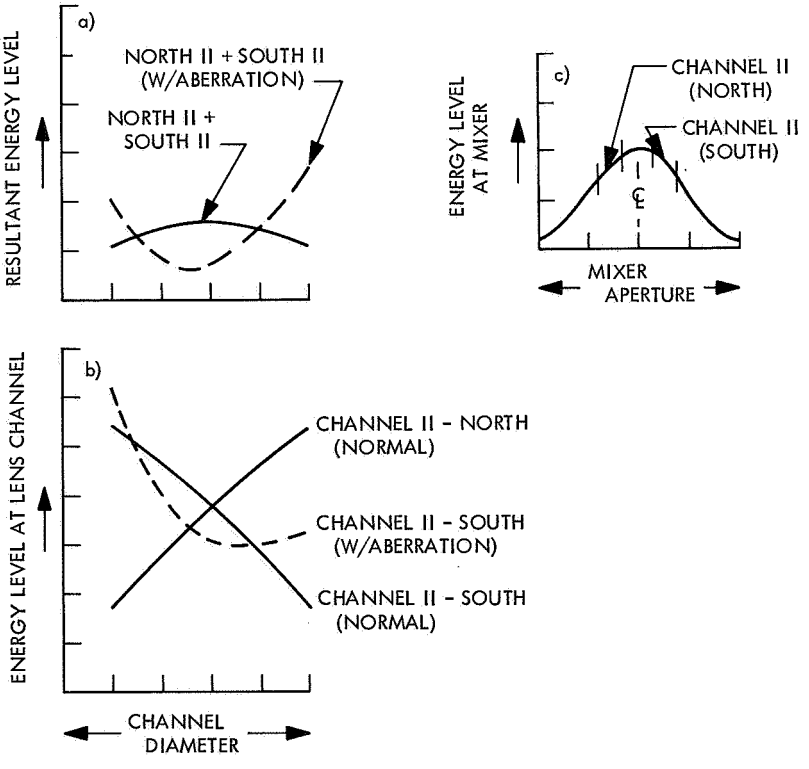


**Fig. 19. Asymmetric utilization of lens aberration**

## IV. Light Sources

### A. Description

The light source for the SS15B solar simulator is provided by a hexagonal array of thirty-seven 20-kW compact xenon arc lamps located in a special lamp basement below the entrance optics. The lamp basement provides an enclosure for the lamps and their related hardware; it is pressurized at about 1 in. of water above atmospheric pressure to provide a cleanroom-type environment for the lamps and optics. An airlock is provided at the basement entrance to maintain the required overpressure in the lamp area.

The lamp array is completely enclosed by a solar hood on the top and air baffles on the outside to provide cooling air flow through the lamp array. The solar hood extends from the lens room all the way down to the second floor of the lamp basement. At this level, a view port is provided to visually observe the condition of the lamps during operation (Fig. 20). The solar hood is lined with an air-cooled stainless-steel radiation shield from the level of the lamps to a height of 20 ft to keep the outside solar hood temperature down when the lamps are operating.

The second floor of the lamp basement also encloses the lamp electrical power conduit wiring and busses. A special area is provided along the east and west walls to isolate the high-voltage ignition portion of the lamp circuit, which consists of individual lamp ignitors, contactors, and negative bus feeders. Access to this area is restricted during system operation.

The third floor basement contains the mechanical support structure for the lamps and their hardware. The basic support structure consists of five trusses which run the full width of the basement. These trusses are designed to perform several functions in that they support the collector gimbals, contain integral water cooling paths for the collector cooling and act as an isolating conduit for the high-voltage, negative lamp feeder busses. The base of the trusses supports the individual lamp coolant shutoff solenoids and control wiring.

The lamp collectors are mounted in their individual gimbal mounts to permit aiming the collectors toward the system aperture. The gimbals are located at 60-deg intervals rather than the customary 90-deg to permit close packing of the collectors. The gimbal mounts are designed to permit the collectors to be rotated upside

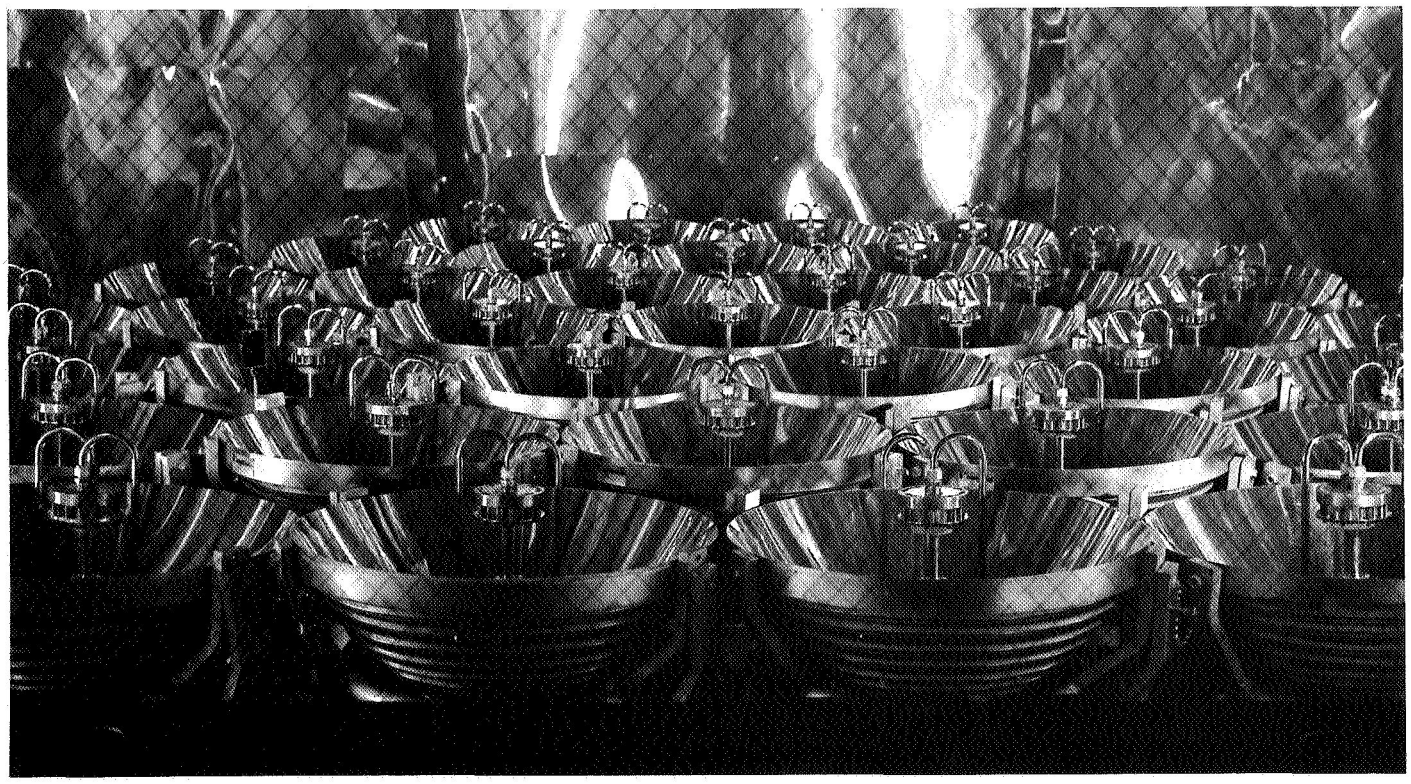

**Fig. 20. Installed lamps and collectors through viewport**

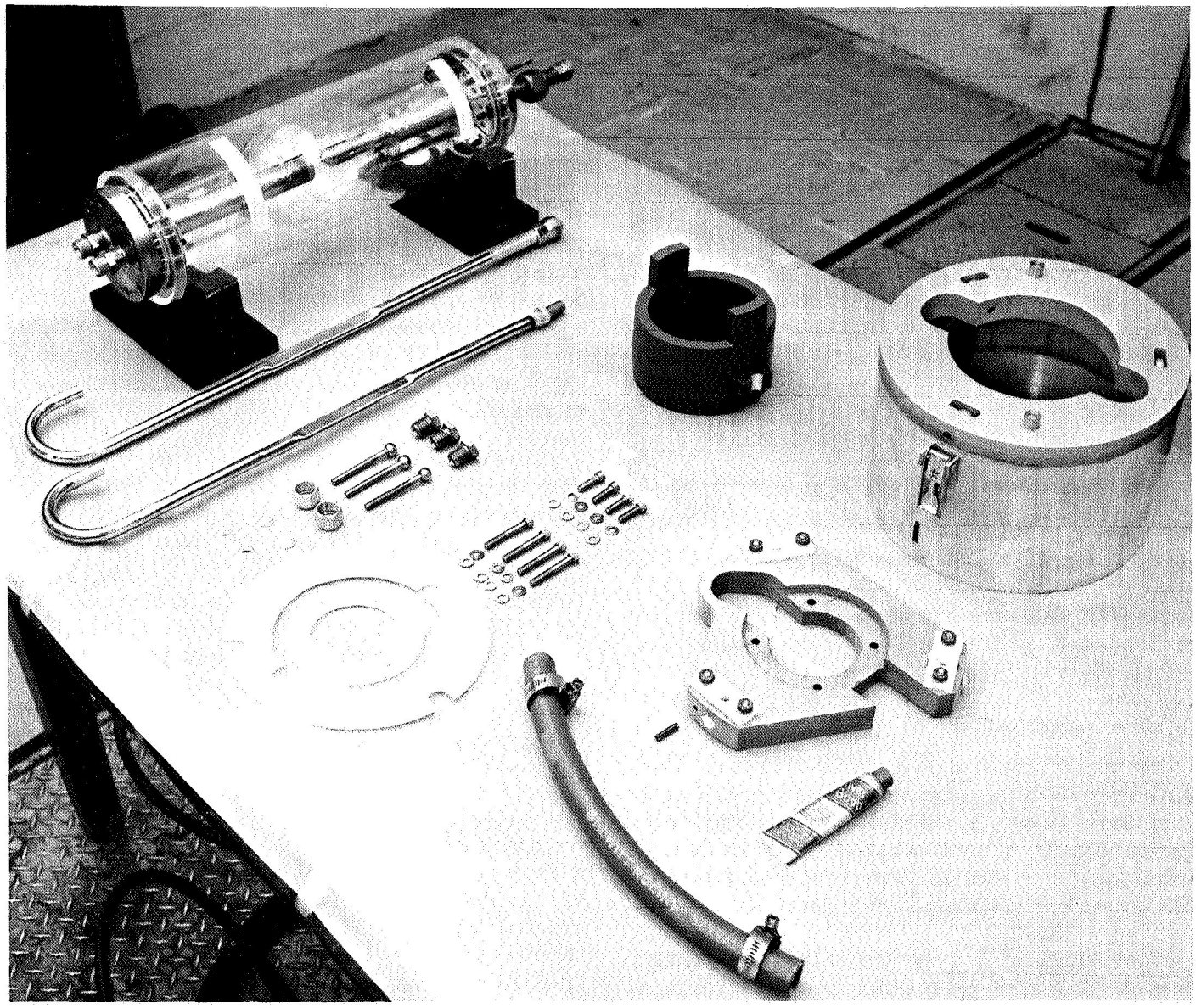

**Fig. 21. Lamp mount (disassembled)**

down for cleaning or maintenance in place from the ground level so that access in the lamp hood area is unnecessary.

The lamp is contained in an adjustable mount that is fastened directly to the rear of each collector with two quick-disconnect fasteners (Fig. 21). Each lamp is prefocused for its particular collector, and each mount and collector are maintained in alignment with respect to each other by accurately located dowel pins. The focus of each collector varies slightly, and a record is maintained for the coordinates of the focus located from the mating dowel pins and interface surface. Each mounted lamp is then accurately prealigned to its particular collector before being installed.

Installation and removal of the mounted lamp is done from below the array. The lamp is drawn directly through the base of the collector. Since the water coolant is contained in the electrical system, there are only two hoses to make or break per lamp installation.

The lamp is cooled with the water going through the anode and cathode in series. A 12-in. dielectric hose (Fig. 22) separates the anode and the cathode electrically. The conductivity of the coolant is maintained

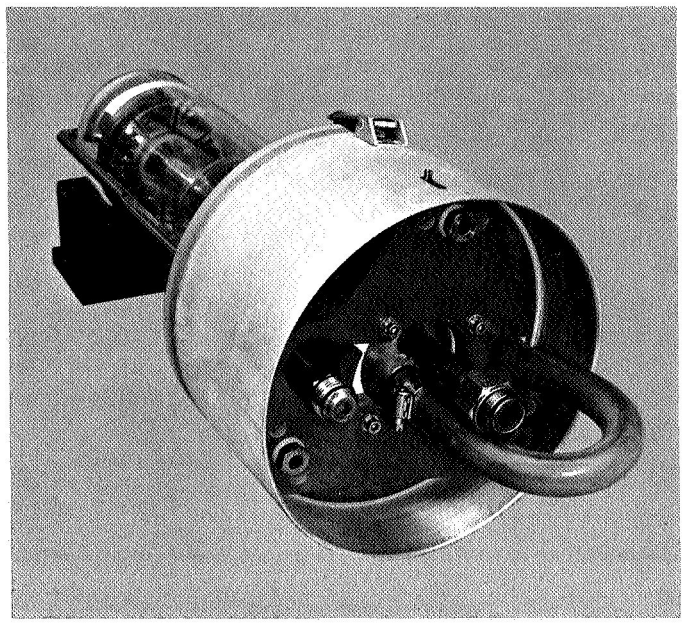

**Fig. 22. Mounted lamp (bottom view)**

below 6000 μmhos/cm so that the current flow between the anode and cathode is very low at the operating lamp voltage (50 V).

### B. Lamp Coolant System

The 20-kW lamps used in this system have water-cooled electrodes that remove approximately 40% of the lamp input power. A closed-loop, recirculating water system (Fig. 23) is used to provide water to the individual lamp electrodes. The water used is deionized and filtered and contains a corrosion-inhibitor additive.

In the sequence listed, the flow of the lamp coolant is from the circulating pump outlet to the rectifier room, lamp array, gas separator, header tank, water-to-water heat exchanger, filter, and returns to the pump inlet. In detail, starting at the pump outlet, the water flows through a throttling valve and then to the rectifier room. At the rectifier room it is discharged into a 4-in.-square copper electrical bus with ½-in. walls, and becomes integral with the positive side of the lamp electrical circuit. The water flows through the common, positive bus down to the third floor basement level where it enters the lamp inlet manifold located around the lamp array.

Between the lamp inlet manifold and the lamp outlet manifold, there is a bypass gate valve and an accumulator tank (Fig. 24). The purpose of the accumulator is to relieve the hydraulic shock on the lamp coolant system when the lamp coolant solenoid shutoff valves close.

The lamp manifold branches into 10 separate distribution manifolds that have individual filter screens and drain plugs. Each of these distribution manifolds supplies water to the lamps through a solenoid operated valve and an electrical conducting flexible hose. From the lamp, the water returns through an electrical conducting, flexible hose, a water check valve, a copper pipe bus, water flow switch and dielectric pipe into the return manifold. Downstream of the return manifold are a conductivity probe and instrumentation, which are used to monitor and indicate the condition of the coolant at the control console (Fig. 25). The coolant must be maintained below 6000 μmho/cm to eliminate short-circuiting the lamp electrodes which are cooled in series – anode to cathode.

After the water returns up and out of the basement, it flows through a gas separator system, surge tank, and throttling valve. The surge tank contains about 100 gal of coolant and is equipped with sight gage, burst diaphragms, and relief valves (Fig. 26). The tank is normally pressurized to 20 psig with $N_2$ to reduce the dissolved $O_2$ and $CO_2$ in the coolant system. The throttling valve adjacent to the surge tank is used to provide sufficient pressure to circulate coolant and gasses from the trap through the surge tank. Because the surge tank is the highest part of the lamp coolant system, the coolant is normally serviced at this point, and a 6-in. flange and blanking plate are provided on the top of the tank for this purpose.

From the surge tank, the coolant is piped to the water-to-water heat exchanger located at ground level (Fig. 27). The shell side of the heat exchanger is supplied by the wind tunnel facility cooling tower water which is regulated to 150 psig maximum. There are temperature and pressure probes on all inlets and outlets of the heat exchanger to monitor flows and temperatures. A replaceable-cartridge filter is located between the heat exchanger and the pump inlet to remove all particles from the coolant >50 μm. The filter is protected by a bypass valve set to 25 psig in case of system back pressure buildup due to filter clogging. Pressure gages are used on both sides of the filter to observe the condition of the filter cartridges. A gate valve ahead of the heat exchanger and downstream of the pump may be used to isolate this portion of the system for maintenance of the components.

The pump used to circulate the lamp coolant is an in-line, centrifugal pump driven by a 75-hp electric motor. It is rated for 500 ft head at 250 gal/min

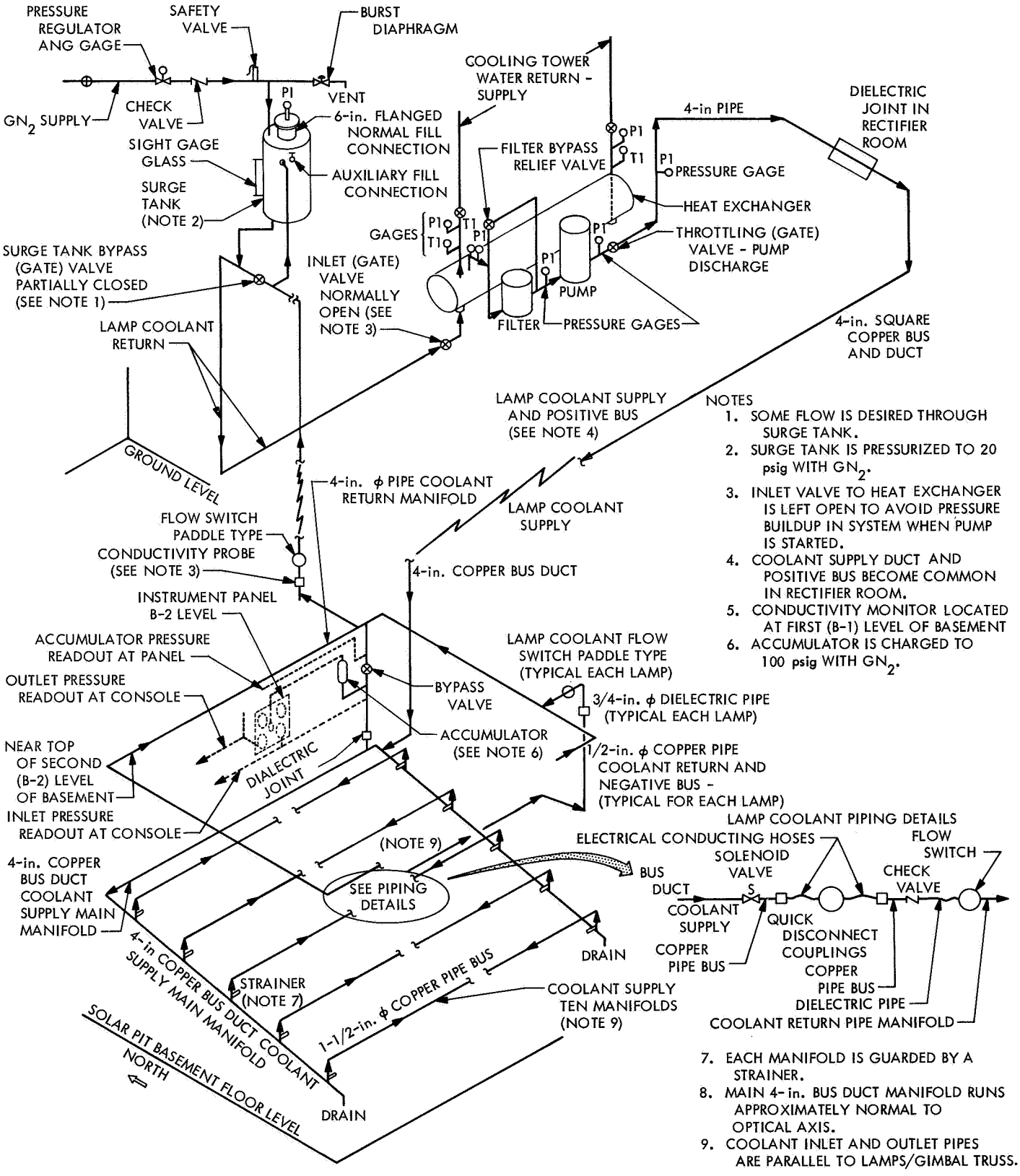


**Fig. 23. Lamp coolant schematic**

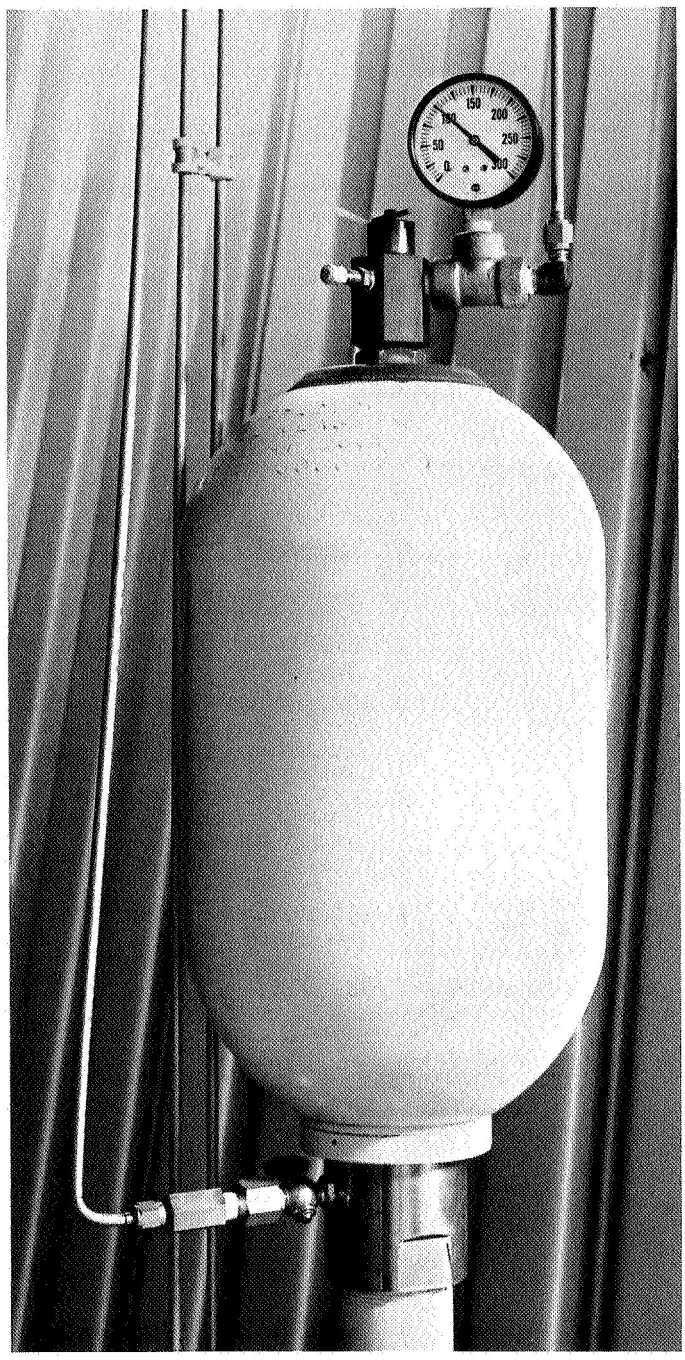

Fig. 24. Hydraulic accumulator, lamp coolant system

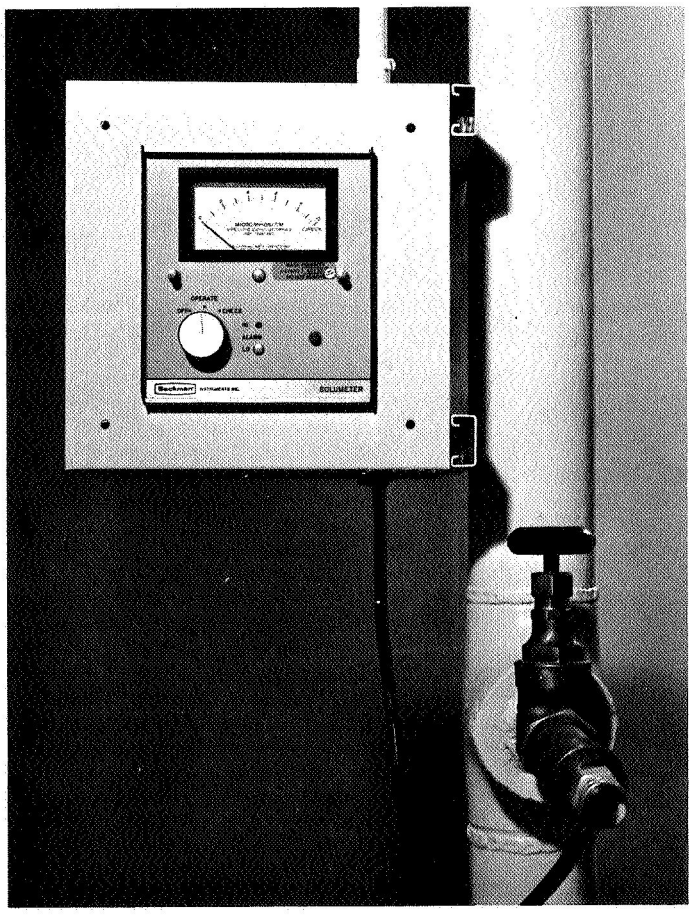


Fig. 25. Conductivity monitor, lamp coolant system

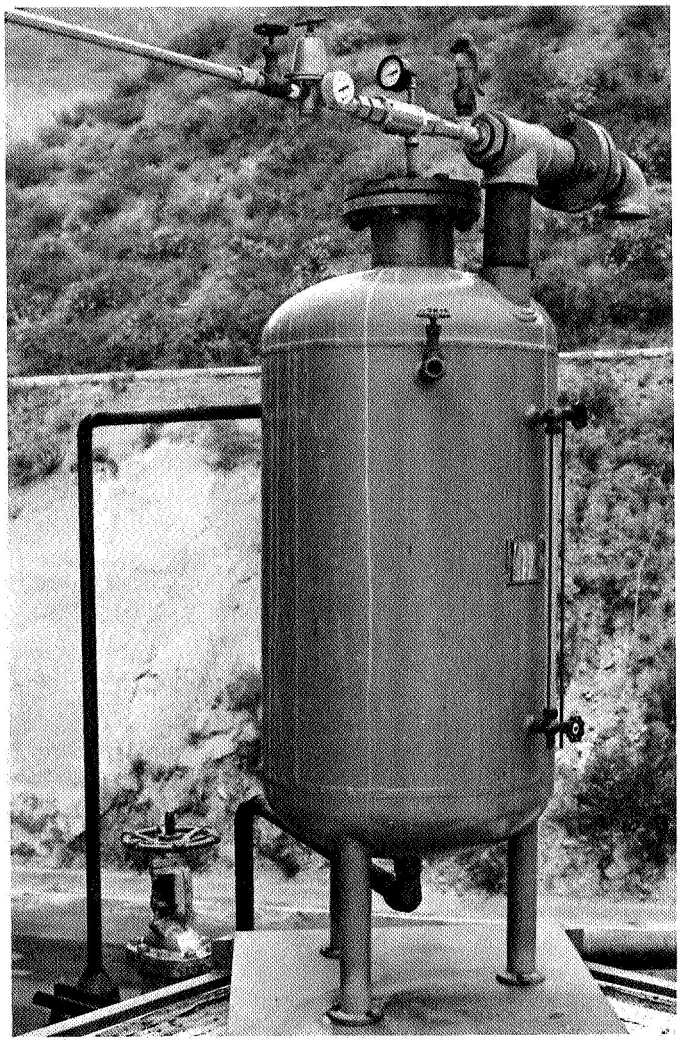

**Fig. 26. Surge tank, lamp coolant system**

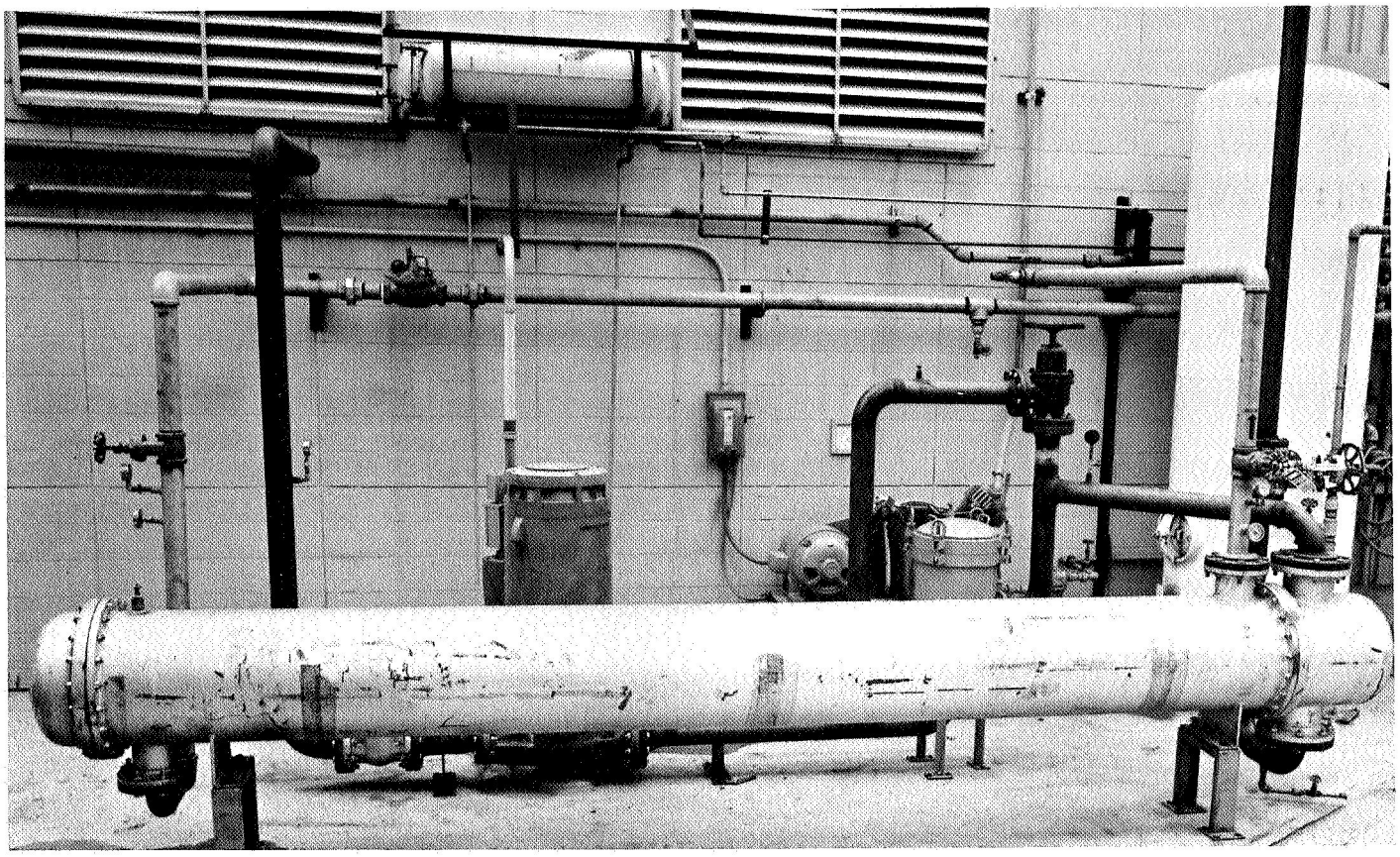

**Fig. 27. Lamp coolant pump area**

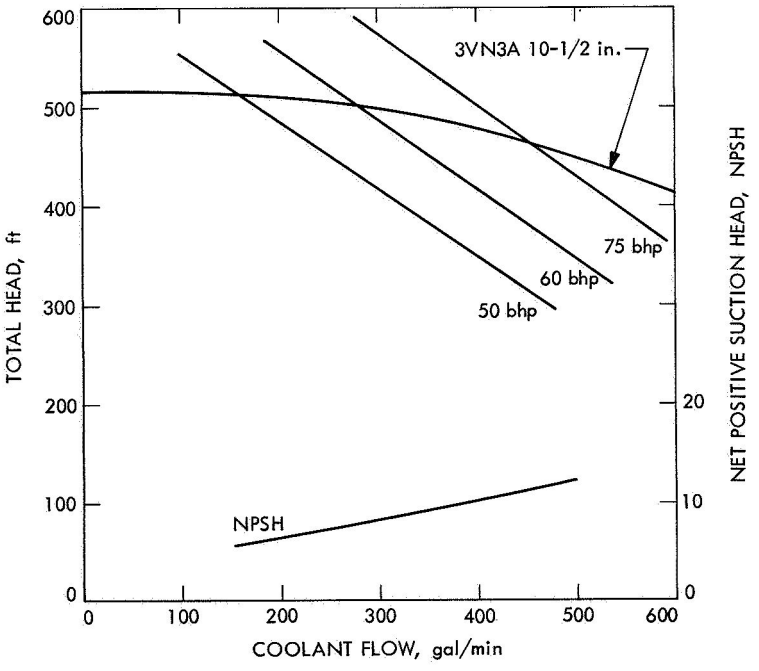


**Fig. 28. Total head available vs coolant flow**

(Fig. 28). The entire system contains approximately 500 gal of coolant. It is designed to accommodate sixty-one 30-kW lamps. Portions of the system not presently in use are blocked off, and the throttling valve is used to maintain an operating lamp inlet pressure of 200 psig and an outlet pressure of 50 psig (Fig. 29). A spare, or standby, pump was not provided, because any loss of lamp coolant flow would automatically shut the system off faster than another pump could be brought up to speed to prevent anode burnout.

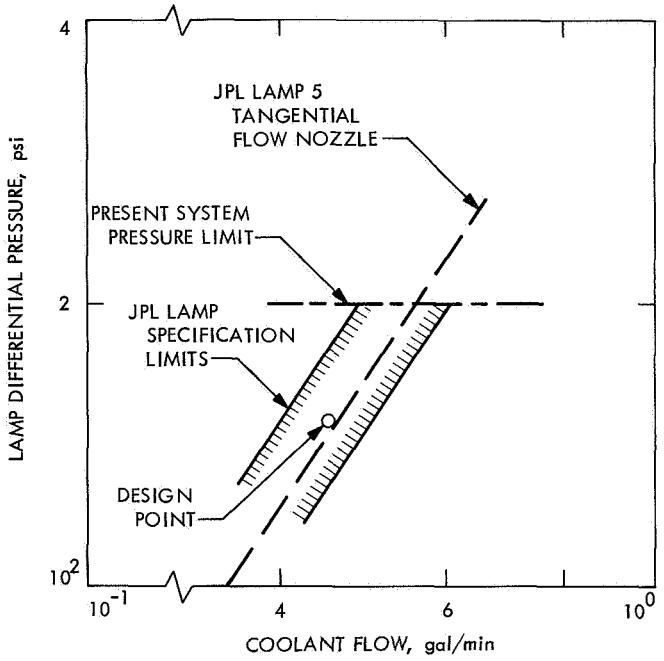


**Fig. 29. Lamp differential pressure vs coolant flow**

Lamp coolant flow to individual lamps can be shut off — either automatically, by the flow switch sensor, or manually, by the use of a remote switch on panel RA (Fig. 30) located on the second floor basement. These manual switches are illuminated to indicate the condition of lamp coolant flow and can be used to stop and restart individual lamp coolant flow. The lamp coolant flow sensing switch is also used to shut down the lamp electrical system in case of low flow. Since all rectifiers and lamp solenoids are held in by the power control switch at the console, this power control switch can be used in an emergency to shut down the entire lamp coolant and electrical system.

### C. Collector Cooling System

The lamp collectors for the 20-kW xenon arc lamps are water-cooled to prevent overheating and burning of the aluminized reflecting surface. The heat transfer to the water is accomplished by flowing water through copper tubing which is uniformly bonded to the rear of the collector casting with an epoxy-base material. Approximately 50 ft of ¼-in. tubing is used to cover the collector with about 1½ in. between the tubes. The tubing is spaced slightly closer together and the water inlet is placed near the base because the heat load is higher in this region.

The lamp support trusses are used to manifold the cooling water to and from the collectors (Fig. 31). The base of the truss contains the supply water and the top contains the return water. Rubber hoses with no-leak quick disconnect fittings are used to hook up the water to each collector. A combination filter screen and flow indicator is mounted in each supply line to prevent accidental clogging of the cooling tube and to provide assurance that the collector has sufficient coolant flow.

A collector absorbs about 1300 W from a lamp operating at its rated (20 kW) power. The collector cooling coil will transfer this energy with a flow rate of approximately 0.6 gal/min (Fig. 32) and a water temperature difference of 15°F. With a water in temperature of 70°F, the maximum surface temperature of the collector does not exceed 120°F. At collector temperatures below the dew point, moisture will form on the aluminized reflecting surface and destroy the coating. Care must be taken during simulator operation to maintain the collector temperatures above the dew point, either by warming the collectors or by dehumidifying the area.

### D. Lamp Electrical System

The direct current electrical power for each individual arc lamp is provided by three commercial, welder-type, silicon-controlled rectifiers wired in parallel (Fig. 33). These rectifiers, rated at 12.5 kW output at 180 A each, are supplied with 60-cycle 480 Vac. The use of these three small rectifiers in parallel to power one lamp was based on the convenience and economy of using the installed equipment previously provided for the 133-2.5 kW mercury xenon lamps in the 6-ft-diam system. The power factor of these rectifiers has been improved by the addition of external line capacitors. The present current ripple of approximately 13% can be improved by the addition of a suitable filter network if desired in the future.

Two of the rectifiers (A, B) are turned on remotely from the control console with the lamp power switch to provide power during lamp ignition. The third (C) rectifier is turned on automatically upon lamp ignition. The

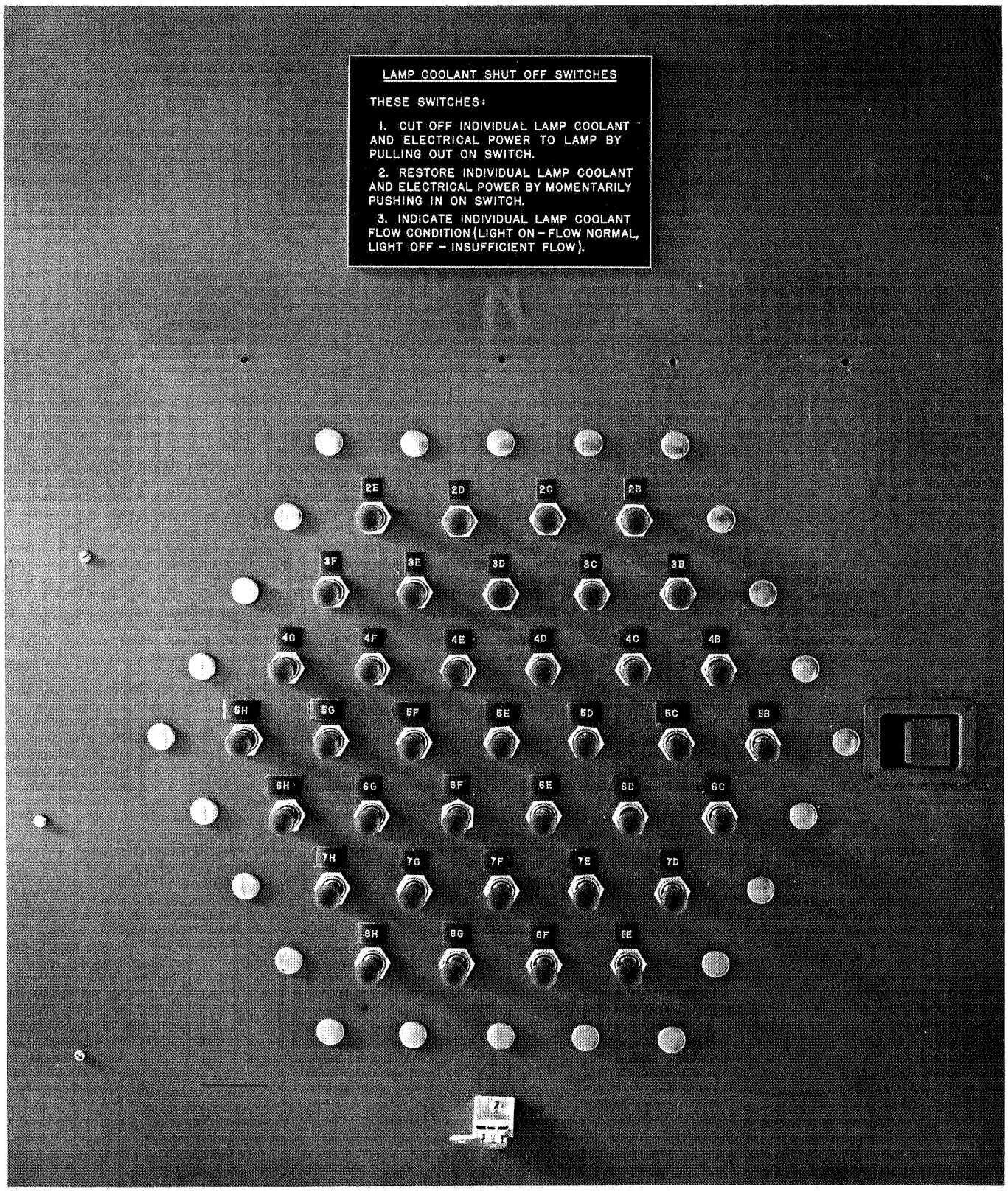


**Fig. 30. Panel RA, lamp coolant system**

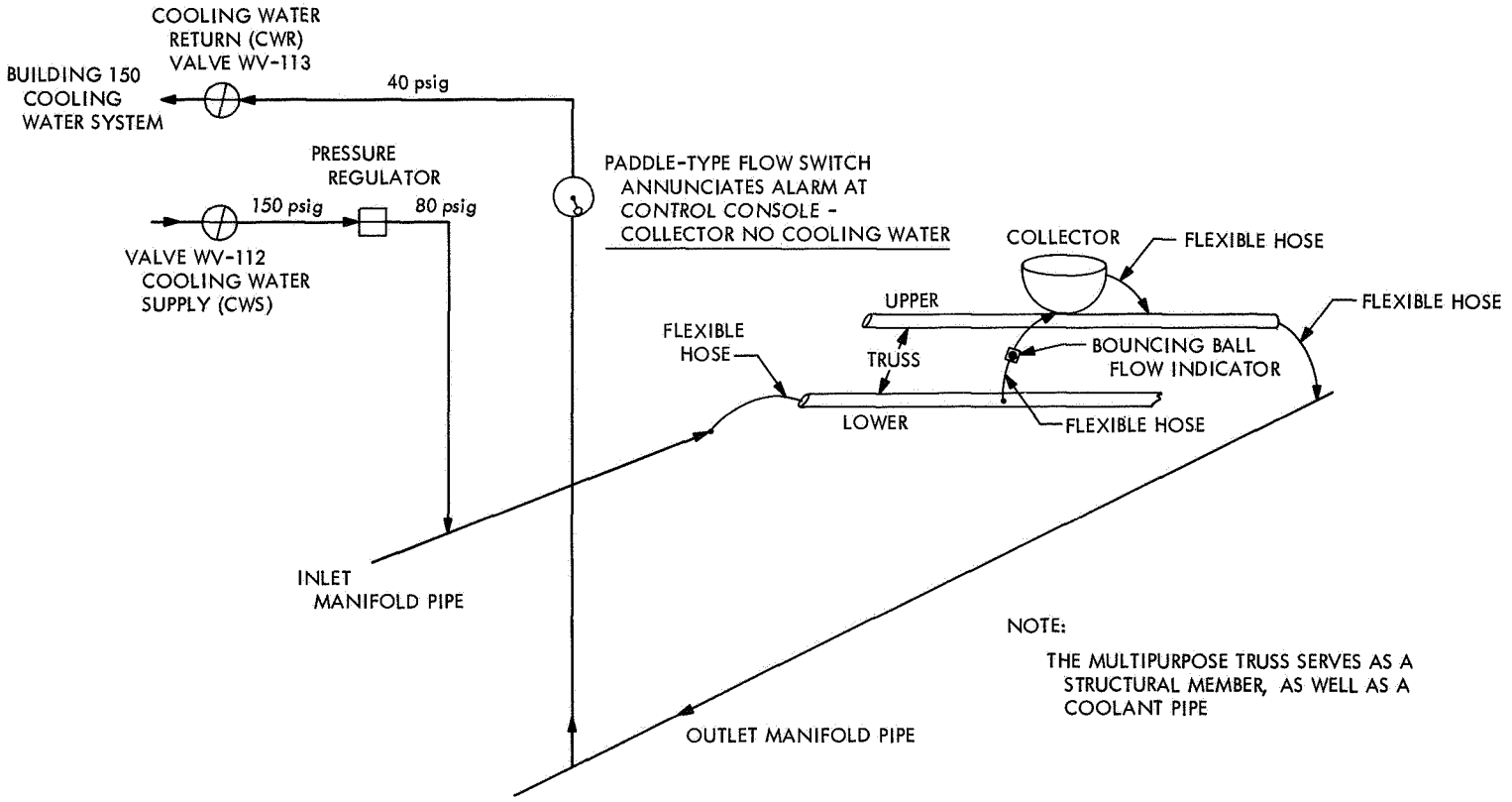


**Fig. 31. Collector coolant schematic**

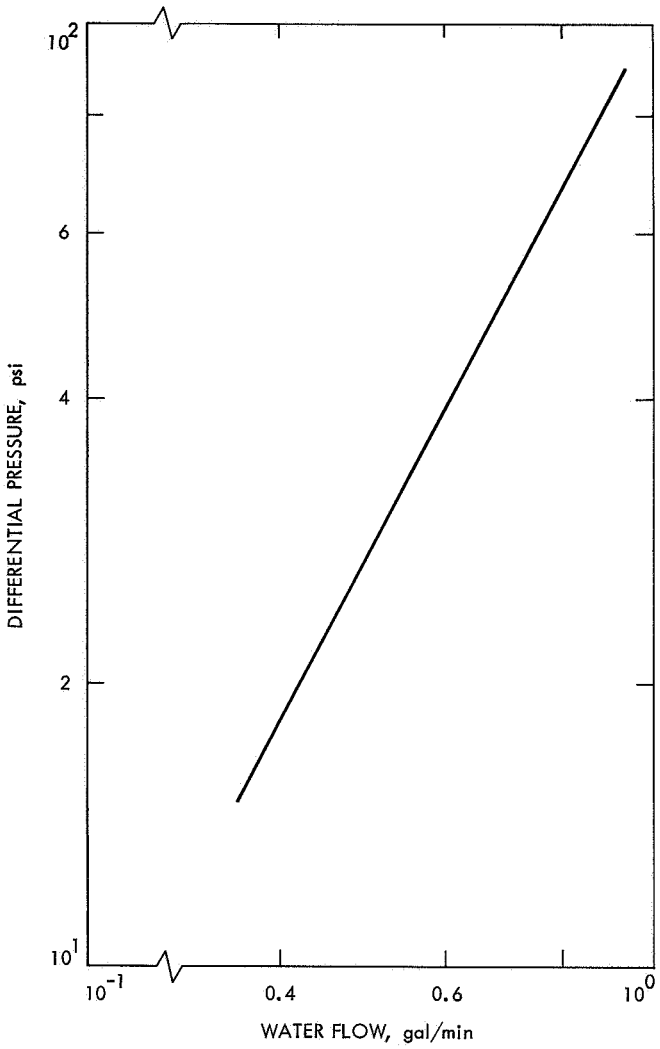


**Fig. 32. Collector differential pressure vs coolant flow**

A rectifier output is controlled directly from the control console. The B and C rectifiers are automatically adjusted to within 10% of the A rectifier output by means of current-sensing coils and a special balancing circuit. More rectifiers can be added to the parallel direct current lamp circuit if greater power levels are required of future lamps.

The lamp ignition is provided by a remotely positioned (30 ft) ignitor-contactor circuit to provide isolation of the high-voltage circuit and greater access to the lamps. The ignition pulse is created by a two-stage, capacitor-discharge-transformer circuit that converts a 150-Vdc input into an RF pulse, of a few milliseconds duration, >50,000 V. The frequency of the pulses is controlled by the storage rate of the capacitor system and occurs about every 3 s. A current-sensing relay switches the ignitor circuit *off* when the lamp has ignited. The purpose of the contactor is to shunt out the ignitor once the lamp is operating, since it is rated at only 200 A. The lamp is grounded electrically at the lamp mount with a braided copper strap to provide a low impedance return path for the RF ignition pulse.

The distribution of electrical power from the rectifier rack to the lamps (about 75 ft) is made by a common positive bus and individual negative cables. The positive bus consists of a 4 × 4-in. copper duct with ½-in. walls, which is grounded electrically to the building at the rectifier rack. Each set of three rectifiers is connected to the positive bus through a 5%, 600-A shunt for lamp control metering purposes. Each rectifier also has an individual 10% shunt-ammeter circuit at the control console for trouble shooting purposes. The positive bus also serves as a water pressure manifold for the lamp coolant system and reduces the number and size of cabling to the lamps. An 18-in. neoprene hose isolates the copper bus from the steel lamp coolant system to reduce galvanic corrosion.

The negative cables from each rectifier are terminated in the lamp basement at the ignitor-contactor. From the ignitor-contactor, the negative side of the lamp circuit is bussed to the lamp through a ⅞-in.-OD copper pipe that serves as part of the lamp return water circuit. The negative bus is isolated from ground for the high-voltage ignition pulse, as well as the normal operating lamp voltage, by a Mylar insulation on the bus and an 18-in. polyvinyl chloride dielectric pipe to the lamp coolant return manifold. The conductivity of the water used as coolant is maintained sufficiently low so that current flow through the coolant is negligible. The lamp operating voltage is read at the control console across the ignitor terminals; the error due to bus resistances is <1%. A wattmeter is used at the control console in conjunction with the precision ammeter and voltmeter circuits to selectively read out lamp operating power. An 18-position telephone stepping switch and digital position readout is used to speed up this process for the console operator (Fig. 34).

### E. Air Cooling System

The purpose of the air cooling system is to cool the lamps, lamp mounts, solar hood and lenses and related support structures in the lens room. The air cooling system is of the recirculating, closed-loop type system (Fig. 35). The air is filtered, humidity controlled, and

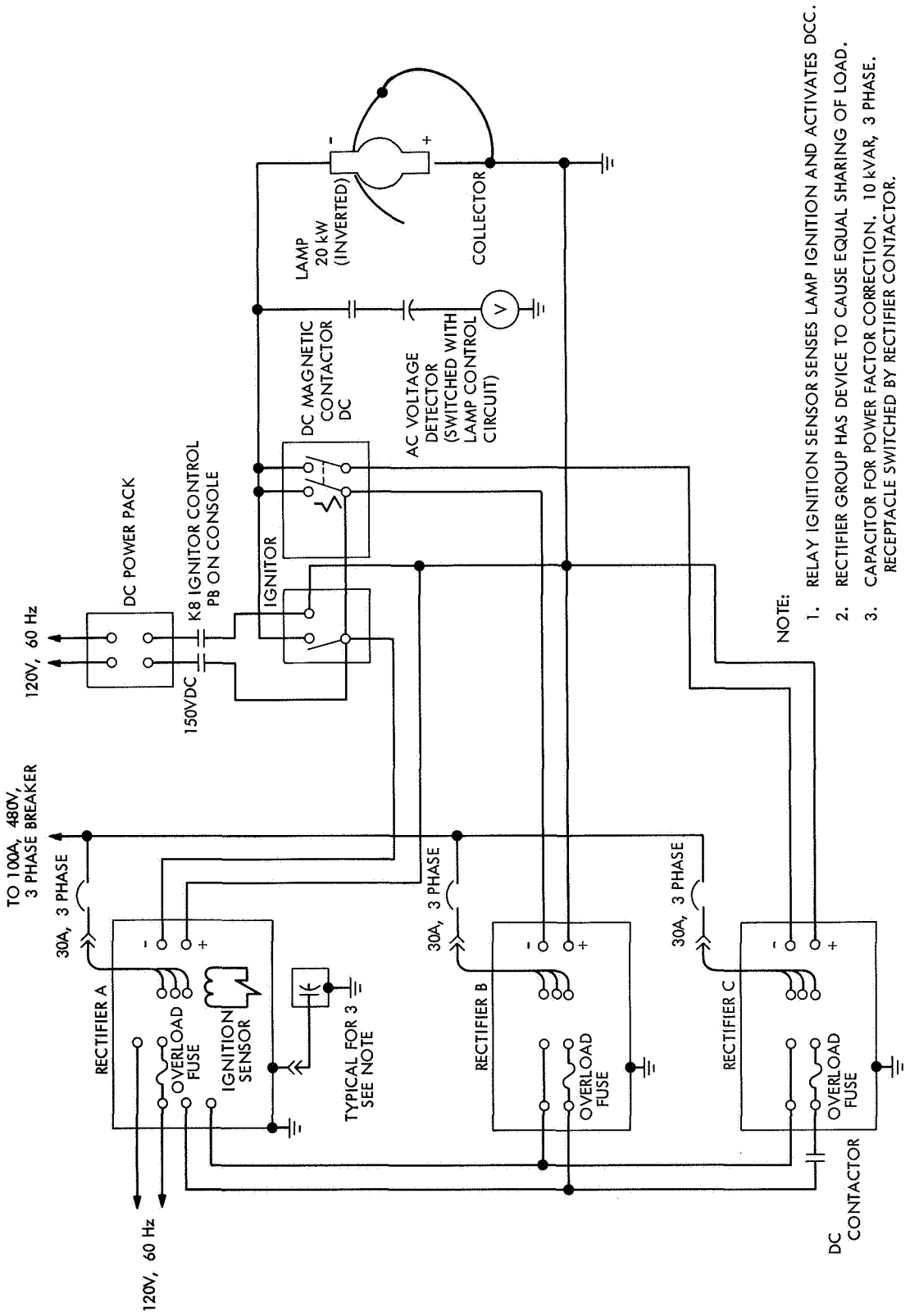


**Fig. 33. Lamp electrical power schematic**

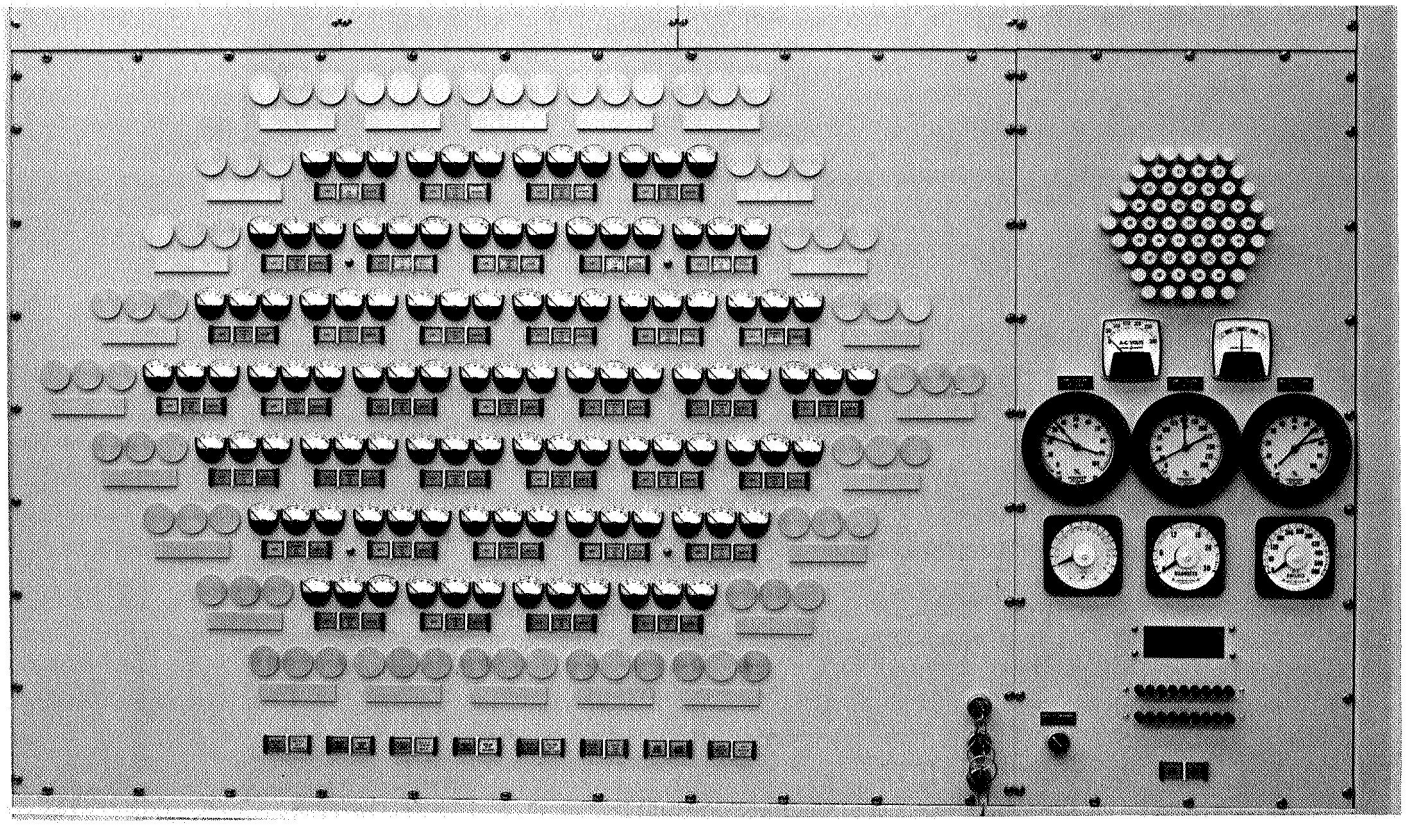

**Fig. 34. Lamp control console**

temperature controlled through a water–air heat exchanger. The filter consists of a 50 $\mu$m prefilter, an activated carbon filter, and final 2 $\mu$m particulate filter. The 50 $\mu$m filter keeps the carbon filters reasonably clean when using outside air. The activated carbon filter absorbs the ozone and other various gases and hydrocarbons. The final filters remove particles down to 2 $\mu$m in size (particles as small as tobacco smoke).

The atmosphere used inside the solar simulator is air, to allow access of personnel to the area during operation. The use of nitrogen would be hazardous and difficult to maintain in such a large system. The use of activated carbon filters ensures that the air entering the basement is free from ozone.

The humidity of the air must be maintained as low as possible to prevent the first surface, aluminized optics, from degrading during operation. Commercial dehumidifiers located in the third floor basement are used for this purpose. A humidity recorder monitors the moisture content in the lamp plenum continuously. If rainy weather or spilled coolant produces more humidity than the dehumidifiers can remove, the dry air from the wind tunnel facility is used.

The lamp plenum is located about 30 ft below the simulator ground level, and the possibility of $GN_2$ gas accumulating in the plenum exists. Oxygen analyzer check points are located on the second and third floor basement levels to detect a shortage of oxygen. If the oxygen falls below a preset danger level, an annunciator is sounded at the control console and an alarm horn in the lamp plenum warns personnel to vacate the area.

There are provisions for recirculating or venting the air in the system. In the recirculating mode, the air from the blower discharges to the lamp plenum, through the lamp bank and radiation shield, up to the lens room area, through the filter bank, and returns to the blower inlet. In the vent mode, the air is drawn in from the outside, passes through the auxiliary blower, through the filter bank, through the main blower into the lamp plenum, through the lamp bank and radiation shield, up through the lens room, and is then vented outside.

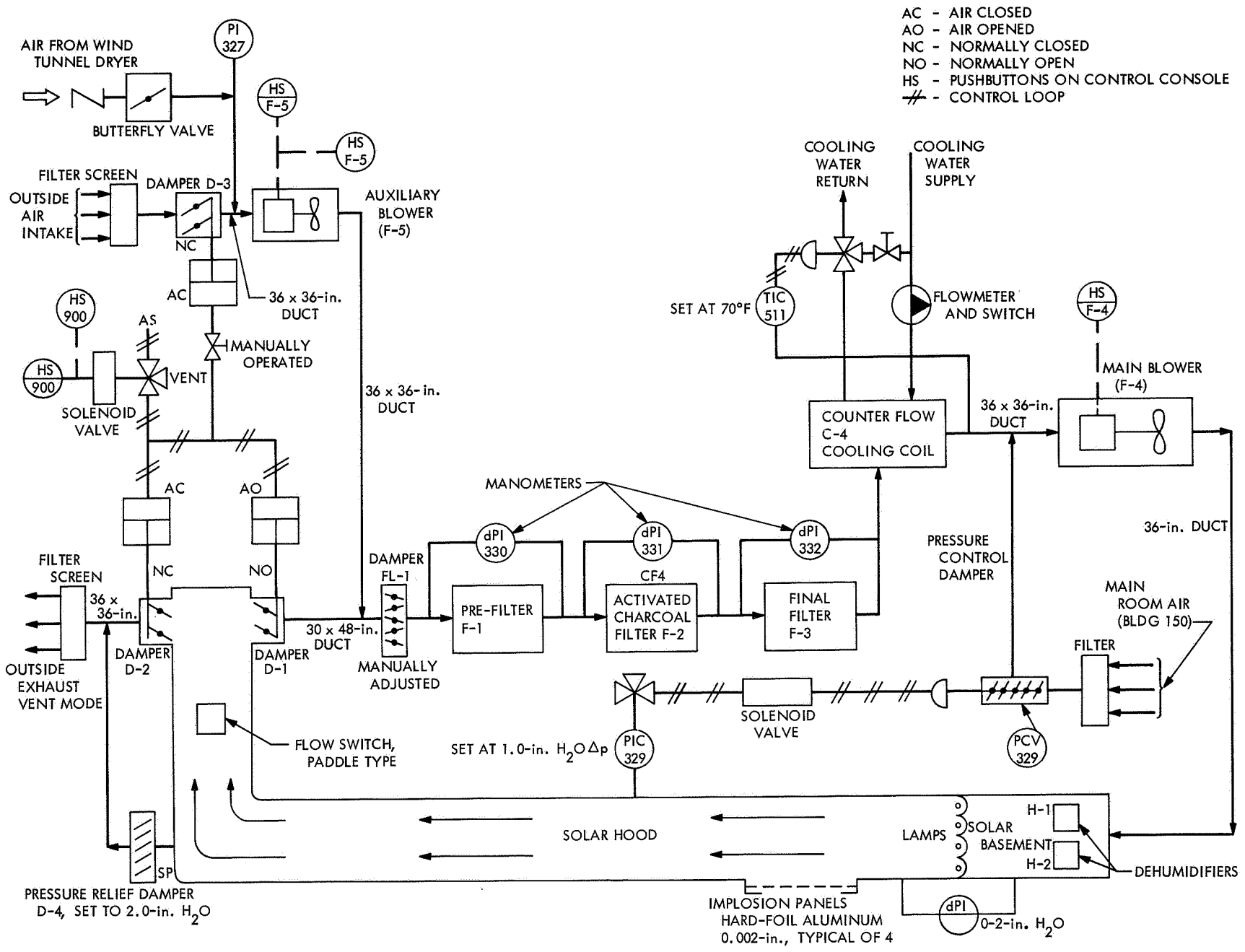


**Fig. 35. Lamp cooling air schematic**

The normal circulation for this system is upward from the lamp room in the same direction as natural convection. In all cases, only treated air is admitted to the lamp plenum, which assures fresh air for observers on the second floor basement. The dry air from the wind tunnel facility may be used instead of outside air, if desired, by proper valving. The wind tunnel air is vented in the same manner as the normal vent cycle.

The temperature of the air delivered to the lamp plenum is controlled by the water–air heat exchanger located downstream of the filter bank. The water is provided from the cooling tower system for the space simulator building. The control for the air temperature, located at the console, senses the air temperature as it leaves the heat exchanger and either bypasses the water around the exchanger or allows it to flow through, depending on the position of the set point. The temperature of the air in the solar simulator can never be maintained below the temperature of the cooling tower water.

The solar simulator air system is designed to operate with the lamp plenum, solar hood, and lens room pressurized above ambient to keep the area as clean as possible. An air lock is provided for access to the lamp plenum, and all other areas are maintained closed or as air tight as possible. A pressure controller senses the pressure in the solar hood and actuates a valve located just ahead of the main blower inlet to admit or close off make-up air as required. A set of filters is used to condition the make-up air before it enters the duct. This make-up valve is automatically closed when the circulate mode switch is placed in the vent position so that the vent air will not be lost through the valve.

The venting and recirculating provisions are controlled from the console by means of remotely operated air cylinders. There are two blowers used to vent or recirculate the air. The main blower, used for normal recirculating, is rated at 34,000 $ft^3$/min at 2½ in. of water; it uses a 50-hp motor. The auxiliary, or vent, blower is rated at 15,000 $ft^3$/min at 2½ in. of water; this blower has a 10-hp motor. These blowers can be used individually or in series for venting, or drawing dry air from, the wind tunnel facility; however, only the main blower may be used to recirculate the air.

### F. Operation of the Solar Simulator

The operation of the solar simulator is accomplished by following the detailed instructions in the operation and maintenance instruction manual. A pre-run inspection is made to assure that all subsystems are operating or ready for operation. A preliminary phase then places all subsystems in operation and ready for lamp ignition. The lamp ignition is carried out individually by turning on the lamp power and pressing the ignitor button. The operation of the ignitor cutout, ignitor bypass contactor, and parallel power supply operation is automatically controlled by current sensing relays upon lamp ignition.

After the lamp is ignited, the lamp power is monitored and raised or lowered as desired. The irradiance level at the test volume is maintained by varying the number of lamps operating and/or adjusting the power level of the lamps from the control console. Provision is made for future automatic control of the simulator power from the console if desired.

The operation of the solar simulator is monitored by various alarms and interlocks and by routine visual inspections of the various operating subsystems. The electrical and mechanical subsystems have interlocks designed to prevent startup of equipment until all necessary preliminary operations have been met, and to initiate a safe shutdown of equipment in the event of a failure (Fig. 36). The philosophy of the system used is to give the operator freedom to exercise judgment in all matters except where an immediate reaction is required to prevent injury to personnel or damage to equipment. The interlocks and alarms are augmented by standard temperature and pressure gauges, flow switches, lockout switches, and audio and visual alarms (Fig. 37).

Additionally, access to potentially hazardous areas is controlled by means of door keys that are an integral part of the interlock system. Areas that are considered unsafe during system operation are made inaccessible. Removal of the key for these areas will shut the system down or make it inoperable. Areas accessible during system operation by key such as the lamp operation observation area actuate a warning buzzer and a light to warn the console operator of occupancy.

The solar simulator is normally shut down by turning off the individual lamp power switches. The remainder of the subsystems are then shut down in the sequence listed in the operation manual. All subsystems are then given a thorough post-run inspection to check the condition of the solar simulator and to place the simulator in a standby status for the next run.

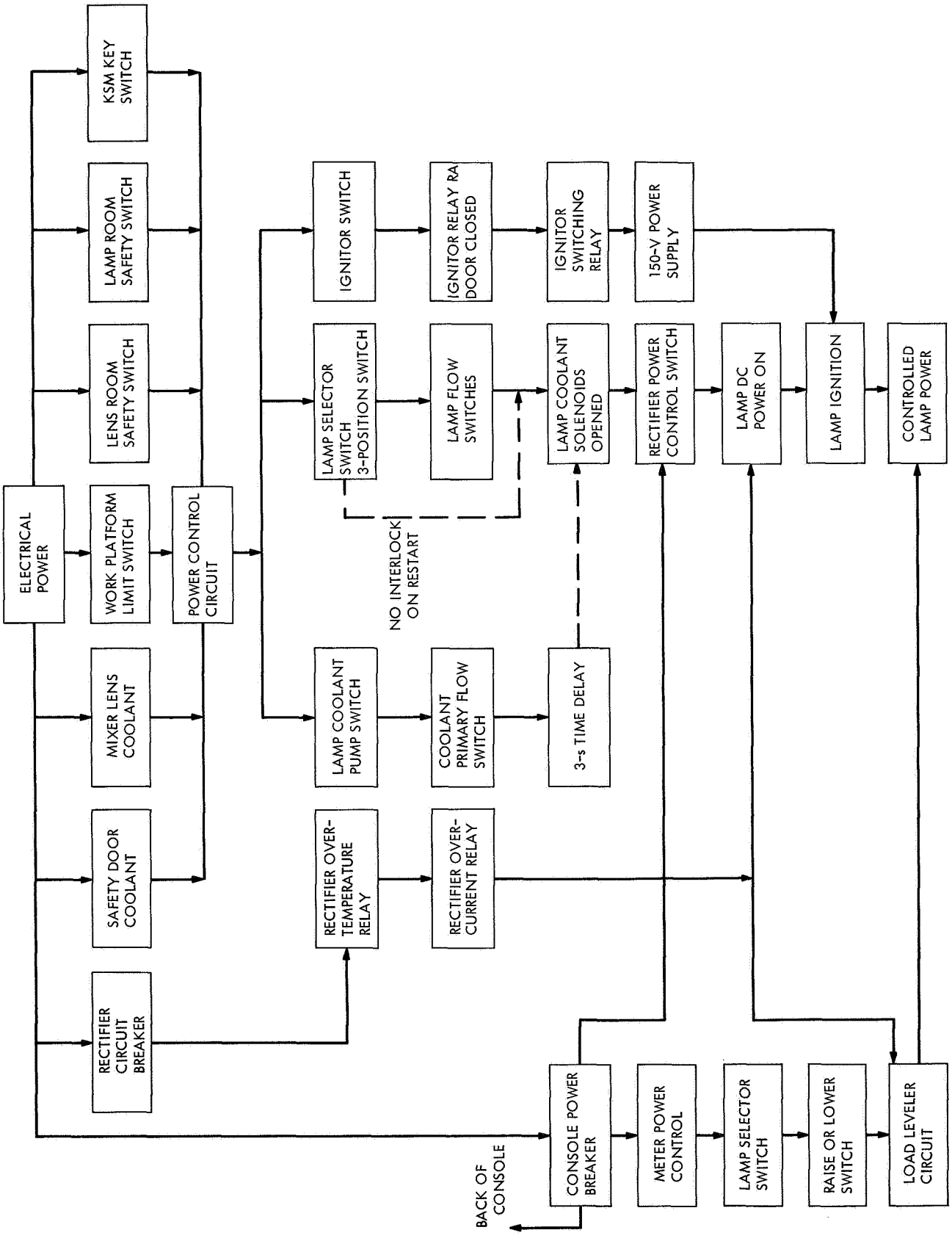


**Fig. 36. SS15B interlock system**

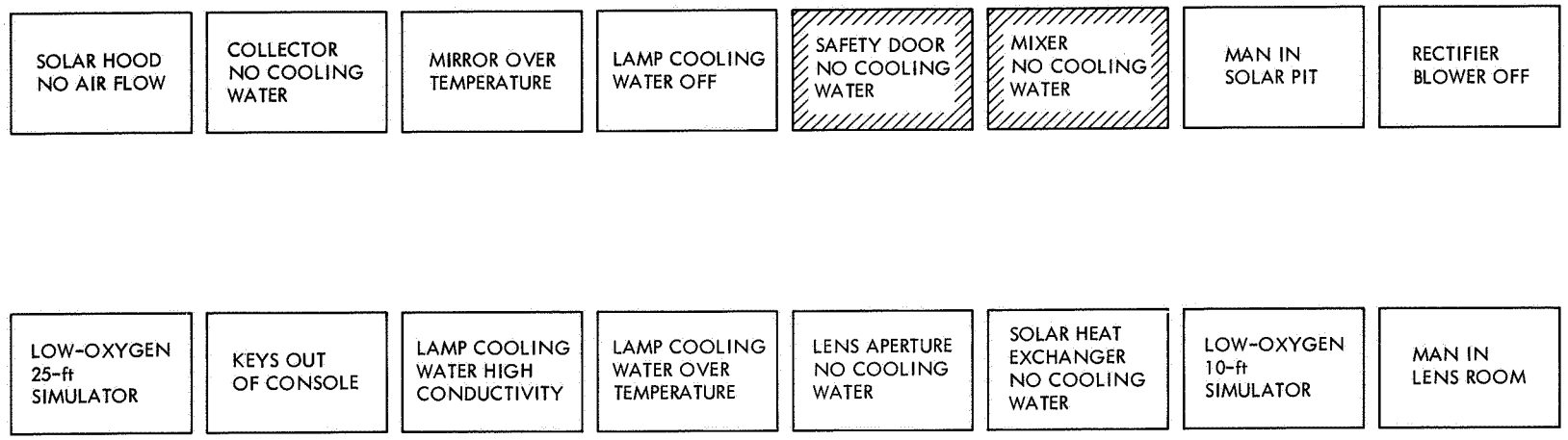


1. ALARM TEST AND ACKNOWLEDGE PUSHBUTTONS ARE NOT SHOWN (SEE TEXT).
2. WHEN ACTUATED BY THE APPROPRIATE SENSOR, AN AUDIO (BUZZER) ALARM WILL BE SOUNDED AND APPROPRIATE MALFUNCTION WILL BE ILLUMINATED BY A FLASHING WHITE LIGHT.
3. WHEN ACKNOWLEDGE PUSHBUTTON IS PRESSED BY CONSOLE OPERATOR, THE BUZZER SIGNAL IS OVERRIDDEN (CUT OUT) AND THE FLASHING WHITE LIGHT COMES ON STEADY AND WILL REMAIN SO UNTIL THE MALFUNCTION OR OFF-NORMAL CONDITION IS CORRECTED.
4. HATCHED SIGNALS - SAFETY DOOR NO COOLING WATER AND MIXER NO COOLING WATER ARE ALSO ELECTRICALLY INTERLOCKED TO THE POWER CONTROL CIRCUIT (SEE TEXT).
5. THE ALARM TEST PUSHBUTTON IS USED TO CHECK THE LIGHT CIRCUITRY PRIOR TO SYSTEM OPERATION. WHEN PRESSED, ALL LIGHTS IN THE PANEL SHOULD FLASH.

**Fig. 37. SS15B annunciator system**

## V. Lamp-Collector Configuration Design

At the time the SS15B system was in the preliminary design stage, the only known reliable high-powered arc lamp was the 5- to 6-kW radiation-cooled xenon lamp. Calculations based on previous studies showed that the power needed to operate the 20-ft solar simulator would require a hexagonal array of one hundred sixty-nine 5-kW lamps. The outer two rows of lamps could be left out, initially, to provide an array of ninety-one 5-kW lamp positions for the 15-ft beam. Calorimetric measurements of power output of a 16-in. collector through a 20-in. aperture demonstrated that ninety-one 5-kW lamps would provide sufficient power for one solar constant plus a 30% factor for lamp degradation and 10% factor for spares. A hexagonal array of the one hundred sixty-nine 16-in. collectors would require a second focal length of 45 ft to fit all the lamps within the solid entrance angle of the optics involved.

The new water-cooled lamps, which were just being developed at this time, looked very attractive from a design point of view because of their power output vs size. The use of the 20-kW lamps would require a smaller number of lamps and their related optics and support equipment and, thus, reduce the system cost considerably. It remained to be proved whether these new lamps would provide sufficient economy to warrant their use.

A parallel design was initiated to accommodate the one hundred sixty-nine 5-kW lamp array into the solar basement as a first consideration and to design a 20-kW lamp array that could use the same basement and hood, etc., should the 20-kW lamp prove feasible. At the same time, a prototype 20-kW lamp test setup was started so that performance estimates could be confirmed. The two systems would be evaluated at a later date. If the 20-kW lamp did not look good, the tried and proven 5-kW lamp system could be used; if they did look good, full effort would be given to the water cooled lamp system and the 5-kW design would be abandoned.

A complete prototype SS15B lamp-collector assembly was manufactured and set up to verify analytical designs and to enable predicting future performance of the system with 20-kW lamps (Fig. 38). The greatest concern in the prototype stage of development was the lack of knowledge of the power collected from the 20-kW lamp and projected into the system aperture. Measurement of this projected power and the energy distribution at the mixer aperture could be extrapolated with performance

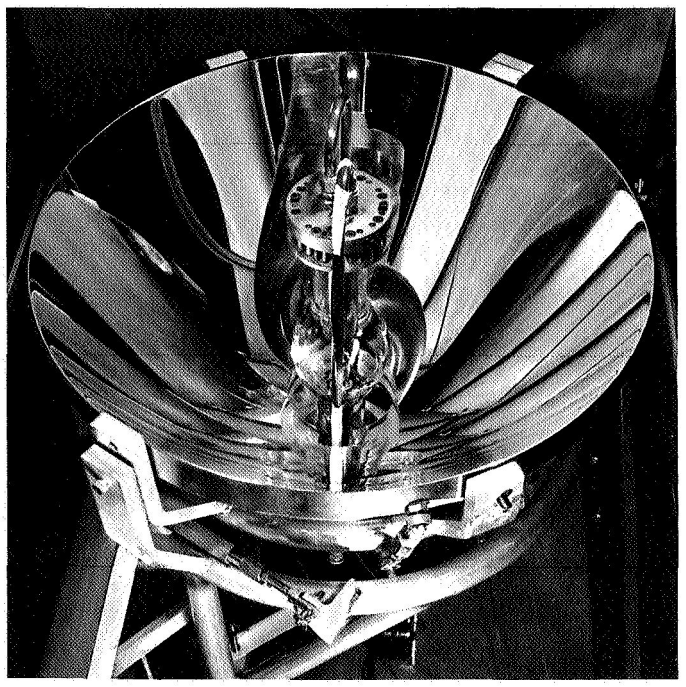

**Fig. 38. Prototype lamp and collector**

characteristics of the JPL series A solar simulators to assure that performance specifications could be met.

Figure 39 shows the measurements of power through the aperture ($A$) vs aperture sizes for a typical 20-kW lamp tested in the prototype hardware. A sketch on this curve describes the test setup. The 17.5-in. aperture used in the SS15B system could pass 3900 watts with the prototype 20-kW lamp operating at rated power ($P$) when the focus was adjusted for maximum through put. The previous A type solar simulators have a transfer coefficient of 0.485 (energy through aperture to energy in test volume). The data obtained from these prototype tests could be used to predict a gross test volume flux of:

$$\Phi = \frac{P}{A_{hex}} = \frac{37 \text{ (lamps)} \times 3900 \text{ W}}{(190 \text{ in.}^2 \times 0.866)/144} \times 0.485 \text{ (the mixer transfer coefficient, type A)} \times 0.875 \text{ [the losses in mixer lens (type B) support]} = \frac{282 \text{ W}}{\text{ft}^2}$$

The 190-in. diameter is used for a conservative 15-ft beam. The area is calculated for a hexagonal beam to correlate with the mixer transfer coefficient.

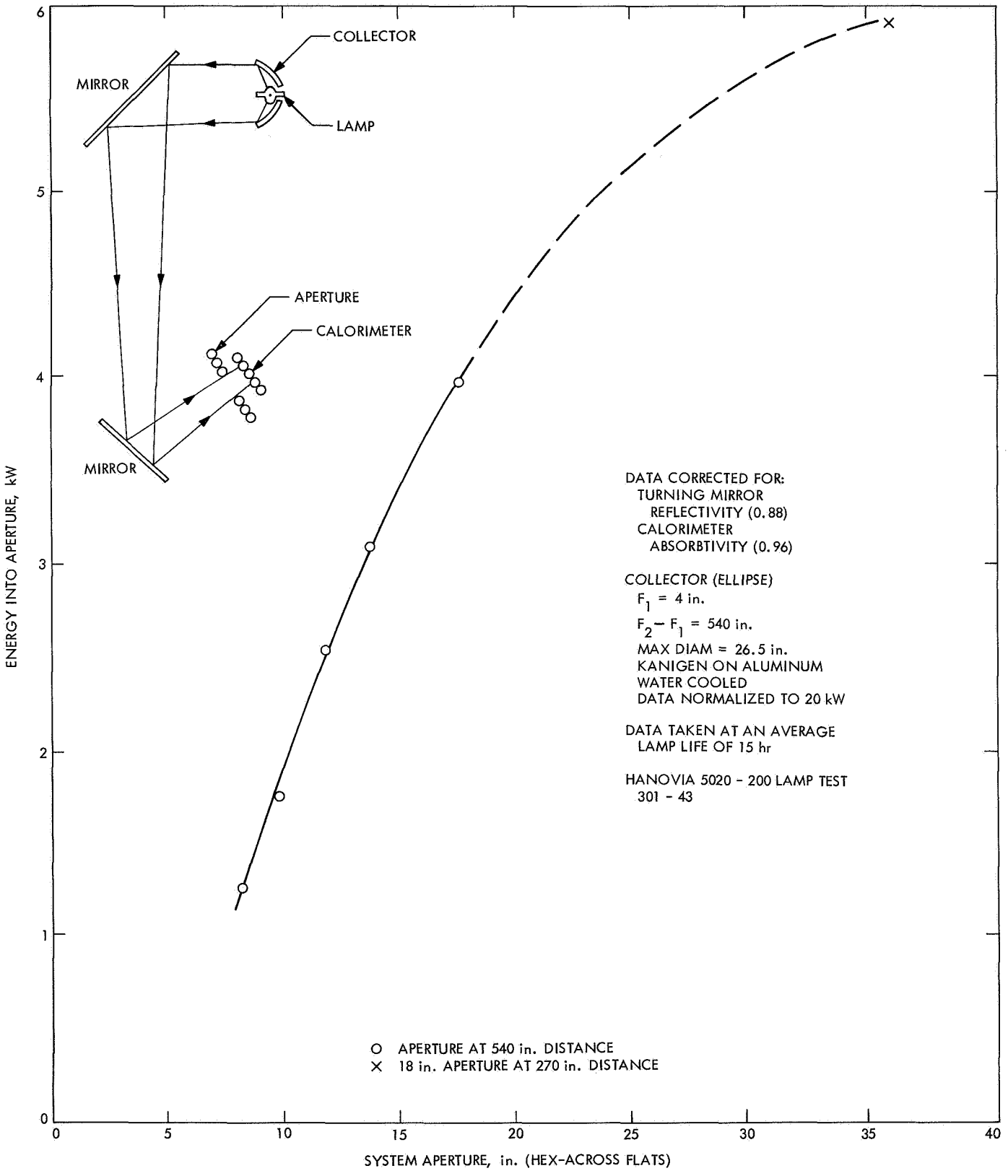


**Fig. 39. Lamp test data, energy vs aperture**

To be realistic, the new lamp performance data should be modified by coefficients to take into consideration the number of spare lamp assemblies desired and the observed degradation of the lamp-collector system with time. The SS15B system was designed around factors of 10% for spares and 30% for degradation of the lamp-collector output during 400 h of operation.

Multiplication of the expected test volume flux by these numbers yields an operational test volume flux of:

$$\Phi_{\text{operational}} = \Phi_{\text{new lamp}} \times 0.9 \times 0.7$$

$$= 282\,(0.63) = 178\,\frac{\text{W}}{\text{ft}^2}$$

Although these numbers make the design appear overconservative, it should be noted that the 20-kW lamp development at the time for decision as to which lamp to use was not certain by any means, but looked promising in the near future. Based on these tests, it appeared that the advantages of the water-cooled lamp system outweighed those of the radiation-cooled lamps. The decision was made to go ahead with the solar simulator design based on these lamps, and also press the developmental testing of the lamps in the hope that they would be suitable for production when needed.

### A. Optimum Lamp-Collector Configuration

There are several important things to consider when designing a collector for the SS15B type system. The solid entrance angle to the mixer lens aperture from the lamp array is fixed by the collimator diameter and focal length; the angle cannot be exceeded because sources outside of this solid angle will not pass energy to the test volume. The maximum realistic packing of sources into the circular source array is a hexagonal pattern, which means that the number of sources will occur in groups of 1, 7, 19, 37, 61, 91, etc. Figure 40 shows the relationship between number and size of inscribed circles to that of the circumscribed hexagon. Using the maximum acceptance angle for the one hundred sixty-nine 16-in. collectors, it is possible to use this hexagonal packing relationship to determine the diameters of the collectors vs the second focus distance by using the number of grouped collectors as a parameter (Fig. 41).

It is obvious that, for a given collector focal length, a greater number of smaller collectors could be packed in. This will not necessarily produce the maximum energy from the array, however, because the smaller diameter

n = NUMBER OF CIRCLES
R = CIRCUMSCRIBED CIRCLE RAD
E = INSCRIBED CIRCLE RAD
d = MAXIMUM DIAMETER OF SMALL CIRCLES

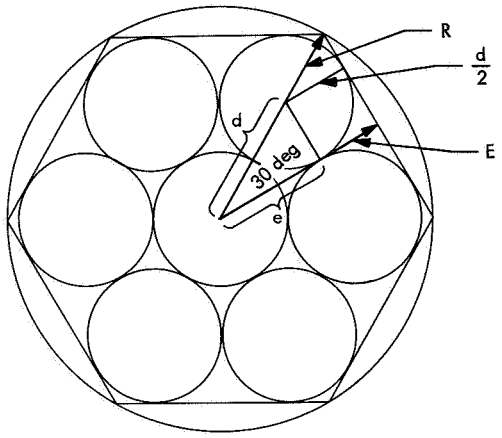


$e = 0.866\,d \qquad E = 0.866\,R$

$f(n)\ e + \frac{d}{2} = E$

$f(n)\ 0.866\,d + 0.5\,d = 0.866\,R$

$$\left\{\frac{-1 + \sqrt{1 + \frac{4}{3}(n-1)}}{2}\right\}\ 0.866\,d + 0.5\,d = 0.866\,R$$

$$\left\{-1 + \sqrt{1 + \frac{4}{3}(n-1)}\right\}\ 0.866\,d + d = 1.732\,R$$

FOR n = , 7, 19, 37, 61, 91, 127, 169... NUMBER OF LAMPS

**Fig. 40. Lamp packing relationship**

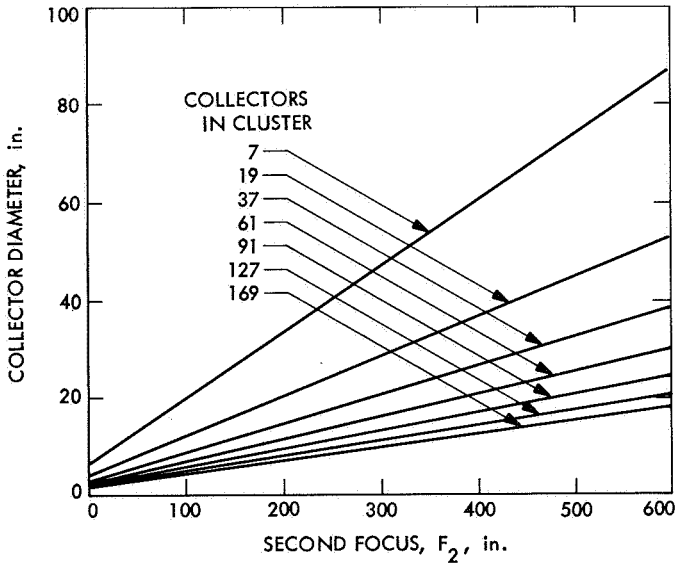


**Fig. 41. Collector diameter vs collector focal length**

collectors may not be capturing the available energy efficiently and passing it through the system aperture at the mixer lens. If the collectors were made larger and placed farther back from the system aperture, the system would again reach a point where the magnification effect of the collector would make passing the collected energy through the aperture more difficult.

It is possible to choose the optimum collector by integrating the relative energy from the polar distribution of the lamp output that is reflected by the surrounding elliptical collector through an aperture at the second focus. This integrated energy passed through the system aperture is then compared to the total energy available from the lamp to obtain a system efficiency for the conditions selected. A great number of repetitive-type calculations make this problem especially suited for a computer. Figure 42 is a sample curve obtained from these calculations; it shows the system efficiency vs collector eccentricity for the design collector diameter (27 in.) when the lamp array is located at a second focal length of 45 ft and the system aperture is 20 in. in diameter. When a number of calculations such as in Fig. 42 are made for many focal lengths, the maximum efficiency points can be plotted versus collector diameter using focal length as a parameter. The dashed lines of Fig. 43, which represent these data combined with Fig. 41 data, show overall efficiencies of systems made up of various lamp groupings.

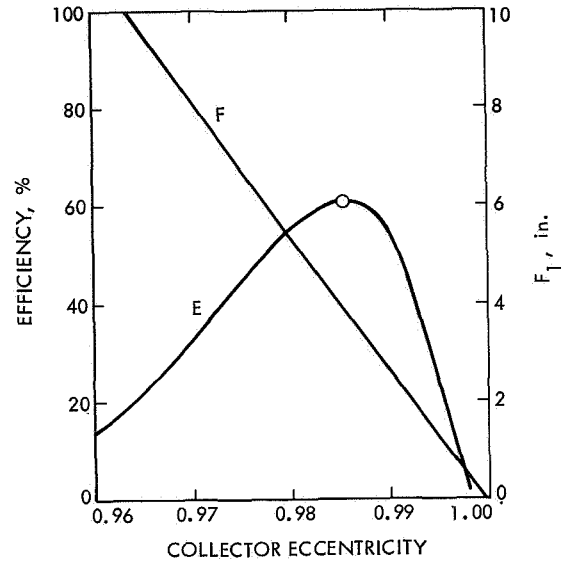


**Fig. 42. Design collector efficiency vs eccentricity**

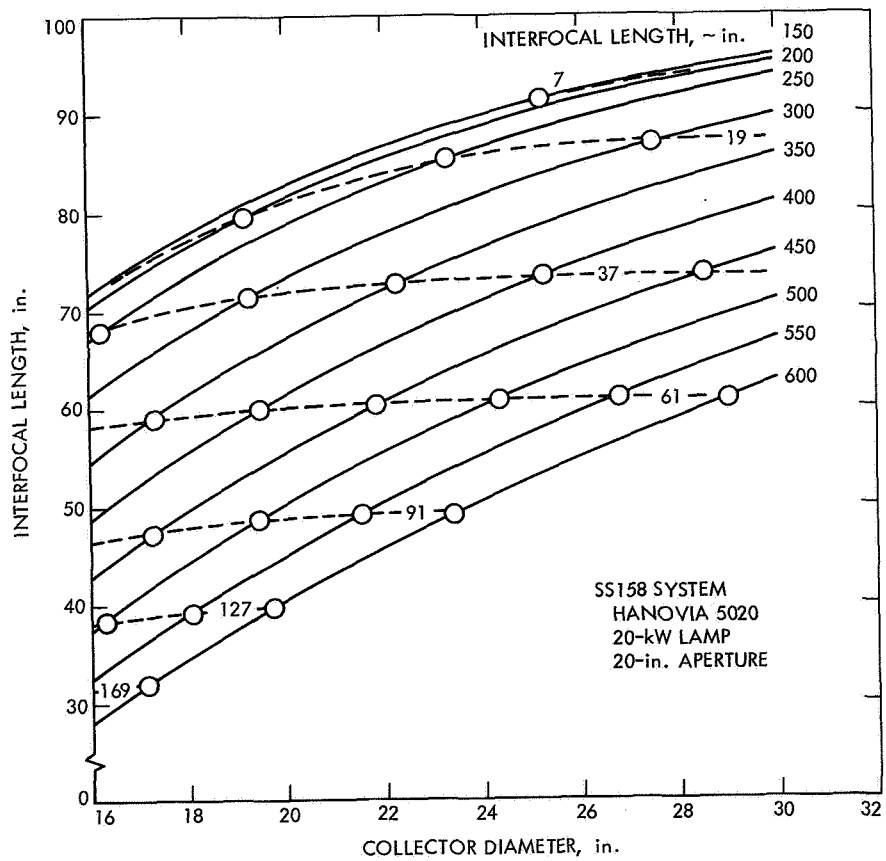


**Fig. 43. Efficiency vs collector diameter and number of lamps in cluster**

There are other factors to consider when determining the number of lamps in an array. More collectors of smaller size may produce greater total energy through the mixer aperture, but less efficiently, and at a cost roughly proportional to the number of lamps. Too few lamps could be considered as a disadvantage from an operational point of view, because of the number of spare lamps required and the necessity of making up for losses from normal lamp degradation or spectral filtering. Smaller sizes of lamp collectors also lead to crowding of systems and poor access to adjustments, etc., which may introduce design or maintenance problems.

At this point, a compromise must be made of the various system parameters and human factors involved to assure the best design payoff. For the SS15B system, it was decided to follow a conservative design approach of providing sixty-one 20-kW lamp positions for the ultimate 20-ft beam and install an inner cluster of thirty-seven 20-kW lamps for the initial 15-ft beam. Figure 43 shows the system efficiency of 61% for the design point picked. The flatness of this efficiency curve shows that an equally efficient system could have been constructed at a focal length of 500 in. with a 24½-in. collector. Because the lamp basement dimensions had previously been sized to accommodate one hundred sixty-nine 16-in.-diam collectors, however, it proved more desirable to use the full basement area available. The resulting design for the water-cooled lamps provided additional space for accommodating the various lamp support systems and improved the accessibility to the lamps for maintenance when a 27-in. center-to-center collector spacing was picked.

### B. Collector Fabrication

The lamp collectors are manufactured from 356 aluminum alloy castings. These castings are uniformly heated in an oven at 440 ±10°F for 7 to 9 h to make them conform to T-51 standards. The optical locating dowel holes and other tapped holes are machined into the casting, and then, it is machined internally to produce the elliptical mirror surface: a large-diameter grinding tool is revolved against the inside of the revolving casting while the locus of the tool is tape controlled to the elliptical coordinates.

Next, the casting is rough-ground to remove the grinding tool steps and prepare the aluminum surface for the 0.006-in. electroless nickel plating. The electroless nickel is heat treated for 1 h at 350 ±10°F to raise the hardness from 45 to 60 Rc. The nickel plating at this point should have sufficient adhesion to prevent peeling during the optical polishing cycle.

The inner nickel surface is then polished to a highly specular finish of the correct figure. To inspect the optical properties, a very small light source 0.006 × 0.015 in. is placed at the focus and the image is examined at the second focus. All the light must be contained within a circle whose diameter is made up of the maximum magnification of the source, plus the slope deviation tolerance allowed (±5 min) for the figure.

The polished nickel surface is coated with vacuum-evaporated aluminum approximately 900 to 1000 Å thick. The aluminized collector is not overcoated because experience at JPL has shown that energy losses and spectral distortion with time are lower and more predictable without overcoating. (Periodic stripping and realuminizing of the collector is accomplished quickly and easily without an overcoat.) Proper humidity control of the circulating cooling air results in low degradation of the uncoated mirror surface.

## VI. Prototype Testing of Lamps and Collectors

The test setup used to determine performance measurements was also used to measure actual pressure drops, flows, and temperatures of the various components under actual operating conditions. It was very useful in demonstrating the functional design of the gimbals, focusing adjustments, clearances, etc. The electrical power system, lamp control system, ignitor circuit, and water cooling requirements could be mocked up and tested before production hardware was ordered. Where problems occurred, the test setup provided an ideal device to enable a fix to be worked out and incorporated into the final production design hardware.

### A. Lamp Comparisons

The use of the prototype test setup with various types of lamps indicated that some were better than others when measuring power at aperture vs operating power. The influence of the lamp envelope quality was immediately apparent when lamps with wavy, or with other poor optical quality envelopes would pass considerably less energy through the aperture than lamps with good envelopes. Figure 44 shows how the energy distribution at the second focus and energy through the aperture is affected by distortions in the lamp envelope. The differences between spherical and elliptical envelopes were

not able to be determined because of the magnitude of the deviation due to the waviness factor.

Comparison of lamps of different types was also complicated by the fact that some manufacturers prefer to fill and operate their lamps at a lower gas pressure. Lower gas pressures reduce the brightness of the arc and this causes reduced efficiency in the lamp collector system. The operating gas pressure can be estimated by observing the electrical characteristics of various lamps. Higher gas pressures and increased arc gap size cause the lamps to operate at higher voltages (Fig. 45). There are other factors that affect the lamp electrical characteristics – such as type of gas, electrode materials, electrode shape, and electromagnetic environment of the lamp – but these are usually of less significance, because most lamps of this type are of similar configuration and differ only in detail design.

If all the lamps tested will produce in excess of a certain minimum amount of energy in the system, the most important lamp characteristic to use in comparing lamps becomes useful-lamp-hours/unit-cost, and initial power output becomes less important. Figure 46 shows the advantage of using lamp B over lamp A, even though both lamps meet the warranted hours. Most of the SS15B lamp

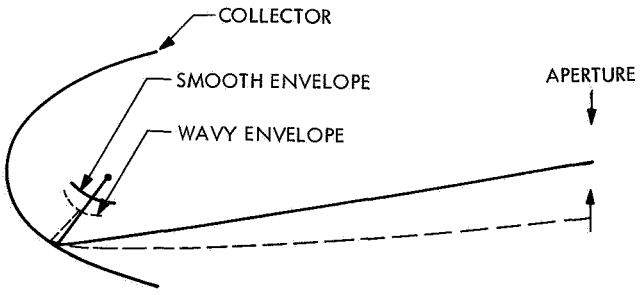


**Fig. 44. Vignetting effect of wavy envelope**

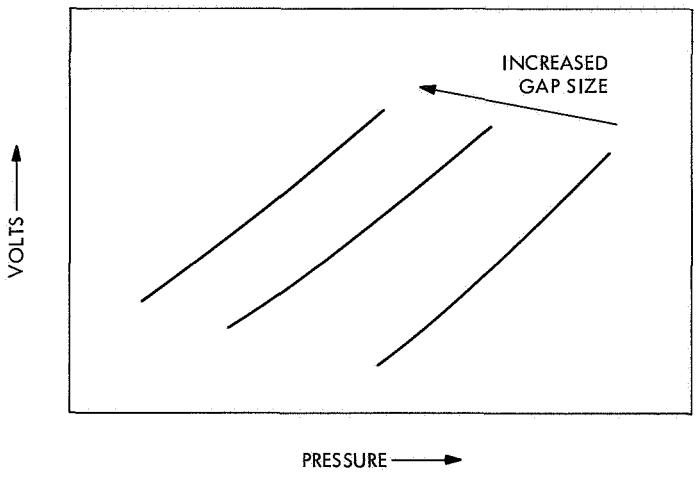


**Fig. 45. General lamp voltage–pressure characteristics**

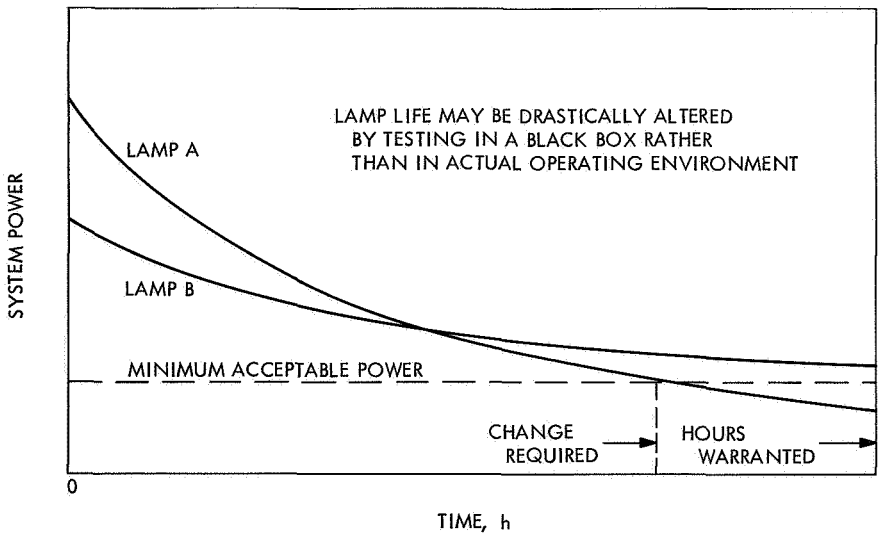


**Fig. 46. System power vs lamp life**

test program is based on studying the lamp-system degradation vs time for various lamps, rather than initial lamp output. The lamp-system power through the aperture can be used to predict performance based upon the earlier testing with the A systems.

### B. Lamp Inclination

The maximum inclination of the lamps installed in the 37-lamp array is approximately 21 deg from the vertical and for the 61 lamp array is approximately 26 deg from the vertical. The lamp testing conducted for the SS15B was done at the 26-deg angle to check on possible problems that might possibly occur from inclination.

There appears to be no significant difference in end seal temperature between an inclined lamp and a vertical lamp installed in the collector-mount assembly. Some lamps that have blackened prematurely are noticeably darker on the high side. Also, some lamps which developed molten areas on the anode end showed drips forming on the low side, but the darkening and melting are believed to be caused by factors other than inclination.

The lamps in the 37-lamp array have not shown any pattern of behavior, such as instability, that would correlate with any particular angle of inclination, although many angles between 0 and 21 deg are represented.

### C. Lamp Ignition Circuit

Operation of the water coolant system with the anode and cathode in series, which was desirable because of its simplicity, presented the problem of maintaining the water at a sufficiently high resistance so that the lamp would not be short-circuited. A test was performed to determine how the conductivity of the coolant and the path length of the dielectric hose connecting the electrodes would affect the lamp ignition. Table 2 and Fig. 47 show the results obtained when attempting lamp ignitions with various coolants and dielectric tube lengths. All lamp power rectifiers were turned off for this testing.

Based on these tests, a dielectric hose length of 12 in. was picked, which would allow 100% ignition with the water at a conductivity expected with the treated coolant.

There were other areas where lamp ignition became a problem in the system which were not apparent during the lamp-collector prototype testing. The ignitors and high-voltage busses to the lamps were routed in such a manner as to completely isolate them from the working area beneath the lamps to reduce congestion and make the area safer to work in. The ignitors were mounted above, and to the side of, the lamp array in a restricted caged-off area, and the negative busses were brought down to the lamps inside of the lamp support trusses, which were shielded. The prototype tests demonstrated

**Table 2. Lamp ignition vs dielectric length**

| Dimension A, in. | Coolant conductivity, ntho/cm | Number of ignitions | | |
|---|---|---|---|---|
| | | *Strong* | *Weak* | *None* |
| 1 | $4.0 \times 10^{-4}$ | 10 | | |
| ¾ | $4.0 \times 10^{-4}$ | 10 | | |
| ¾ | $4.0 \times 10^{-3}$ | | | 10 |
| 1 | $4.0 \times 10^{-3}$ | | | 10 |
| 1½ | $4.0 \times 10^{-3}$ | | | 10 |
| 2 | $4.0 \times 10^{-3}$ | | | 10 |
| 4 | $4.0 \times 10^{-3}$ | 6 | 4 | |
| 5 | $4.0 \times 10^{-3}$ | 7 | 3 | |
| 6 | $4.0 \times 10^{-3}$ | 6 | 4 | |
| 7 | $4.0 \times 10^{-3}$ | 7 | 3 | |
| 9 | $4.0 \times 10^{-3}$ | 10 | | |
| 11 | $4.0 \times 10^{-3}$ | 10 | | |
| 12 | $4.0 \times 10^{-3}$ | 10 | | |
| 13 | $4.0 \times 10^{-3}$ | 9 | 1 | |
| 18 | $4.0 \times 10^{-3}$ | 10 | | |

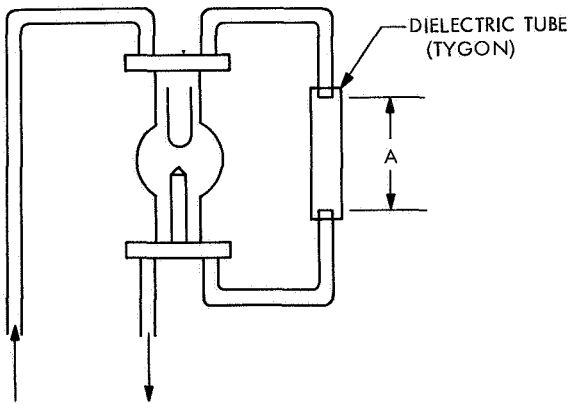


**Fig. 47. Dielectric tube schematic**

that satisfactory lamp ignitions could be obtained with the capacitor discharge ignitor separated by as much as 35 ft from the lamp; this distance was the maximum expected.

The changes in physical arrangement between the prototype and the actual installation introduced new problems when the lamp ignition was attempted in the lamp array in the simulator basement area. The long, high-voltage negative buses, which were closely packed in the lamp support trusses, were leaking energy into the trusses and surrounding basement area so that the lamp would not ignite. The first approach to the problem was to step up the discharge voltage of the ignitor, but this proved futile, even when the voltage was doubled. The lamp ignition circuit had simply too many *holes* and too high an impedance.

To better insulate the negative buses, the entire length of the bus within the truss was covered with 3 to 5 layers of 3-mil Mylar sheet. The sheets were overlapped a minimum of 2 in. at the joints. Any portion of the negative bus that came within 2 in. of any other surface or insulator was similarly wrapped with Mylar sheet all the way back to the ignitor. The ignitor bypass contactors, which were also at high-voltage during lamp ignition, were modified to enlarge the contactor *open* gap and, also, covered with plexiglass shields to eliminate arc discharge from the sharp edges of the contacts and linkages.

The impedance of the ignition circuit was further reduced by wire-braid bonding the anode directly to ground at the collector and bonding the ignitor positive terminal to ground at the ignitor. These modifications to the ignitor circuit allowed the ignitor voltage to be reduced to the original 50 kV with very good ignition characteristics. Some lamps occasionally will not start on the first attempt, even though there is a strong discharge at the electrode gap. This phenomenon is believed to be due to the lamp electrode condition however, and not the ignitor. At some times the ignition process appears to be more reliable when the humidity is lower in the lamp area, but sufficient operating experience is unavailable to confirm this.

### D. Lamp Coolant System

The prototype 20-kW lamps specified ordinary tap water to be used as a coolant. Early lamp evaluation tests showed that tap water was probably sufficient for their type of anode cooling, but the lamp life was so short that the importance of the coolant was not recognized.

The SS15B coolant system was designed around the requirements of the prototype and early production lamps that used a water cooled tungsten anode. The water used was de-ionized and contained a soluble, high PH additive to reduce corrosion in the system. The equilibrium ionization of this water system made the conductivity of the coolant low enough and sufficiently stable with time that a water system de-ionizer was not required.

A nitrogen purge system is used to reduce the oxygen and carbon dioxide in the coolant, and a filter is added to block all particles larger than 50 $\mu$m.

The newer 20-kW lamps with the small, tangential flow nozzle anode cooling systems may present problems when used with an additive in the coolant. Tests conducted by JPL and others (Ref. 7) indicate that lamp coolant systems will have to become much more sophisticated than the early tap water systems to achieve the heat-transfer efficiencies required for long life at increased power levels.

Changes currently being considered for the SS15B system to adapt to the newer lamps include: highly filtered (5 $\mu$m) de-ionized water, complete de-aeration of all dissolved gases, and increased operating water pressures.

### E. Lamp Stability

The water coolant lines to the lamp anode were routed as close to the lamp envelope as possible to reduce the amount of collector surface to be cut away and to allow the lamp to be serviced from the rear of the collector (Fig. 48). Rear servicing reduced the exposure to the bare lamps above the array, and a series anode-cathode flow path meant fewer hose connections to service for lamp removal.

It was felt, initially, that the current could be shunted effectively between the two opposing anode conductors so that their magnetic fields would cancel and the arc would not be deflected seriously. The prototype design called for a $\frac{1}{8} \times \frac{3}{4}$-in. copper shunt strap connecting the two water tubes at the base. This seemed to work satisfactorily at up to 10 kW; but at higher power levels, the arc was noticeably deflected away from the conductor carrying the most current and became unstable.

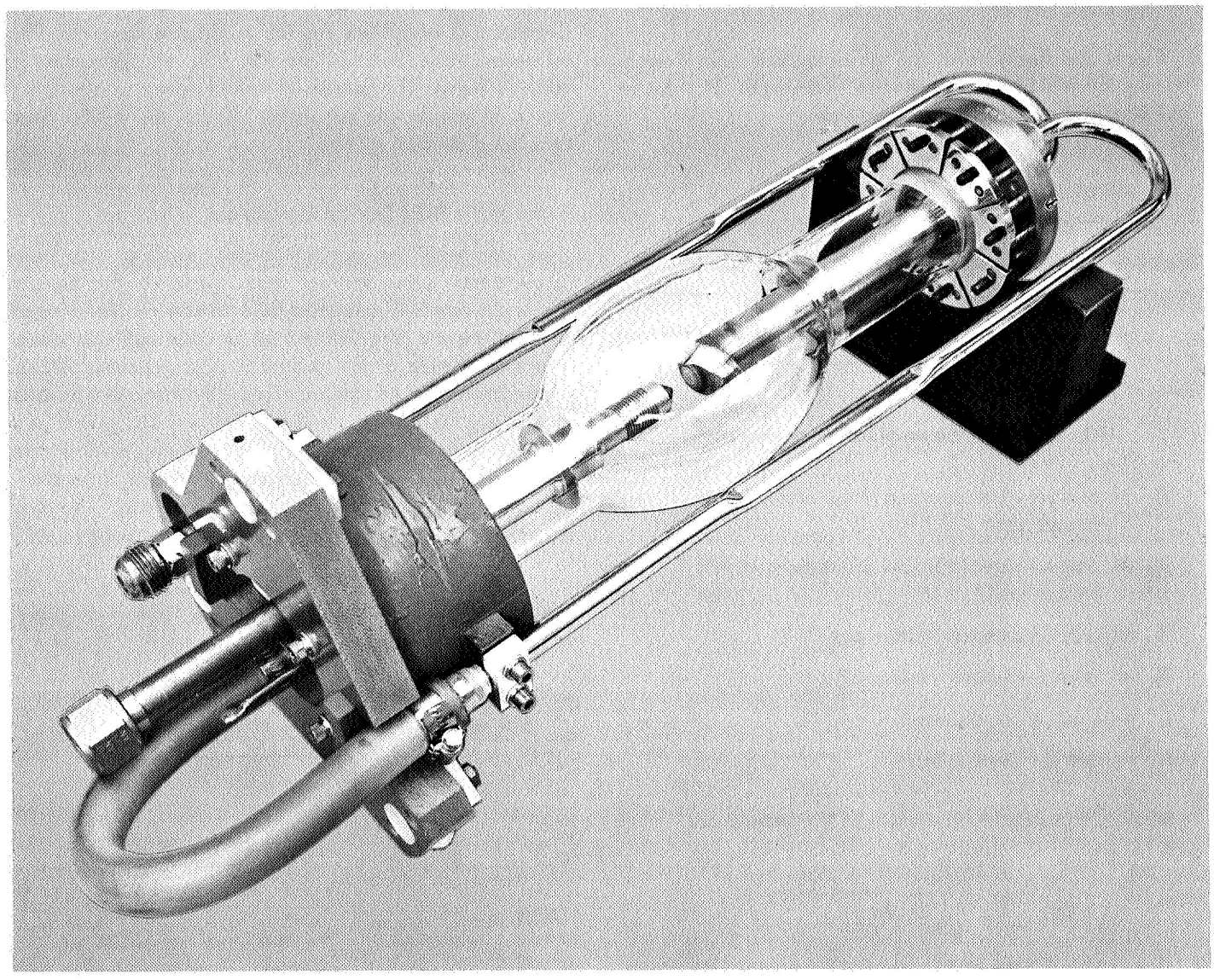

**Fig. 48. Water tubes on mounted lamp**

Doubling the current capacity of the shunt appeared to solve the problem, but it was later discovered by the lamp manufacturer, and verified by a JPL lamp test, that small changes in the contact resistance of the shunt would cause instability and deflection of the arc. The contact resistance was apparently affected not only by installation procedure but, also, by aging in the lamp mount after assembly.

Figure 49 shows how the problem was solved electrically by making the conducting tubes ($R_3$, $R_4$) out of 321 stainless steel, rather than copper.

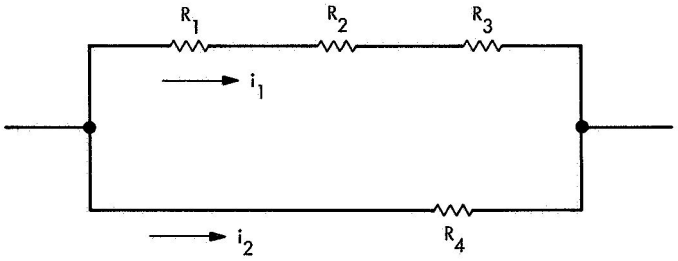


**Fig. 49. Lamp mount electrical schematic**

$R_1$ = contact resistance and shunt resistance/2 (water in)

$R_2$ = contact resistance and shunt resistance/2 (water out)

$R_3$ = tube resistance (water out)

$R_4$ = tube resistance (water in)

$i_1$ = current (water out)

$i_2$ = current (water in)

The current divides in a ratio of the resistances

$$\frac{i_2}{i_1} = \frac{R_1 + R_2 + R_3}{R_4}$$

It is very difficult to get the shunt contact resistances $R_1$ and $R_2$ lower, but if $R_3$ and $R_4$ are made large compared with $R_1$ and $R_2$ and it is assumed that the tube resistances are nearly alike, the current ratio will converge to 1.0. The noticeably unstable lamps with copper tubes and silvered contacts were observed to have current ratios as high as

$$\frac{i_2}{i_1} = \frac{0.00017 + 0.00017 + 0.00034}{0.00034} = 3.0$$

When the copper tubes were replaced with stainless steel, the current ratio is reduced to

$$\frac{i_2}{i_1} = \frac{0.00017 + 0.00017 + 0.00683}{0.00683} = 1.05$$

This modification appears to have solved the arc deflection and instability for the conductor magnetic field influence at a cost of an $i^2R$ loss of approximately 1000 W/lamp. The increased voltage drop of about 2 V was well within the capability of the arc welder rectifiers used in this system.

### F. Magnetic Field Control Experiment

At the time the arc instability problem was being investigated, some studies were made of the possible use of an external magnetic field to control the environment of the arc (Fig. 50). An 18-in.-diam coil was placed at the back side of the collector, approximately 1½ in. below the center of the arc. This 200-turn coil was energized by a highly regulated and filtered DC power supply. By increasing the flux level of the coil, it was possible to make an unstable lamp operate in a stable manner with a noticeably constricted arc. The constricted arc was noticed to pass approximately 1½%

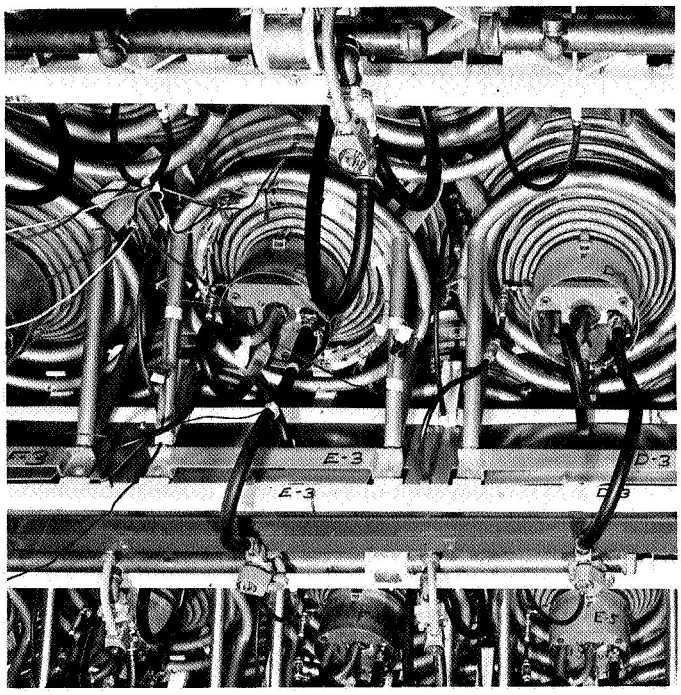

**Fig. 50. External magnetic coil experiment**

more energy into the test volume by observing the test volume radiometer and to reduce the upper seal temperature by 10°F. When the flux level was raised above 30 G, the arc was restricted still further and became unstable once more. At the optimum stability level, the flux was mapped (Fig. 51) in the vicinity of the lamp with the lamp power *off*. No flux measurements were made with the lamps operating.

An interesting observation was made while operating the magnetically controlled lamp in the full lamp array. Rapidly varying the flux level surrounding the controlled lamp by turning the coil *off* and *on* produced a noticeable flicker in the operating voltage of the adjacent lamps. The field strength was estimated to be $<1$ G at the adjacent lamps because of the coil. When all adjacent lamps except one were turned *off*, this one could be made slightly unstable by turning *off* the coil of the adjacent controlled lamp and allowing the controlled lamp to go unstable. Apparently the oscillating field of the unstable lamp was sufficient to affect the normally stable lamp with a very small field level. No measurements were made of the field levels and all testing was terminated at this time to get ready for the acceptance testing of the solar simulator. It seems possible that future problems may be encountered with the magnetic environment of these high current lamps tightly clustered as in the SS15B system.

### G. Mechanical Design of Lamp Mount

The mechanical design of the production lamp mounts were altered to overcome deficiencies noted in the prototype testing. The lamp base plate, which appeared to operate satisfactorily with one type of lamp, was badly burned when operated with a lamp having more energy in the solid angle toward the base (Fig. 52). To remedy this situation, a ¼-in. Teflon baffle was located between the lamp and the base to shield the radiant energy (Fig. 53).

The gimballing adjustments, which were originally designed with standard ¼–28 threads were too coarse for accurate optical alignment of the collector, and the turnbuckles were changed to 32 thread for greater accuracy.

Optical alignment of the lamps and collectors with the lamps operating proved to be a time consuming, uncomfortable, and potentially dangerous operation. A point source lamp fixture previously developed for the acceptance inspection of the lamp collector was incorporated with an alignment device to eliminate this requirement.

A lamp was first operated in the collector and the focus adjusted to give the optimum energy transfer through the aperture. This lamp was then removed and placed in the alignment device (Fig. 54). The crosshairs

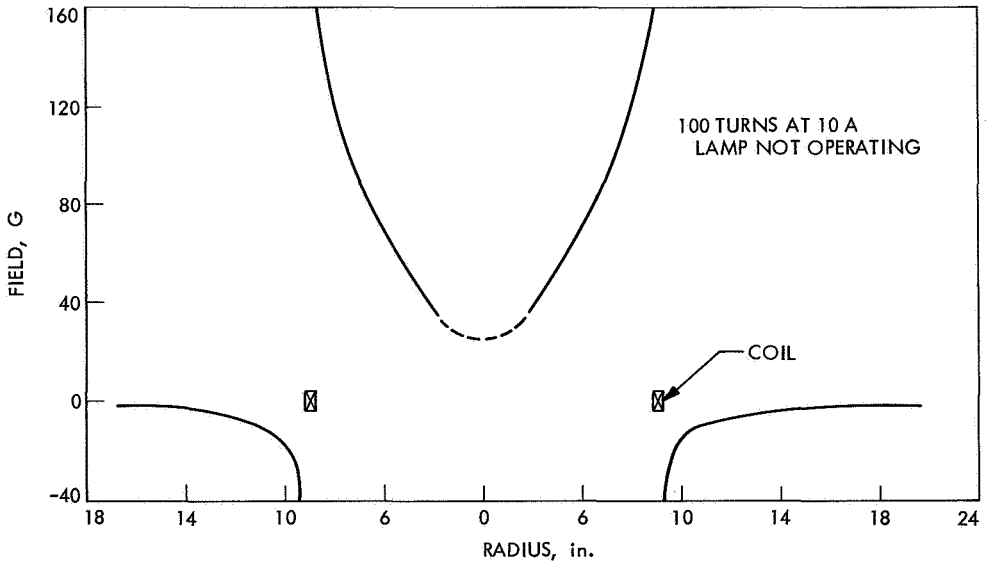


**Fig. 51. Magnetic field induced upon lamp using external coil**

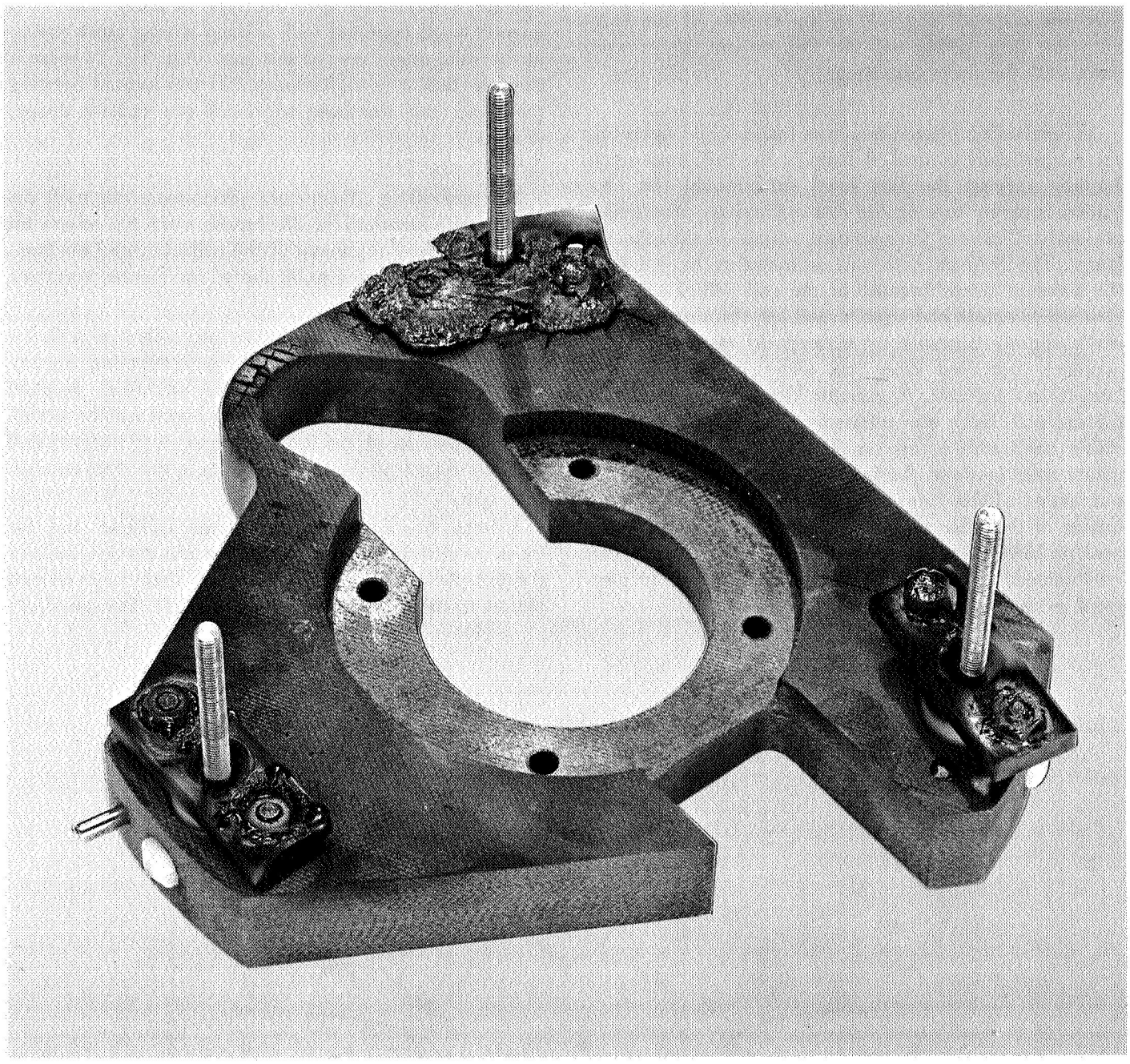

**Fig. 52. Burned lamp mounting base**

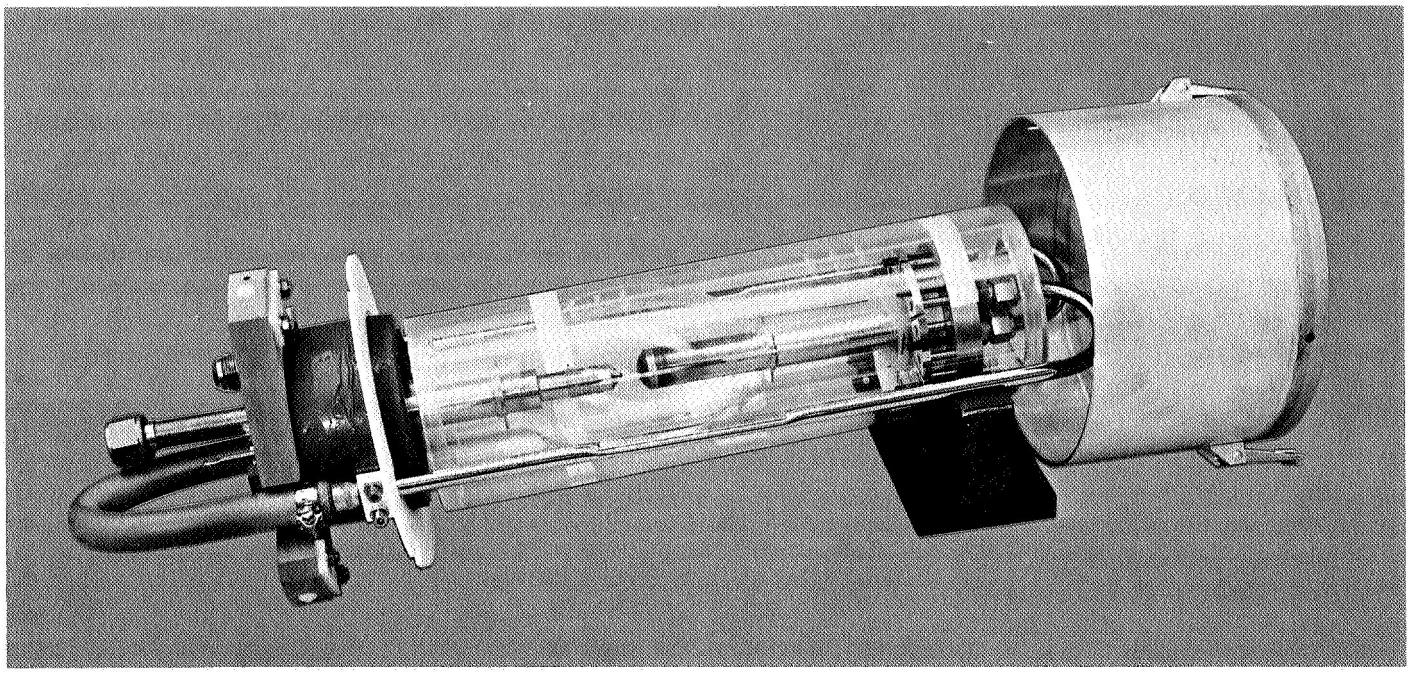

**Fig. 53. Teflon baffle on mounted lamp**

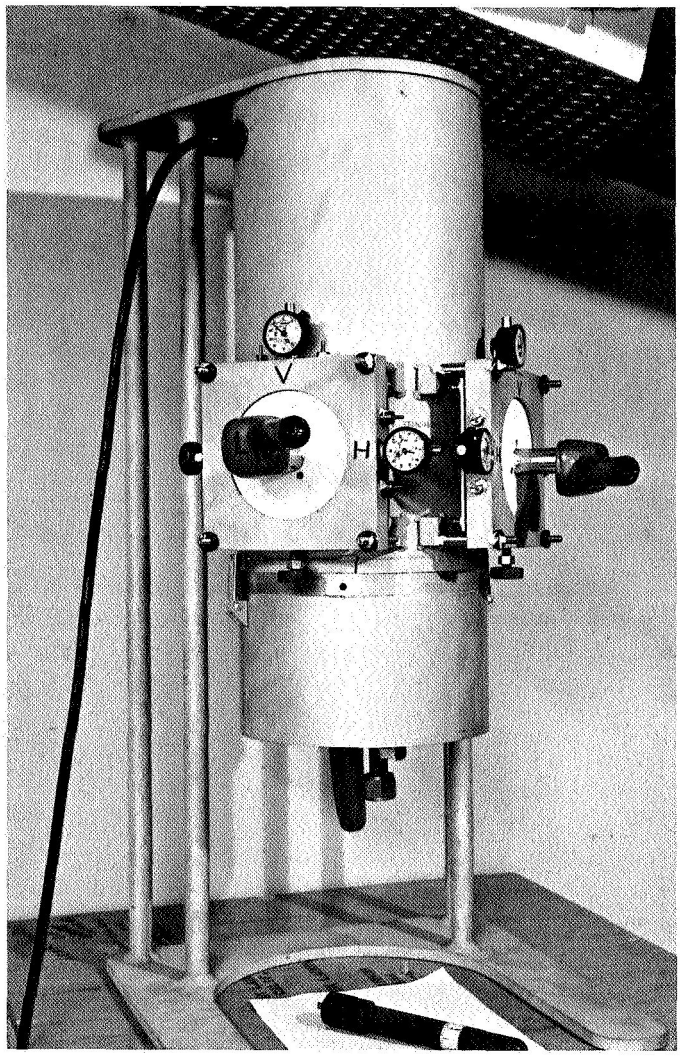


**Fig. 54. Lamp alignment device**

of the 90-deg telescopes mounted on calibrated crossfeeds were adjusted on the extreme cathode tip and locked. The lamp was then removed, and the point source fixture was locked in the alignment device. The point source lamp (0.006 × 0.015 in.) was then positioned at the crosshairs of the alignment device. When the point source fixture was then removed from the alignment device and placed in the same collector that had previously been used, the image size at the second focus was approximately 18 in. in diameter. A target was constructed with a circle 18 in. in diameter and placed over the integrating optics of the system.

Alignment of the collectors and prefocusing of the lamps can next be accomplished by a reverse order of the initial procedure. The alignment target is placed over the integrating optics, and the point source fixture (Fig. 55) is placed in the collector. The point source lamp is moved about until the image is the smallest size (3-in.-diam) and concentric. The point source is then locked into the fixture so it cannot be moved, and the collector is gimballed until the small, 3-in.-diam image is centered on the target. The collector is now properly aimed and the turnbuckle adjustments are locked.

When the collector is aimed, the axial position of the point source lamp is unlocked, and the point source is brought back until the image at the target is enlarged to fill the 18-in.-diam target circle. The point source is then locked in position, and the fixture is removed and indexed into the alignment device (Fig. 56). The crosshairs are moved to the position of the point source lamp, and the opposing crossfeed indicator readings are logged. Any lamp to be installed in this collector position can now be prefocused to these telescope coordinates by placing it in the alignment device and centering the cathode on the crosshairs.

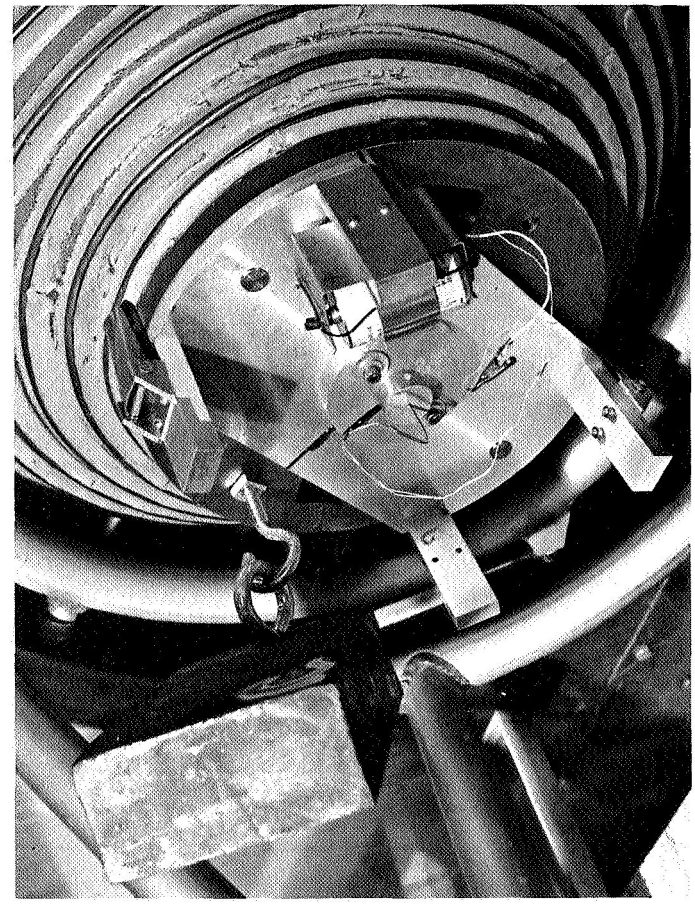

**Fig. 55. Point source fixture installed in collector**

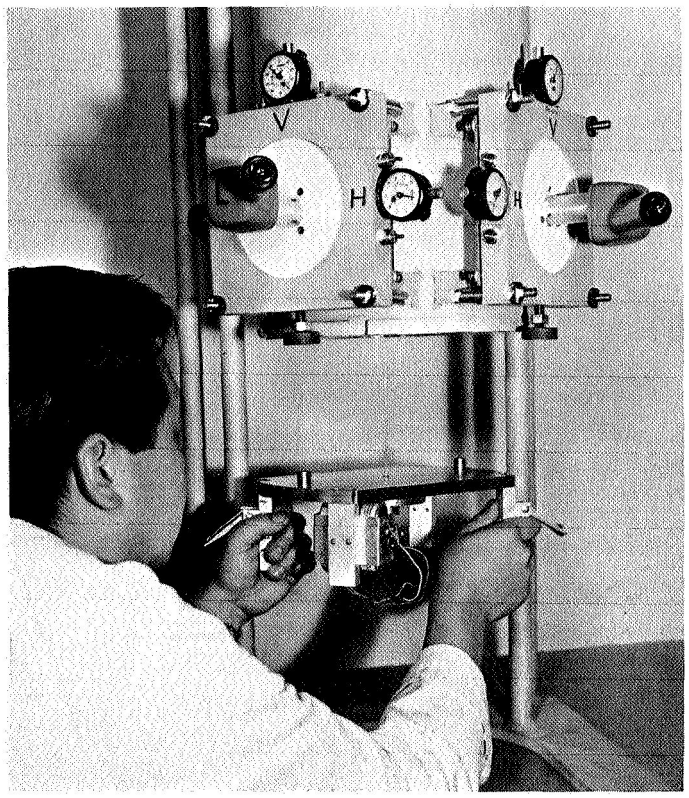


**Fig. 56. Installing point source fixture in alignment device**

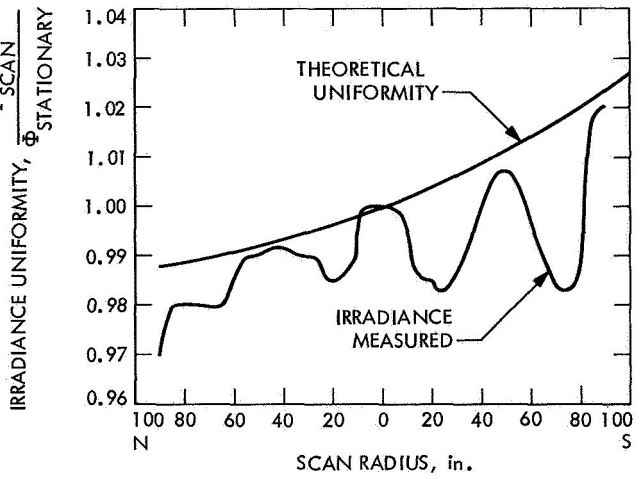


**Fig. 57. Irradiance uniformity vs scan radius**

## VII. System Tuning and Uniformity of Irradiance Tests

### A. Description of Runs

Because of the possibility of improving the uniformity of irradiance by using the aberration effect of the condensing lenses, several runs were made with different lens configurations. As the lenses were progressively inverted (Fig. 14) more energy was spread into the outer portions of the beam, and better overall uniformity was produced. It can be seen that the amount of change is roughly proportional to the amount of energy in the lens channels being used. The irregular behavior of the curve is believed to result from collimator reflectivity and not to be affected by the lens aberration process. Superpositioning the measured irradiance uniformity over the theoretical uniformity due to the collimator aberrations (Fig. 57) shows the approximate magnitude of the mirror reflectivity influence. Direct correlation is not possible because the contribution of the mirror reflectivity is a three-dimensional problem and only limited two-dimensional data are available. Figure 58 shows the total reflectivity of the mirror as measured after these runs.

These data were obtained by operating only one centrally located lamp, because only the magnitude of the change was of interest. As more lamps are used, the uniformity becomes better because, although each lamp illuminates the entire test volume, it illuminates it from slightly different zones of the collimator (Fig. 59). These contributing zones effect an averaging process on the test volume irradiance. The averaging is related to the number of lamps used and, if very good uniformity is desired during a test, all the lamps should be run at a uniformly low power, even if a few lamps run at rated power could do the job.

### B. Lamp Focus Effects

The optimum position of the lamp electrodes with respect to the collector focus was determined in prototype testing for the maximum energy transfer through the aperture. It was noticed during these tests that the lamp focusing readjustment would be required for lamps during their early life because the erosion of the cathode tip is most pronounced at this period. After 50 h, the cathode tip seems to reach an equilibrium radius, and the arc plasma will remain near the same location during the rest of the lamp's useful life. The focus for the lamps used in this system was based on the *burned in* location of the cathode tip rather than the new lamp position.

Figure 60 shows the irradiance in the test volume as a function of cathode position for a new lamp. It can be seen that maximum energy transfer occurs when the cathode tip has eroded approximately 0.036 in. The initial loss resulting from this adjustment compensation is about 5% until the cathode has rounded. There are some

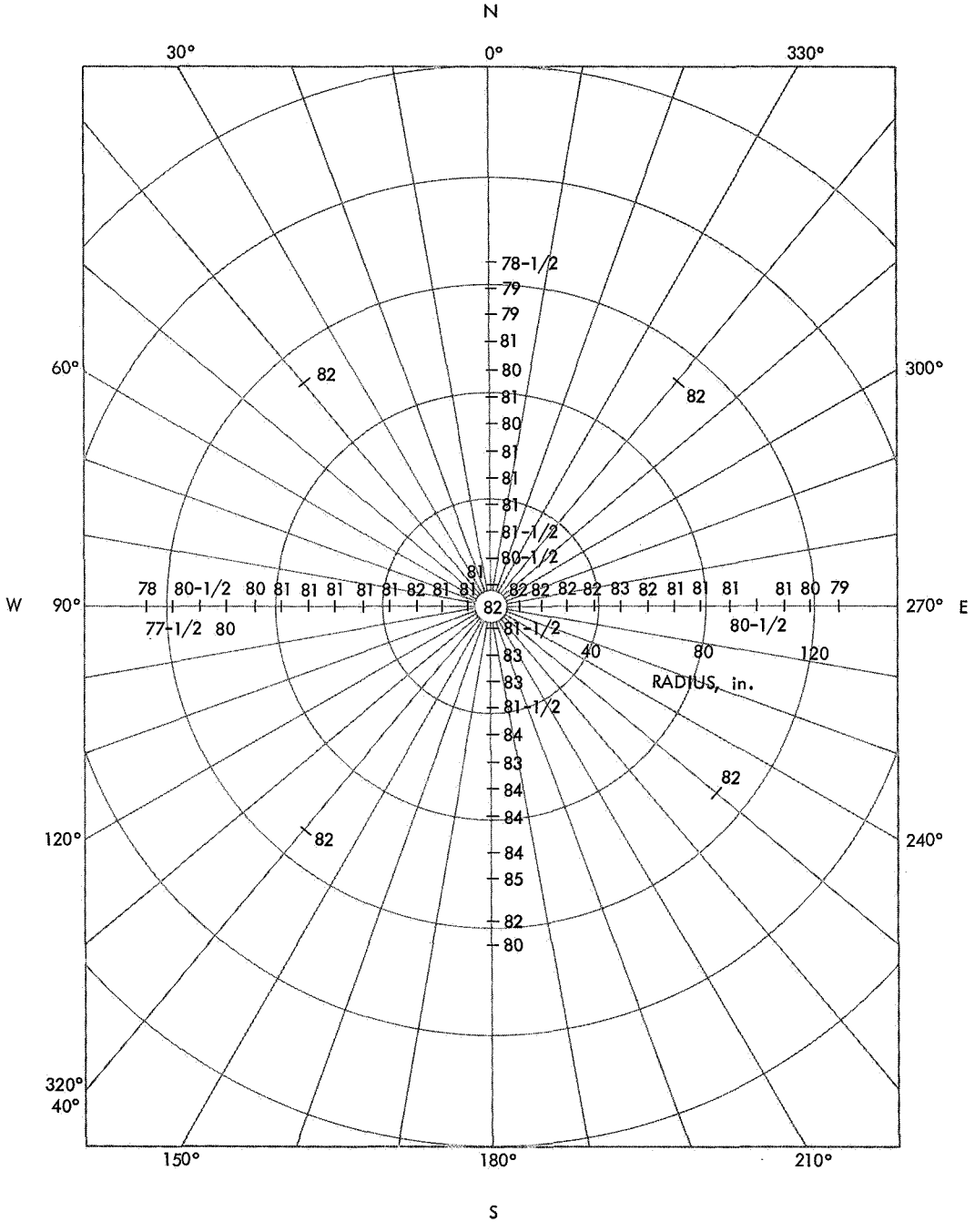


**Fig. 58. Reflectivity of 23-ft mirror**

additional losses from the reduced brightness with the rounder cathode, but these have not been determined quantitatively.

The effect of the focus of the lamp on the system uniformity is shown in Fig. 61. The first interpretation of these data was that the uniformity could be improved by defocusing the lamp somewhat – which appeared true, but the accompanying loss of energy to the test volume makes this solution less desirable. A closer examination of the focus effect on the uniformity was made to see why the uniformity appeared to be worst at the optimum energy transfer; it was found that the original lamp was slightly misaimed. The flag marks show the same type of data obtained from a more closely aimed lamp where the test volume uniformity of irradiance is improved.

The importance of proper aiming can be shown as in Fig. 62 where the distribution of energy from the lamp is displaced on the integrating lens system. It can be seen that the defocused beam distribution will produce an improved uniformity for a lamp that is not aimed properly, but will not produce significant changes for a properly aimed lamp.

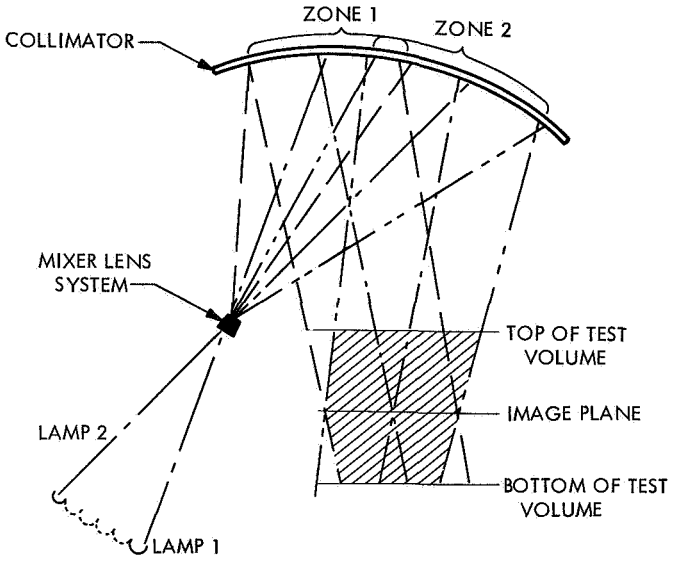


**Fig. 59. Zonal illumination of collimator**

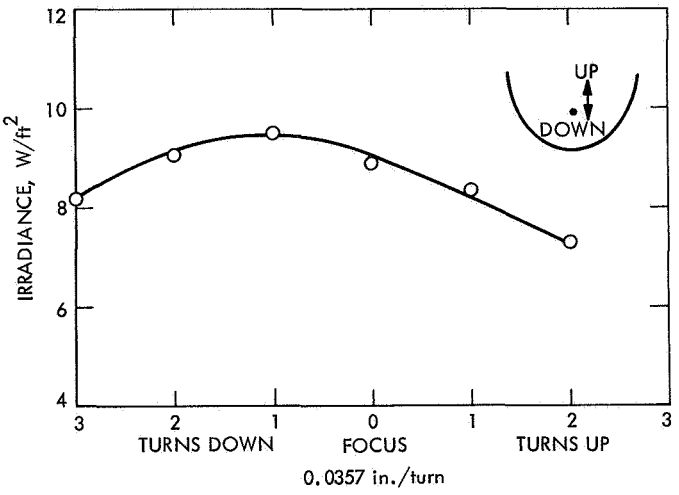


**Fig. 60. Test volume irradiance vs lamp focus**

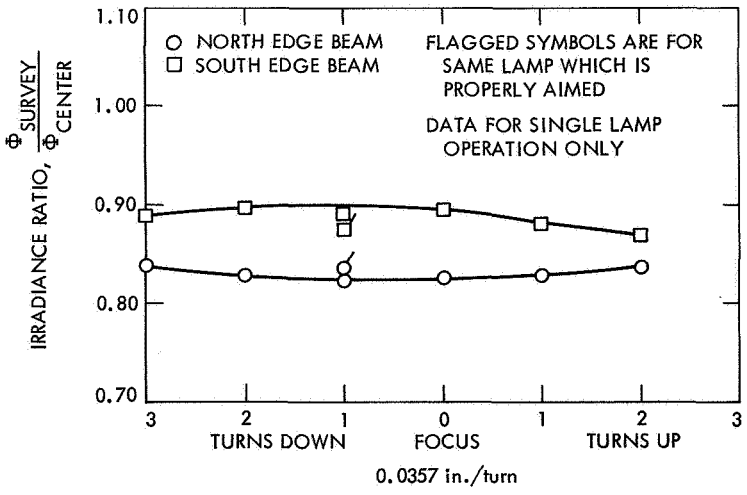


**Fig. 61. Irradiance uniformity effect vs lamp focus**

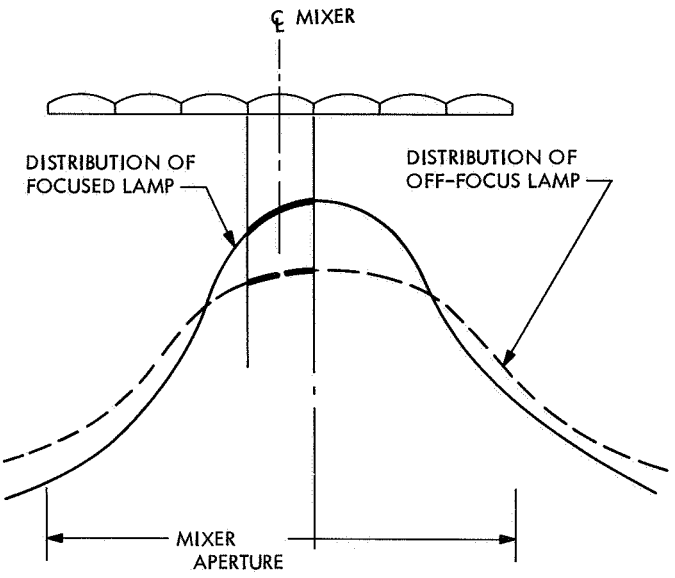


**Fig. 62. Distribution of energy at mixer lenses (misaimed)**

The effect of nonuniformity as a result of the beam position on the mixer is reduced by the averaging process of operating a large number of lamps at lower power, rather than a small number of lamps at higher power. The averaging can also be accomplished by using more lens elements in the integrating lens system; but if a sufficiently large number of lamps is used, this method becomes less attractive.

## VIII. Acceptance Testing and Calibration

The acceptance testing demonstrated that the SS15B system exceeded all the design specifications. The early analytical studies based on prior operation of the type A simulators predicted a system efficiency of 7.5% overall.

$$\text{eff} = \frac{\text{power in test volume}}{\text{power into lamps}} \times 100$$

calculated efficiency

$$\text{eff} = \frac{\Phi \times A}{\text{No.} \times \text{power}} = \frac{282 \times 197}{37 \times 20{,}000} \times 100 = 7.5\%$$

measured efficiency

$$\text{eff} = \frac{133 \times 197}{341{,}300} \times 100 = 7.7\%$$

The denominator represents the average kW input during 7 runs at 133 W/ft².

### A. Collimation

The collimation was measured by use of a theodolite at a 6.0-ft elevation and sighting on the image of the

**Table 3. Collimation of SS15B beam**

| Point of measurement on beam | Angle of beam with test floor | | | Deviation from vertical | |
|---|---|---|---|---|---|
| | Angle A[a] | Angle B[a] | Angle C[a] | A − B | Mean difference |
| | 4-ft radius at 6 ft elevation | | | | |
| N | 180° 59′ 33″ | 179° 5′ 29″ | 2′ 31″ N | 1° 54′ 4″ | 1° 55′ 0″ |
| S | 180° 49′ 57″ | 178° 54′ 1″ | 3′ 1″ N | 1° 55′ 56″ | |
| E | 180° 46′ 51″ | 179° 4′ 52″ | 4′ 8″ W | 1° 41′ 59″ | 1° 42′ 15″ |
| W | 180° 43′ 0″ | 179° 0′ 29″ | 8′ 15″ E | 1° 42′ 31″ | |
| | 7.5 ft radius at 6 ft elevation | | | | |
| N | (Interference with lens cutout prevented measurement) | | | | 1° 58′ 31″ |
| S | 180° 54′ 45″ | 178° 56′ 14″ | 4′ 30″ N | 1° 58′ 31″ | |
| E | 180° 41′ 55″ | 178° 58′14″ | 9′ 55″ W | 1° 43′ 41″ | 1° 43′ 46″ |
| W | 180° 37′ 55″ | 178° 54′ 4″ | 14′ E | 1° 43′ 51″ | |

[a]See Fig. 64 for description of angle.

lamp array on the projection lens system of the mixer to determine the virtual source size. The lamps need not be turned on to make this measurement if the lamp array image is brightened by turning on the maintenance lights in the lamp hood area. Figure 63 shows the measuring points used in calibrating the system and Fig. 64 shows the angle convention used. The data obtained from these measurements are contained in Table 3.

It should be noted that this method takes into account only the extreme rays of the system. Most of the energy is more highly collimated. Table 4, derived from the mixer energy distribution, gives a better presentation of the effectiveness of the solar simulator with respect to the collimation. Note here that the concentrated energy distribution at the mixer is more effective from a collimation standpoint than from a uniform energy distribution.

**Table 4. Percentage of energy within collimation half angles**

| Lens channel | Collimation half angle, deg | Energy, % |
|---|---|---|
| I | 0.0 to 0.23 | 9.6 |
| II | 0.23 to 0.62 | 43.4 |
| III | 0.30 to 0.87 | 26.5 |
| IV | 0.62 to 0.99 | 20.5 |

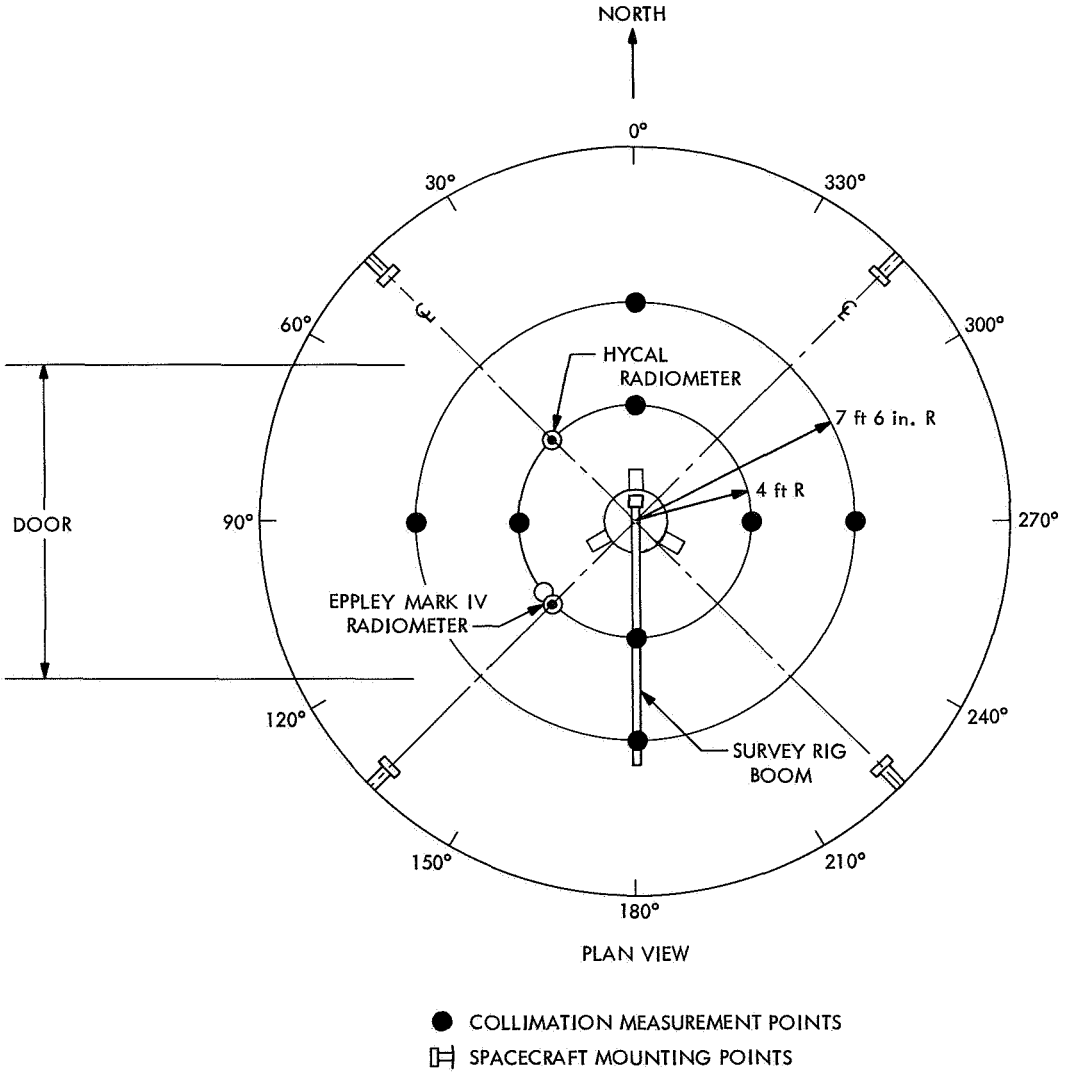


**Fig. 63. Acceptance test measurement points**

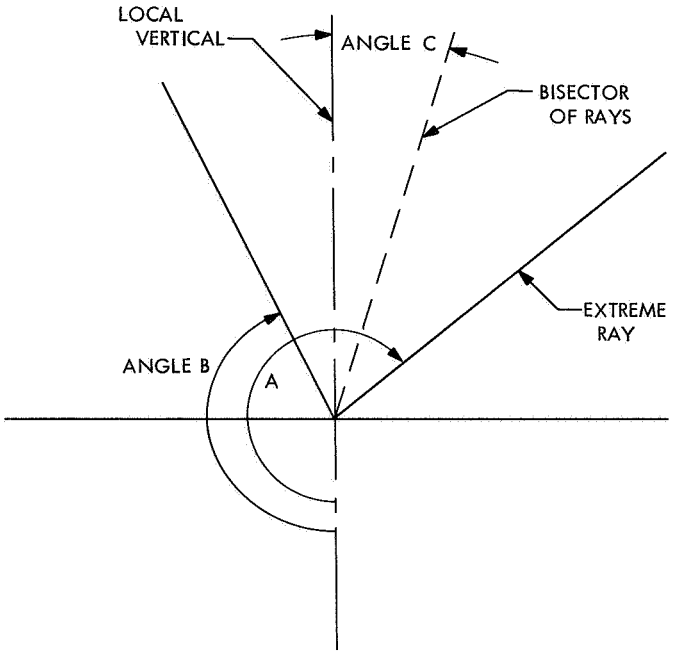


**Fig. 64. The angle convention used for collimation measurements**

### B. Spectrum

The spectrum was measured with an Eppley Mark IV filter radiometer with a B9 filter wheel. Figure 65 shows the percentage of radiant flux vs wavelength obtained for the xenon lamp system as modified by the system optics, only. No filtering was attempted. Lamps were operating at ⅔ of the rated power during spectral measurements. No attempt was made to determine the effect of spectrum vs lamp input power.

### C. Irradiance

The irradiance was measured in the test volume with a calibrated Hycal radiometer and a strip chart recorder during all runs. Figure 63 shows the position of the radiometer in relation to the other instruments. Although the instrument was located 4 ft from the center of the beam, the irradiance was representative of the entire beam because of the high degree of uniformity.

### D. Uniformity

The high quality of the solar simulator beam required a new technique to be used to measure the beam uniformity. This method consisted of comparing the voltage output of two 2 × 2-cm silicon cells (short circuited with 1-Ω wire-wound resistors) with a log ratio converter and processing the output signal through an antilog converter to an *X–Y* plotter:

$$\begin{matrix} E_j \\ \rightarrow \\ E_k \\ \rightarrow \end{matrix} \boxed{E_i = -10 \log_{10}\left(\frac{E_j}{E_k}\right)} \begin{matrix} E_i \\ \rightarrow \end{matrix}$$

$$\boxed{E_o = \text{antilog}_{10}\left(-\frac{E_i}{10}\right)} \begin{matrix} E_o \\ \rightarrow \end{matrix} \boxed{\begin{matrix} X\text{–}Y \\ \text{plotter} \end{matrix}}$$

where:

$E_j$ = scan cell voltage

$E_k$ = stationary cell voltage

$E_i$ = log ratio converter output voltage

$E_o$ = antilog converter output voltage

This technique was used to eliminate the possibility of small changes in the irradiance level, due to random facility power changes, from showing up as irradiance nonuniformities. The stationary silicon cell is mounted on the survey boom so that it is only 2 in. from the center of the test volume and at the same elevation as the scan cell. The irradiance ratio is then:

$$\Phi_{\text{ratio}} = \frac{\Phi_{\text{scan}}}{\Phi_{\text{stationary}}} \propto \frac{E_j}{E_k}$$

The irradiance levels were determined by observing a calibrated Hycal radiometer output during all scans with a strip chart recorder. All scans were made at an irradiance level of 133 ±2 W/ft² with approximately 22 lamps running at ⅔ of the rated power. As explained previously, it was expected that better uniformity could be obtained if all 37 lamps were operating, but lamp stability problems prevented this from being done.

Figure 66 shows typical irradiance ratio scans made at ambient conditions in the four directions of major interest. Figure 67 shows a typical uniformity contour plot derived from the complete scanning data under simulated test conditions. There were no significant changes in test volume irradiance uniformity when data were taken at different elevations — either under cold wall conditions or at −100°F to +70°F collimator temperatures.

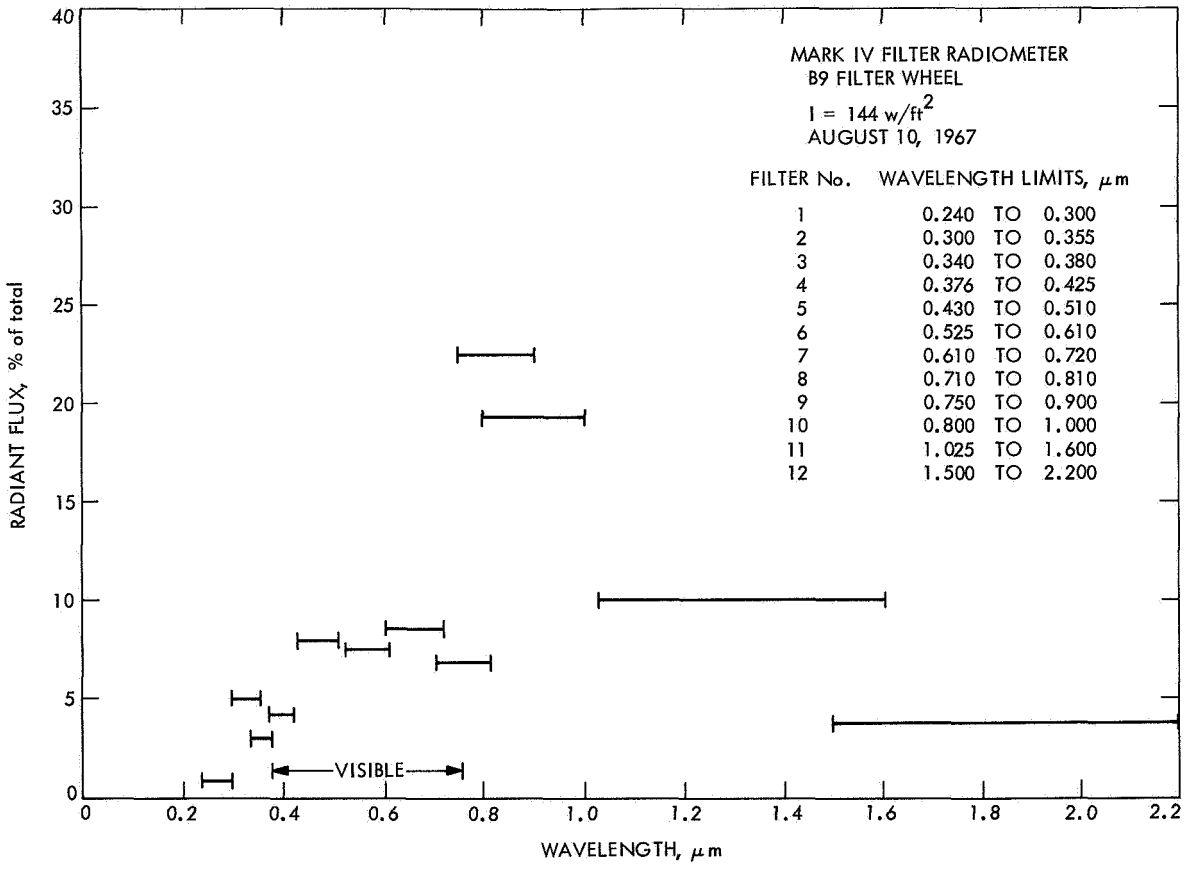


**Fig. 65. Spectral measurement in the 25-ft space simulator**

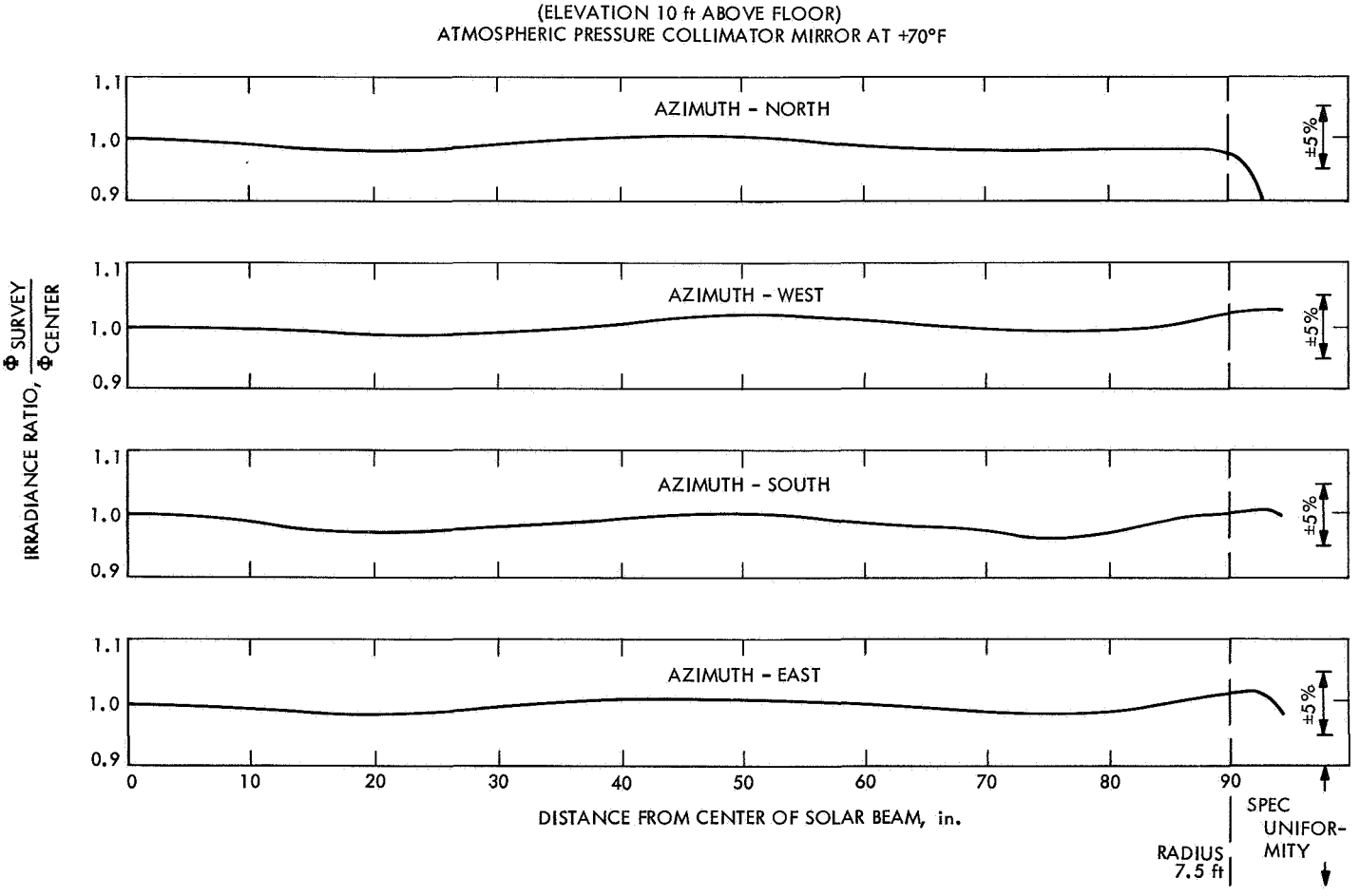


**Fig. 66. Uniformity scans**

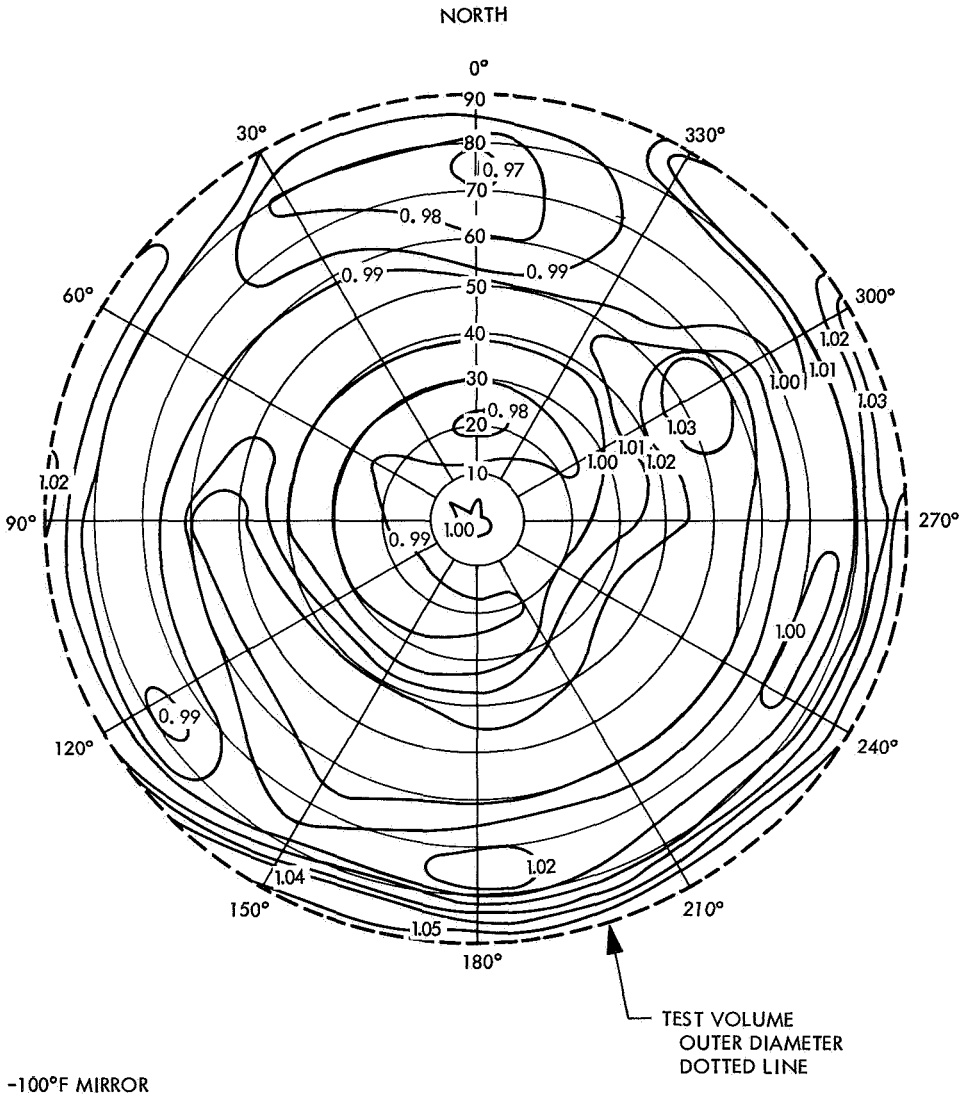


**Fig. 67. Contour plot of irradiance ratios**

## IX. Future Capabilities

The performance of the 25-ft simulator with the existing lamp array and changing only the mixer lenses and lamp power can be extrapolated with confidence for systems of higher irradiance or varying beam size. Figures 68 through 71 show the wide range of options available with these minor changes. Additional changes such as the addition of the 10-ft-diam × 20-ft-focal-length collimator from the 10-ft simulator and suitable mixer lens changes can be used to provide an 8-ft beam with irradiance equivalent to that of the planet Mercury.

## X. Conclusions

Large single-piece collimating mirrors of more than 20 ft in diameter can be fabricated for use in high-quality solar simulators from aluminum weldments. When properly designed and constructed, they will be dimensionally stable and have excellent temperature-control characteristics. The mirror's reflecting surface can be formed by electroplating nickel to the machined weldment, then grinding and polishing the nickel to a highly specular finish. The vacuum deposition of aluminum on this surface by means of a single-source crucible heated by electron beams is capable of producing optimum uniformity of reflectance over the entire diameter. Also, the spherical aberrations of large-diameter, off-axis collimators and the resulting degradation in uniformity of irradiance and collimation can be improved by locating the virtual source off focus.

Transmission optics for large systems such as the SS15B are subjected to extremely high-flux densities at the system aperture. Water-cooled structures to position the optical elements can be designed and fabricated to withstand these thermal loads with relatively small losses. The nonuniformities in the test volume irradiance that result from the cosine type distribution of energy at the mixer aperture can be improved by design of the optical elements in the mixer lens system.

Water-cooled lamps have made possible the design of large solar-simulator beam sizes with a relatively small number of higher-powered lamps. The water coolant and electrical power to these lamps can be joined in common buses to make more efficient use of available space. Initial problems with premature anode failure and plasma instability appear to be near solution and show promise of increased power output and useful lamp life.

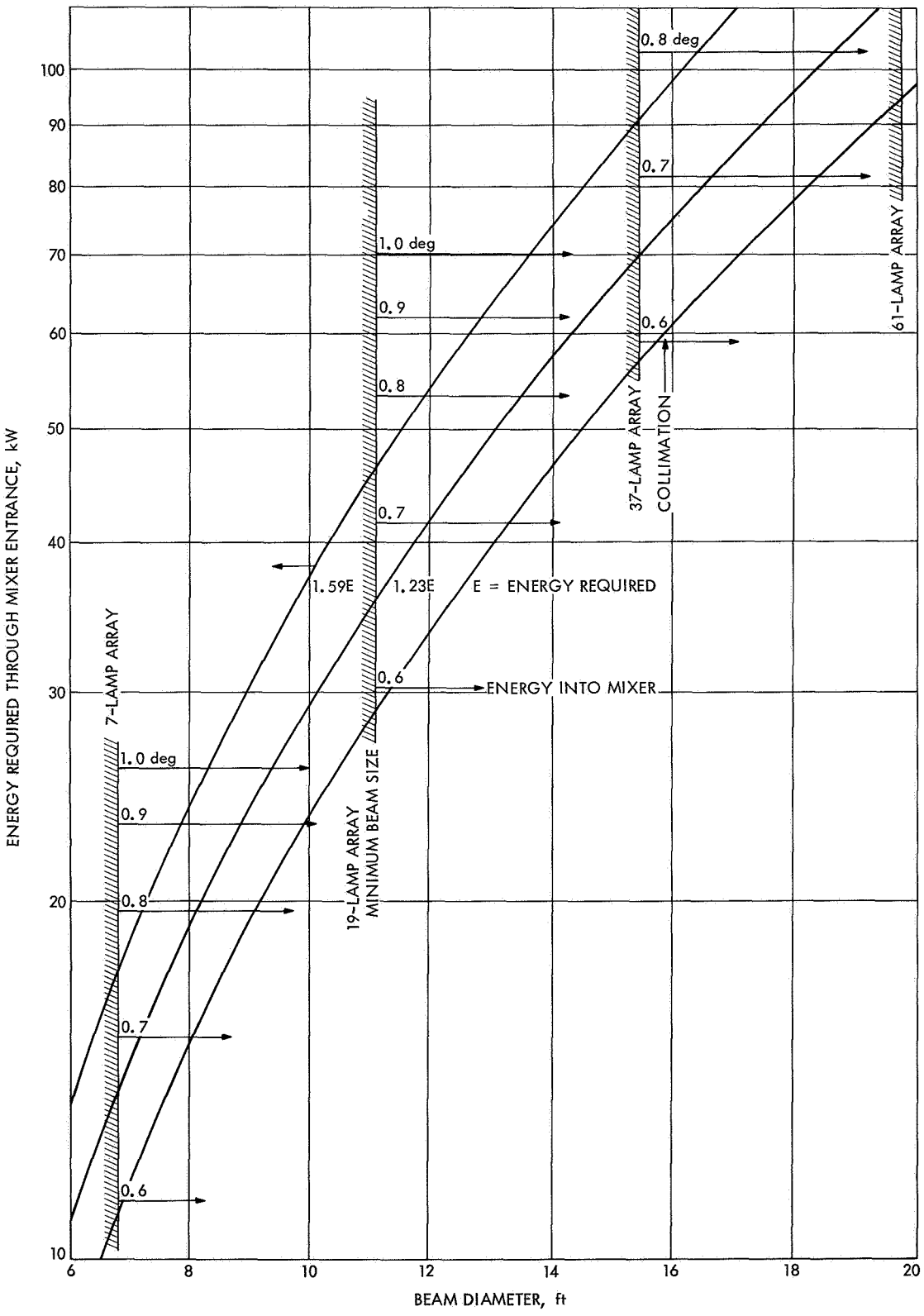


**Fig. 68. Energy through mixer vs beam diameter: earth irradiance, 20-kW lamps**

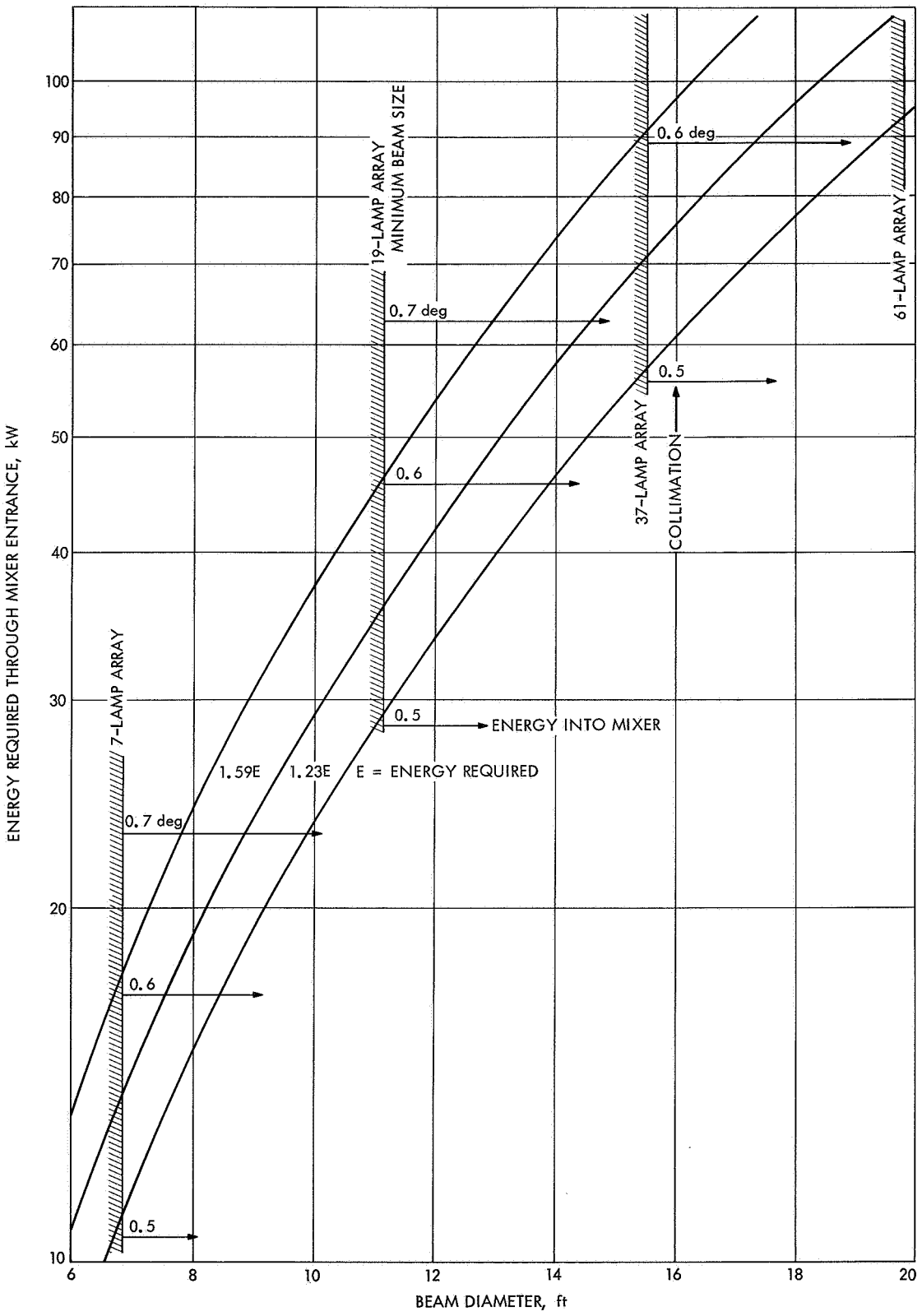


**Fig. 69. Energy through mixer vs beam diameter: earth irradiance, 30-kW lamps**

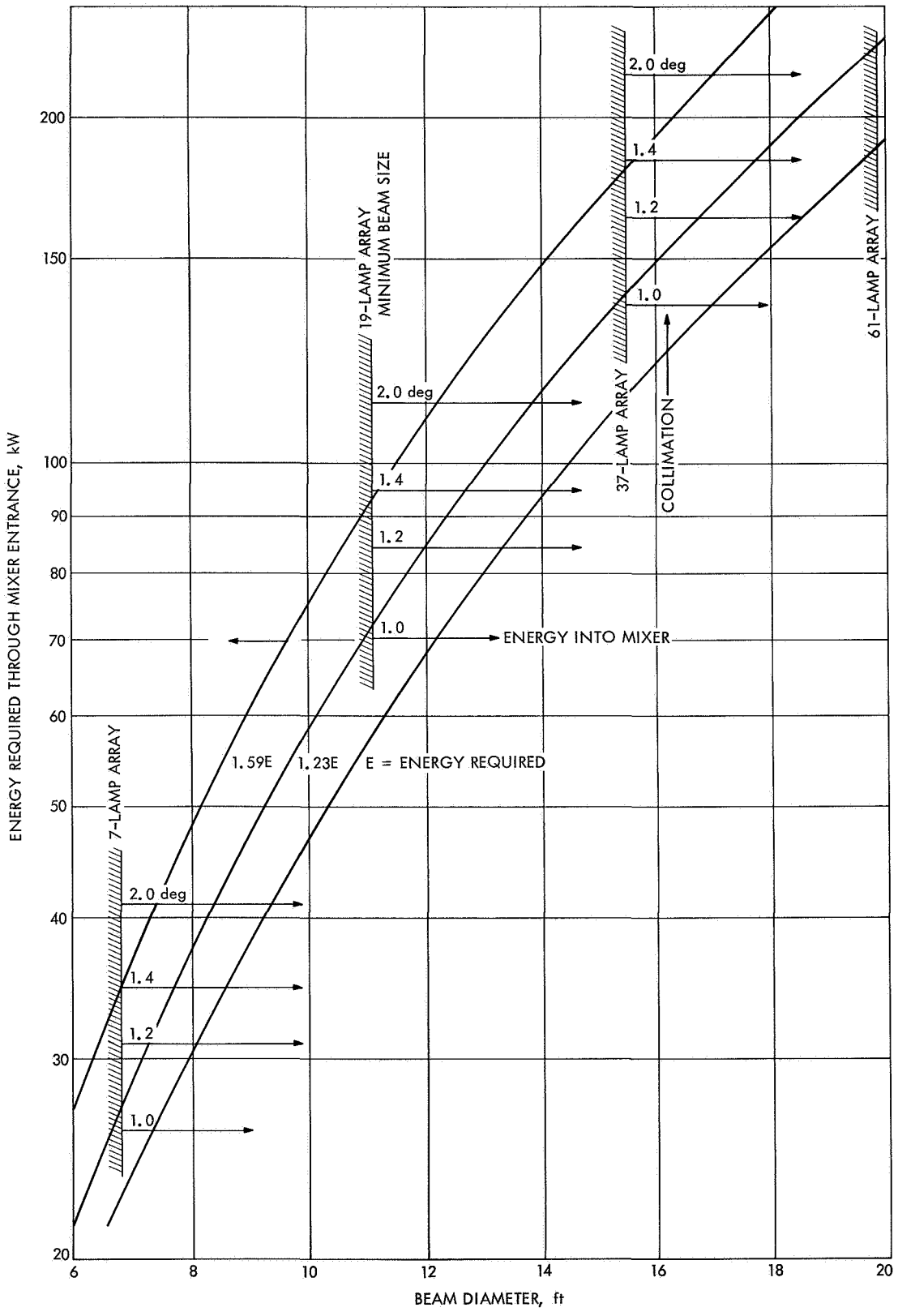


**Fig. 70. Energy through mixer vs beam diameter: Venus irradiance, 20-kW lamps**

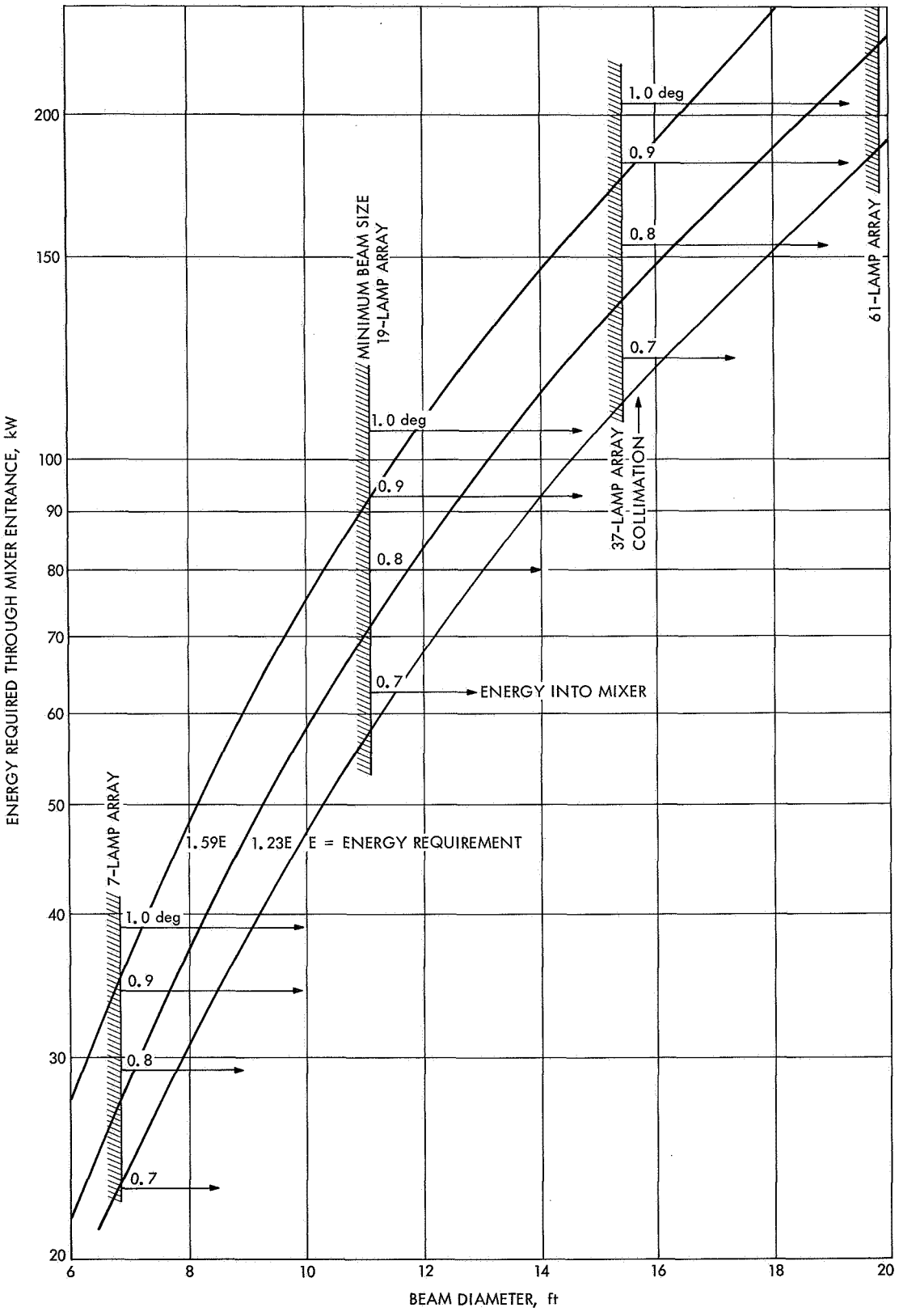


**Fig. 71. Energy through mixer vs beam diameter: Venus irradiance, 30-kW lamps**

## References


1. Barnett, R. M., and Thiele, C., *JPL Advanced Solar Simulator Design, Type A,* Technical Memorandum 33-141. Jet Propulsion Laboratory, Pasadena, Calif., Apr. 23, 1963.

2. Bartera, R. E., and Barnett, R. M., *Development of the JPL Solar Simulator, Type A,* Technical Report 32-638. Jet Propulsion Laboratory, Pasadena, Calif., Jul. 1964.

3. Eddy, R. P., and Heilig, M. R., *Fabrication of the 23-ft Collimating Mirror for the JPL 25-ft Space Simulator,* Technical Report 32-1214. Jet Propulsion Laboratory, Pasadena, Calif., Dec. 15, 1967.

4. Riise, H. N., *Solar Simulator Optimization Through Defocusing: A Result of Computerized Optical System Ray-Tracing Study,* Technical Memorandum 33-384. Jet Propulsion Laboratory, Pasadena, Calif., Sept. 15, 1968.

5. Schmidt, L. F., and Casad, T. A., *Automatic Design of Optical Systems by Means of an IBM Digital Computer Employing the IBJOB Monitor,* Technical Report 32-790. Jet Propulsion Laboratory, Pasadena, Calif., Oct. 1, 1967.

6. Firnett, P. J., and Wilson, L. A., *Fortran Optical Lens Design Program, Volume II,* Technical Report 67-700-10-2. Informatics, Inc., Los Angeles, Calif., Oct. 16, 1967.

7. Lunde, A. R., Yerkes, J. W., and Haslund, R. L., "The Boeing 20-ft Solar Simulator: Progress Report," *The Second ASTM–IES–AIAA Space Simulation Conference, Philadelphia, Sept. 11–13, 1967,* pp. 162–177.